การสังเคราะห์อะลูมิเนียมออกไซด์พิลลาร์เคลย์อิมเพรกเนตด้วยโลหะคลอไรด์สำหรับปฏิกิริยาที่ใช้กรดเร่ง

นางสาว ปิยรัตน์ ตรีกิตติวงศ์

วิทยานิพนธ์นี้เป็นส่วนหนึ่งของการศึกษาตามหลักสูตรปริญญาวิทยาศาสตรดุษฎีบัณฑิต
สาขาวิชาปิโตรเคมี
คณะวิทยาศาสตร์ จุฬาลงกรณ์มหาวิทยาลัย
ปีการศึกษา 2553

SYNTHESIS OF METAL CHLORIDE-IMPREGNATED ALUMINIUM OXIDE-PILLARED CLAY FOR ACID CATALYZED REACTIONS

Miss Piyarat Trikittiwong

A Dissertation Submitted in Partial Fulfillment of the Requirements
for the Degree of Doctor of Philosophy Program in Petrochemistry
Faculty of Science
Chulalongkorn University
Academic Year 2010

Thesis Title	Synthesis of Metal Chloride-impregnated Aluminium Oxide-pillared Clay for Acid Catalyzed Reactions
By	Miss Piyarat Trikittiwong
Field of Study	Petrochemistry
Thesis Advisor	Assistant Professor Warinthorn Chavasiri, Ph.D.
Thesis Co-advisor	Nipaka Sukpirom, Ph.D.

Accepted by the Faculty of Science, Chulalongkorn University in Partial Fulfillment of the Requirements for the Doctoral Degree

S. Hannongbua ....Dean of the Faculty of Science

(Professor Supot Hannongbua, Dr. rer. nat.)

THESIS COMMITTEE

Sirirat Kokpol ....Chairman

(Associate Professor Sirirat Kokpol, Ph.D.)

Warinthorn Chavasiri ....Thesis Advisor

(Assistant Professor Warinthorn Chavasiri, Ph.D.)

Nipaka Sukpirom ....Thesis Co-advisor

(Nipaka Sukpirom, Ph.D.)

W. Trakarnpruk ....Examiner

(Associate Professor Wimonrat Trakarnpruk, Ph.D.)

Nuanphun Chantarasiri ....Examiner

(Associate Professor Nuanphun Chantarasiri, Ph.D.)

Jinda Yeyongchaiwat ....External Examiner

(Assistant Professor Jinda Yeyongchaiwat, Ph.D.)

ปิยรัตน์ ศรีกิตติวงศ์ : การสังเคราะห์อะลูมิเนียมออกไซด์พิลลาร์เคลย์อิมเพรกเนตด้วยโลหะคลอไรด์สำหรับปฏิกิริยาที่ใช้กรดเร่ง. (SYNTHESIS OF METAL CHLORIDE-IMPREGNATED ALUMINIUM OXIDE-PILLARED CLAY FOR ACID CATALYZED REACTIONS) อ. ที่ปรึกษาวิทยานิพนธ์หลัก: ผศ.ดร. วรินทร ชวศิริ, อ. ที่ปรึกษาวิทยานิพนธ์ร่วม: อ.ดร.นิปกา สุขภิรมย์, 156 หน้า

ได้สังเคราะห์ไอรอนออกไซด์พิลลาร์เคลย์ เช่น ไอรอนออกไซด์พิลลาร์เบนโทไนต์ ไอรอนออกไซด์พิลลาร์เฮกโทไรต์ และไอรอนออกไซด์พิลลาร์แทนิโอไลต์ โดยการสอดแทรกไอรอน (III) คลอไรด์เข้าไประหว่างชั้นของเคลย์ นำไปเผาที่ 300°C นาน 5 ชั่วโมง ได้เตรียมอะลูมิเนียมออกไซด์พิลลาร์เบนโทไนต์ด้วยวิธีอินเทอร์คาเลชัน และนำไปเผาที่ 500°C นาน 1 ชั่วโมง จากนั้นอิมเพรกเนตด้วยโลหะคลอไรด์ ($LaCl_3$, $CeCl_3$, $NdCl_3$, $GdCl_3$, $YbCl_3$ และ $DyCl_3$) และนำไปเผาที่ 450°C นาน 4 ชั่วโมง พิสูจน์โครงสร้างของตัวเร่งปฏิกิริยาที่สังเคราะห์ได้และแร่ดินเหนียวด้วยเทคนิคการเลี้ยวเบนของรังสีเอ็กซ์ เทคนิคการดูดซับ-การคายแก๊สไนโตรเจน เทคนิคการคายออกของแอมโมเนียแบบโปรแกรมอุณหภูมิ และเครื่องอินดักทีฟคับเพิลพลาสมาออฟติกเคิลอิมิชชันสเปกโทรโฟโทมิเตอร์ นำตัวเร่งปฏิกิริยาที่สังเคราะห์ได้ไปใช้ใน (1) ปฏิกิริยาฟรีเดลคราฟต์เอซิลเลชัน (2) ปฏิกิริยาการเปลี่ยนวงอิพอกไซด์เป็นแอซีโทไนด์ และ (3) ปฏิกิริยาไอโซเมอร์ไรเซชัน เปรียบเทียบความสามารถในการเร่งปฏิกิริยาของตัวเร่งปฏิกิริยาแร่ดินเหนียวที่สังเคราะห์กับแร่ดินเหนียว ตัวเร่งปฏิกิริยาแร่ดินเหนียวที่สังเคราะห์ให้ปริมาณผลิตภัณฑ์ที่สูงกว่าแร่ดินเหนียวทุกชนิดที่ใช้ ได้พบภาวะที่เหมาะสมสำหรับปฏิกิริยาที่ใช้กรดเร่ง ปฏิกิริยาเหล่านั้นให้ปริมาณผลิตภัณฑ์และมีความเลือกจำเพาะระดับดีถึงดีมากภายใต้ภาวะที่ไม่รุนแรง

สาขาวิชา.........ปิโตรเคมี.......... ลายมือชื่อนิสิต ....ปิยรัตน์ ศรีกิตติวงศ์........
ปีการศึกษา ....2553.............. ลายมือชื่อ อ. ที่ปรึกษาวิทยานิพนธ์หลัก..........
ลายมือชื่อ อ. ที่ปรึกษาวิทยานิพนธ์ร่วม.....นิปกา สุขภิรมย์.....

4973829023: MAJOR PETROCHEMISTRY

KEYWORDS: IMPREGNATED / PILLARED CLAY / EPOXIDE

PIYARAT TRIKITTIWONG: SYNTHESIS OF METAL CHLORIDE-IMPREGNATED ALUMINIUM OXIDE-PILLARED CLAY FOR ACID CATALYZED REACTIONS. ADVISOR: ASST. PROF. WARINTHORN CHAVASIRI, Ph.D., CO-ADVISOR: NIPAKA SUKPIROM, Ph.D., 156 pp.

Iron oxide-pillared clays such as iron oxide-pillared bentonite, iron oxide-pillared hectorite and iron oxide-pillared taeniolite were synthesized by the intercalation of iron (III) chloride into clay interlayers and calcination at 300°C for 5 h. Aluminium oxide-pillared bentonite was prepared by the intercalation method and calcination at 500°C for 1 h. The impregnation with metal chloride ($LaCl_3$, $CeCl_3$, $NdCl_3$, $GdCl_3$, $YbCl_3$ and $DyCl_3$) was carried out with calcination at 450°C for 4 h. The synthesized clays and raw clays were characterized using powder X-ray diffraction, N_2 adsorption-desorption, temperature programmed desorption of ammonia and Inductively Coupled Plasma Optical Emission Spectrometry techniques. These synthesized catalysts were used for acid-catalyzed reactions (1) Friedel-Crafts acylation, (2) the conversion of epoxides to acetonides, and (3) isomerization reaction. The catalytic activity of synthesized clays was compared with raw clays. The synthesized clays provided significantly higher yield than raw clays in all types of clays. The optimized conditions for acid-catalyzed reaction were disclosed. Those reactions could smoothly be proceeded in the presence of synthesized clays to furnish the corresponding products in good to excellent yield and selectivity of products in all reactions under mild conditions.

Field of Study: ... Petrochemistry...... Student's Signature PIYARAT TRIKITTIWONG
Academic Year: ...... 2010 .... Advisor's Signature W. Chavasiri
Co-advisor's Signature Nipaka Sukpirom

ACKNOWLEDGEMENTS

The author wishes to express her deep and sincere gratitude to her advisor Assistant Professor Dr. Warinthorn Chavasiri and co-advisor Dr. Nipaka Sukpirom, for very kind assistance, generous guidance, and encouragement throughout the course of this research.

The author also wishes to express gratitude to Associate Professor Dr. Sirirat Kokpol, Associate Professor Dr. Nuanphun Chantarasiri, Associate Professor Dr. Wimonrat Trakarnpruk and Assistant Professor Dr. Jinda Yeyongchaiwat serving as the chairman and members of this thesis committee, respectively, for all of their valuable discussion and suggestion.

The author would like to gratefully thank volclay siam limited and cernic international Co., Ltd for supporting the clays, hectorite and bentonite. Moreover, the author would like to thank Natural Products Research Unit, Department of Chemistry and Program of Petrochemistry, Faculty of Science, Chulalongkorn University and Center for Petroleum, Petrochemicals, and Advance Materials for the support of chemicals and laboratory facilities and Office of the Higher Education Commission for scholarship.

The author also acknowledges Professor Dr. Shogo Shimazu, Department of Applied Chemistry and Biotechnology, Faculty of Engineering, Chiba University, Japan, for providing the knowledge and practical skill on a new methodology study for the preparation of acetonides from Li-taeniolite (synthetic clay from Japan)

The author would also like to express her special gratitude to her parents, family members for their inspiration, understanding, love, great support and encouragement throughout the entire course of study. The usefulness of this thesis, the author dedicates to my parents and all teachers who have taught me since my childhood. Finally, she would like to thank all members of Natural Products Research Unit and Material Chemistry for their assistance in her experiments and their kind suggestion. For all my frinds, thanks for their friendship, help and encouragement throughout the course of this research.

CONTENTS

Page

CHAPTER

Page

Page

III THE FRIEDEL-CRAFTS ACYLATION BY CLAY CATALSTS

Page

Page

Page

Page

V THE ISOMERIZATION OF α-PINENE BY CLAY CATALSTS ..

Page

Page

LIST OF TABLES

Table **page**

Table **page**

Table **page**

LIST OF FIGURES

Figures **page**

Figures **page**

LIST OF SCHEMES

Scheme **page**

LIST OF ABBREVIATIONS

%	percent
BET	Brunauer-Emmett-Teller
°C	degree of Celsius
Å	Angstrom unit
∑	mass balance
anh	anhydrous
β	beta
$CDCl_3$	deuterate chloroform
CH_2Cl_2	dichloromethane
$CHCl_3$	chloroform
d	doublet (NMR)
dd	doublet of doublet (NMR)
eq	equivalent
Et_2O	diethyl ether
EtOAc	ethyl acetate
Fig	figure
γ	gamma
g	gram (s)
GC	Gas chromatography
Hz	hertz
h	hour (s)
ICP-OES	Inductively coupled plasma-optical emission spectroscopy
J	coupling constant (NMR)
M	molar
m	multiplet (NMR)
m.p.	melting point
mg	milligram (s)
min	minute (s)
mL	milliliter
mm	millimeter
mmol	millimole

MW	molecular weight
nm	nanometer
NaOH	Sodium hydroxide
NMR	nuclear magnetic resonance
q	quatet (NMR)
quant	quantitative
quin	quintet (NMR)
RT	room temperature
s	singlet (NMR)
sex	sextet (NMR)
t	triplet (NMR)
TPD	Temperature Programmed Desorption
THF	tetrahydrofuran
TLC	thin layer chromatography
vol	volume
wt	weight
XRD	X-ray diffraction
α	alpha
θ	theta
δ	chemical shift
λ	wavelength
μg	microgram (s)
μM	micromolar

CHAPTER I

INTRODUCTION

Clays are widely used in catalytic reactions including those for organic synthesis, chemical evolution and environmental problems. Reactions of organic molecules on clay minerals have been investigated from various aspects. Their acidities as both Brønsted and Lewis types have been exploited for catalytic applications. Such clays are employed to catalyze a sequence of acid-catalyzed reactions. Clays and modified clays are used to catalyze various types of organic reactions such as hydrogenation, dehydrogenation, Michael addition, carbene addition and insertion, allylation, alkylation, acylation, condensation, aldol formation, imine synthesis, diazotization, synthesis of heterocycles, oxidation of alcohols, epoxidation, esterification, cyclization, rearrangement/isomerization and several more [1]. Moreover, good enantioselectivity and stereoselectivity are achieved using chiral organic compounds and chiral complexes intercalated between clay layers. These reactions are more efficient, with greater selectivity, under milder conditions, better yields, shorter reaction times, easy reusability and recovery of the catalysts [2,3]. Moreover, the work-up and purification procedures are simple as the catalyst can be filtered or centrifuged out from the reaction mixture.

Clays are the most interesting microporous and/or mesoporous materials in terms of properties and availability. Clay surfaces show modulable electrostatic fields and electric charges as results of their ionic structures [4,5]. Pillared interlayered clays (PILCs) are microporous materials obtained by exchanged cations and polyoxocations bulk in organic into the interlayer of swellable clay, leading to the intercalated clays. The intercalated clays are calcined, the polyoxocations are transformed into pillars, thus leading to the pillared solids. Inorganic oxide-pillared are formed with a permanent separation between the silicate layers. The microporous structure of pillared with high surface area and high thermal stability is obtained. Both Brønsted and Lewis acid sites are present. A variety of pore dimensions and catalytic activities are obtained by different types of pillared clays. Pillared interlayered clays are very efficient catalysts in various applications such as reduction of pollutants, synthesis of fine chemicals and acid catalyzed reactions [6,7] because of pillared interlayered clays have higher thermal stability, surface area and pore volume than those of the raw clays. Organic reactions under acid catalysis can be taken place very efficiently using pillared interlayered clays catalysts. In this thesis, the use of synthesized clays (iron oxide-pillared clays and metal chloride-impregnated aluminium oxide-pillared clays) for acid-catalyzed reaction (the conversion of epoxides to acetonides, Friedel-Crafts acylation and isomerization reaction) has been focused. There is no report on the utilization of iron oxide-pillared clays and metal chloride-impregnated aluminium oxide-pillared clays as catalysts for these reactions. This research concerns with a new and efficient procedure for the preparation of acetonides from epoxides, isomerization of α-pinene and Friedel-Crafts acylation catalyzed by iron oxide-pillared clays and metal chloride-impregnated aluminium oxide-pillared clays under mild conditions.

CHAPTER II

CLAY CATALYSTS

2.1 Clay

Clay minerals are crystalline hydrous aluminosilicates, classified as phyllosilicate, or layered silicate structures. They occur abundantly in nature. The unique properties of clays include high surface area, high sorption, reversible ion-exchange and high acidity. Their acidities as both Brønsted and Lewis types have also been exploited for catalytic applications. Many organic reactions use clays as efficient heterogeneous catalysts. For example, modified smectite clays could be used as highly selective catalyst in organic transformations and green chemistry with excellent yield, high regio- and stereoselectivity. The advantage of clay catalysts over homogeneous catalysts can be clearly seen at the work up step by simple filtration. In addition, it is easy to recover and reusable the heterogeneous catalysts, hence a large reduction in the generation of wasteful products [8].

2.2 The structure of clay minerals

Clay minerals posses a layered structure, and their suspension in aqueous solution contains particles with the average diameter of about 2 µm [9]. The layered units are constructed from the combination of two basic types of layers, a sheet of edge-linked octahedra and a sheet of corner linked tetrahedra. Phyllosilicate minerals have layered structures composing of aluminum octahedral and silica tetrahedral sheets. The tetrahedral and octahedral sheets are held together by sharing apical oxygen atoms [10].

2.2.1 Basic units

2.2.1.1 Tetrahedral sheets

In tetrahedral sheet consists of tetrahedral units. The dominant cation is Si^{4+} (SiO_2), but frequently substituted by Al^{3+} and occasionally by Fe^{3+}. This sheet extends infinitely in two dimensions by three corners of each tetrahedral share oxygen atoms with three other tetrahedral units to form hexagonal network (Fig 2.1).

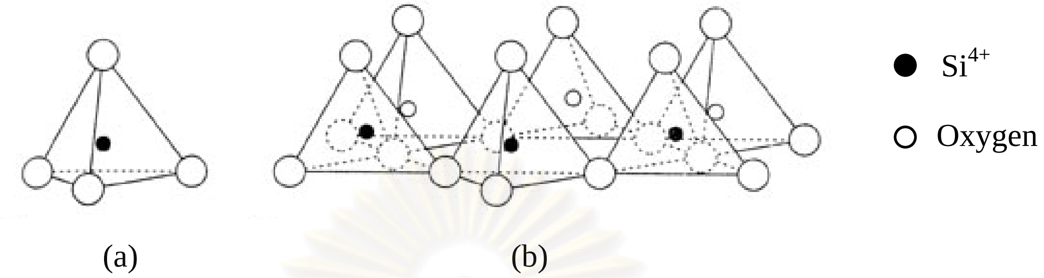

Figure 2.1 A single tetrahedral silica (a), and a sheet structure of silica tetrahedral arranged in a hexagonal network (b).

2.2.1.2 Octahedral sheets

The octahedral sheet is constructed from the other octahedral units similar to the tetrahedral sheet. The dominant cation is Al^{3+}, but substituted frequently by Mg^{2+} and occasionally by Fe^{2+} and Fe^{3+}. Connection of the neighboring oxygen ion forms a sheet of edge-linked octahedral as hexagonal network (Fig 2.2), extending infinitely in two dimensions (b).

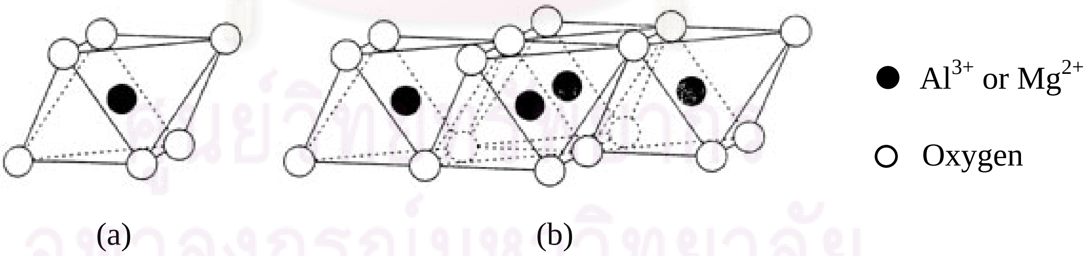

Figure 2.2 A single octahedral unit (a) and a sheet structure of octahedral unit arranged in a hexagonal network (b).

2.2.2 The combination of basic sheets

The combinations of basic sheets of clays could be divided into 2 categories:

2.2.2.1 The 1:1 layered type (T:O)

This combination of one tetrahedral sheet (T) and one octahedral sheet (O) is one unit of clay layer. The oxygen atoms at the edge of tetrahedral sheet are pointed to the octahedral sheet and held together with sharing those atoms (Fig 2.3).

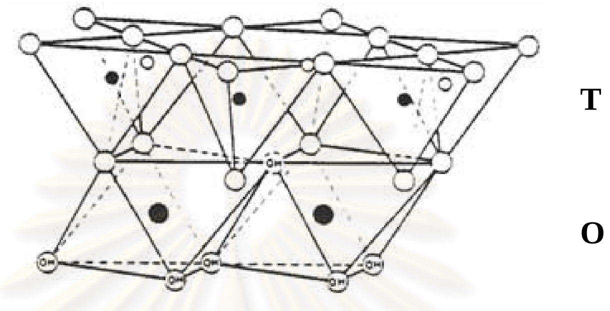

Figure 2.3 Structure of 1:1 layered type (T = tetrahedral sheet, O = octahedral sheet).

Kaolinite is common in 1:1 layered type of clay and has the chemical formula $Al_2Si_2O_5(OH)_4$. It consists of an octahedrally coordinated layer of aluminum ions and a layer of tetrahedrally coordinated silicon atoms in 1:1 structure. Kaolinite layers are held together by Van der Waals forces. The thickness of each clay layer is about 7 Å, which gives rise to a corresponding characteristic X-ray diffraction peak of about 7 Å.

2.2.2.2 The 2:1 layered type (T:O:T)

A 2:1 layer of clay minerals is constituted of two silica tetrahedral layers with one alumina octahedral layer. This combination makes a tetrahedral-octahedral-tetrahedral (T:O:T) sandwich. The assembly makes a T:O:T sandwich layers such as smectite clay minerals. Bentonite, montmorilonite and hectorite are the common smectite clay minerals. The simplest members of this group are shown in Fig 2.4.

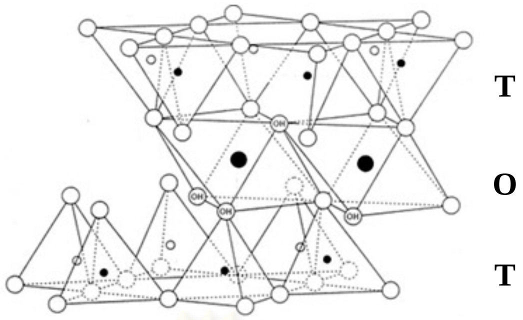

Figure 2.4 Structure of 2:1 layered type (T = Tetrahedral sheet, O = Octahedral sheet).

2.3 Smectite clay minerals

The structures of smectite clays are derived from the mineral talc and pyrophyrite, which consist of a stacking of silica tetrahedral sheet ($Al_4Si_8O_{20}(OH)_4$) and alumina octahedral sheet ($Mg_6Si_8O_{20}(OH)_4$)and, respectively. A layer of smectite clay minerals is constituted of two silica tetrahedral layers with one alumina octahedral layer. Substitution of cation (for example Al^{3+} or occasionally Fe^{3+} substitutes for Si^{4+} in tetrahedral sheets and Mg^{2+} or occasionally Mn^{2+}, Fe^{2+} substitutes for Al^{3+} in octahedral sheets) either in the tetrahedral or octahedral sheet results in the formation of negative layered charge, which is balanced by additional cations located between the interlayer of clay [11]. The structure of smectite clay is shown in Fig 2.5.

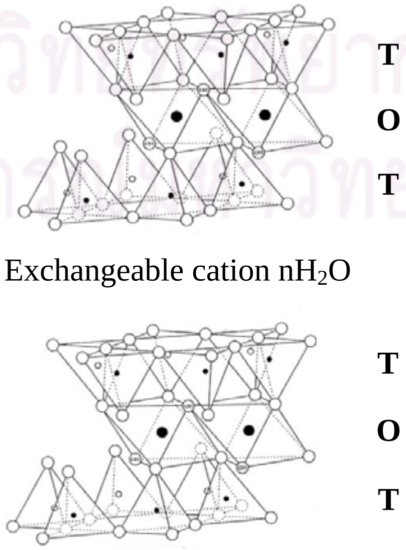

Figure 2.5 Structure of smectite clay.

The important ability of the smectite clay is the adsorption of a large amount of water molecules between the layers, causing the volume of the minerals increase. Thus, the smectites are expanding clays with the basal spacing of 10 to 20 Å. The common smectite is montmorillonite with an ideal formula of $(\frac{1}{2}Ca,Na)(Al,Mg,Fe)_4(Si,Al)_8O_{20}(OH)_4.nH_2O$. Smectite clays normally occur as extremely small crystals (less than 1 μm). The repeating distance between the clay-layer is called the basal spacing, d_{001}. This value is easily identified by X-ray diffraction technique.

2.3.1 Bentonite clay

Montmorillonite is the main constituent of bentonite (typically 80-90 wt%). The remaining impurities in bentonite clay are generally found as quartz, feldspar, crystobalite, and humic acids. Montmorillonite has an ideal formula of $(Si_8)(Al_{4-x}Mg_x)O_{20}(OH)_4A_x.nH_2O$ (where A is a monovalent or divalent cation), which Mg/Al substitution in the octahedral sheet gives the clay layer negative charged [12].

2.3.2 Hectorite clay

The octahedral sheet of hectorite contains Mg^{2+} which is different from bentonite. Hectorite has Li/Mg substitution in the octahedral sheet, resulting to negatively charged layers. The general chemical formula of hectorite is $(Si_8)(Mg_{6-x}Li_x)O_{20}(OH)_4A_x.nH_2O$ (where A is a monovalent or divalent cation) [12].

2.3.3 Taeniolite clay

The general chemical formula of taeniolite is $(Si_8)(Mg_{6-x}Li_x)O_{20}(F)_4A_x.nH_2O$, (where A is a monovalent or divalent cation). The structure of taeniolite contains F^- which is different from bentonite and has the excess of the bivalent ions (Ca^{2+}, Mg^{2+}, Ba^{2+}, Be^{2+} and Pb^{2+} impurities). The crystal structure of taeniolite is a pack consisting of three layers of close cubic packing of F^- anion and O^{2-} anions [13].

2.4 Properties of clay

2.4.1 Ion exchange

Clay minerals have the ability to adsorb and exchange cations from external solution. In general, the ideal neutral structure is disrupted by introduction of charged imbalance into the clay sheets. The two main causes of charged imbalance are (i) isomorphous substitution of cations by lower valent ions, such as the substitution of aluminum cation for silicon in the tetrahedral layer, magnesium for aluminum and lithium for magnesium cations in the octahedral layer, and (ii) crystal defects. Leading to, the clay layers have an overall negative charge which is balanced by adsorption of metal cations into the interlayer of the clay minerals. These balance cations can be readily replaced by other cations in aqueous solution. The ion exchange is great and important property of clay minerals. In the application of clay mineralogy, it is important because the nature of the exchangeable ion may influence substantially the physical properties of the material [8].

In swellable clay minerals such as smectites clay, the cations in interlayer of clays can be exchanged with other cations from external aqueous solutions. When a solution of a metal cation is used to exchange the interlayer cations of clay, it was observed that the smaller the size and the higher the charge of the exchange cations, the more powerful that cation at replacing the interlayer exchangeable cations. Similarly the ease of replacement of interlayer cations follows the reverse trend. The following series can be constructed:

$$\mathbf{M^{+} << M^{2+} << H_2O^{+} \approx K^{+} \approx NH_4^{+} < M^{3+} < M^{4+}}$$

$$\xrightarrow{\hspace{12em}}$$

increasing exchange power

(decreasing ease of exchange)

Scheme 2.1 The exchange properties of cations with clays.

The cation exchange capacity is called CEC. CEC is often measured by uptake and release of ammonium ions from 1 M ammonium acetate solution, although other cations are sometimes used in place of NH_4^+. CEC is usually measured in milliequivalents per 100 gram of dried clay. Smectites clays have relatively high concentration of exchangeable interlayer cations therefore they have the high cation exchange capacities around 50-270 meq/100 g [14].

2.4.2 Swelling

Many clay minerals have also the swelling ability. Clay minerals can adsorb molecule of water into the interlayer of clay, which cause the clay swelling. For efficient swelling, the released energy must be sufficient to overcome the attractive forces between the adjacent layers, such as lattice energy and hydrogen bonding from layer solvation. In aqueous solution, hydroxyl groups on octahedral layers of clays forms strong hydrogen bonds with water [14]. The interlayer separations of extent of clay swelling can be measured by using power X-ray diffraction.

2.4.3 Acidity of clays

Acidity of clays (Brønsted and Lewis acidity) is an important property of clays. Clay catalysts are widely used as catalysts in organic reaction. Their acidic properties and catalytic activity depend on the exchanged cations. Clay minerals have both Brønsted and Lewis acidity. The interlayer cations into the interlayer of the clays lead to the acidity. Some of these cations (*e.g.* Al^{3+}) dissociate their coordinated water molecule to produce acidic proton (Brønsted acidity). Being coordinated between an organic compound to cation, the cation is an electron pair acceptor and can act as Lewis acid catalyst [8].

2.5 Intercalation

Intercalation is the insertion of molecules or cations into the interlayer of clay and consequently the layered structure still remains. Intercalation compound is proven by the XRD pattern, which must unambiguously show an increase in the spacing between adjacent layers, *i.e.* an increase in the basal spacing [15].

2.6 Pillaring

Pillaring is the process using the intercalation procedure of pillaring agents into interlayer space of clays by cation exchange, resulting to a pillared compound or a pillared layered solid, which are high thermal stability and stable microporous and/or mesoporous materials with the preservation of a parent layer structure [15].

2.7 Pillaring agent

The pillaring agents are any guest compounds which could be intercalated between interlayer of clays [15].

2.8 Pillared clay

Pillared interlayered clays (PILCs) are microporous materials obtained by exchanged cations and polyoxocations bulk in organic molecule into the interlayer of swellable clay, leading to the intercalated clays. The intercalated clays are calcined, the polyoxocations are transformed into pillars, thus leading to the pillared solids. Inorganic oxide-pillared are formed with a permanent separation between the silicate layers. The microporous structure of pillared with high surface area and high thermal stability is obtained. Both Lewis and Brønsted acid sites are present. The nature of clay (montmorillonite, hectorite, taeniolite *etc*) and the nature of intercalating cations species (polycations based on Si^{4+}, Zr^{4+}, Ti^{4+}, Al^{3+}, Cr^{3+}, Fe^{3+} or Ca^{2+}, *etc*) have possibility affected on the properties of the pillared solids [16]. A variety of pore dimensions and catalytic activities are obtained by different types of pillared clays. Pillared interlayered clays are very efficient catalysts in various applications such as reduction of pollutants, synthesis of fine chemicals and acid catalyzed reactions because of pillared interlayered clays have higher surface area, thermal stability and pore volume than those of the raw clays. Organic reactions under acid catalysis could be taken place very efficiently using pillared interlayered clays catalysts. Scheme 2.2 shows the example of pillared clay compounds [17].

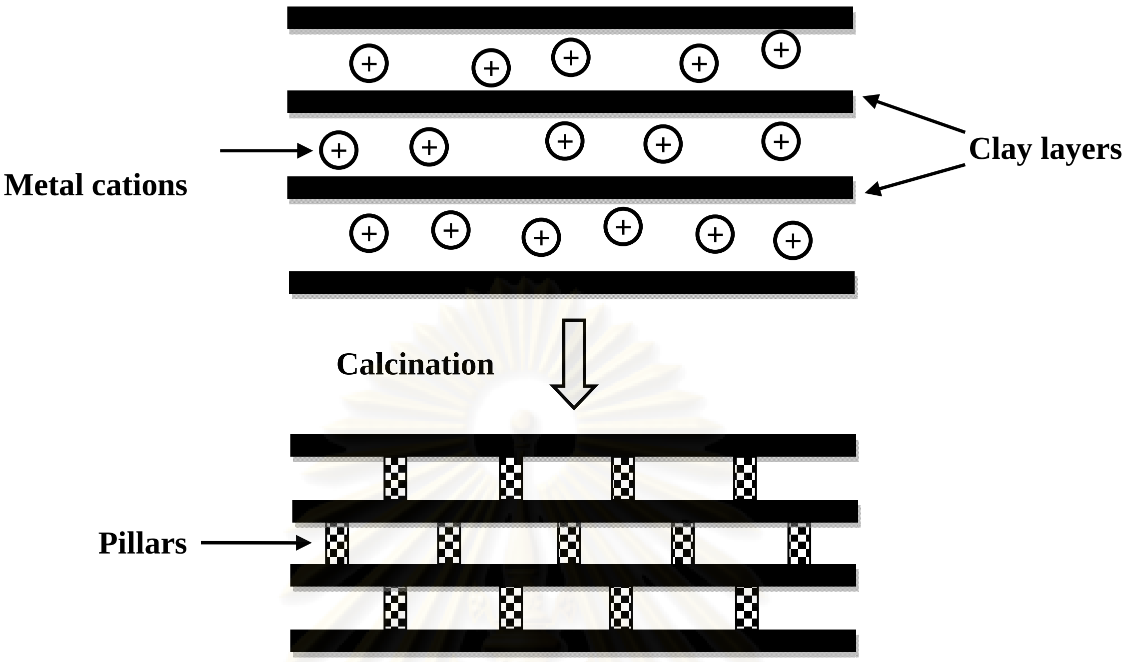

Scheme 2.2 Diagram for the preparation of pillared clay compounds (cross section).

2.9 Impregnation

Impregnation is the method for making a heterogeneous catalyst. Usually, a support or carrier is a porous material will be in contacted with a solution of compounds that little group are held onto the support. The impregnation method requires less equipment since the forming steps, filtering and washing are needless. Scheme 2.3 shows the example of impregnated pillared clay [18].

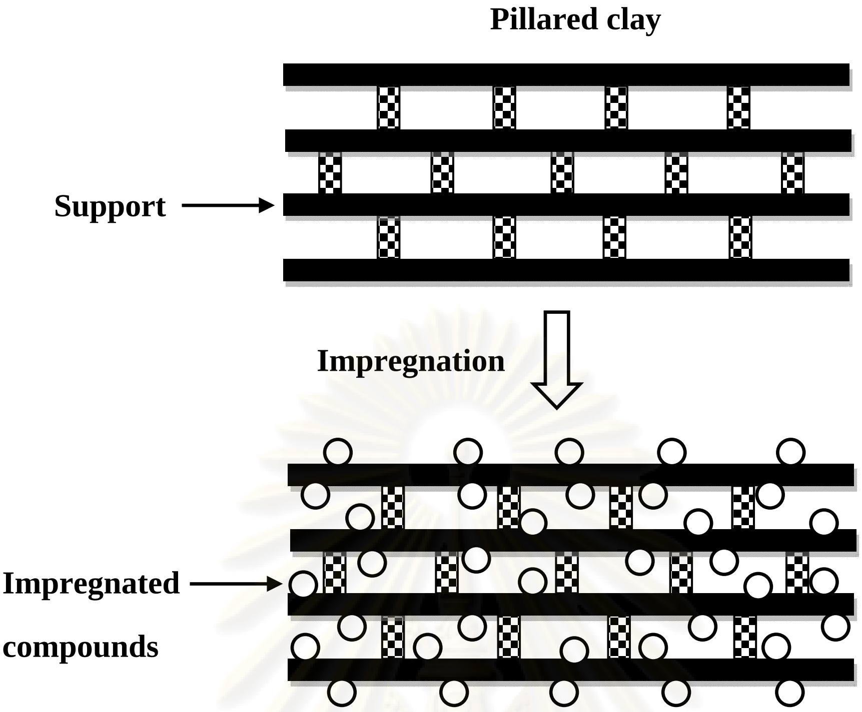

Scheme 2.3 Diagram for the preparation of impregnated pillared clay (cross section).

2.10 Characterization of clays and clay catalysts

2.10.1 Powder X-ray diffraction (XRD)

X-ray diffraction (XRD) is an important instrumental technique for characterization and identification of crystalline materials. A collimated beam of nearly monochromatic is a type of X-rays beam in this technique. X-rays beam is directed onto the flat surface of a thin layer of ground materials causing the diffracted X-ray to specific angles. The additional information from XRD data can be analyzed for the degree of crystallinity of the minerals present, determined the proportion of the different minerals present, the structural state of the minerals and the degree of hydration for minerals [10]. Fig 2.6 shows a monochromatic beam of X-ray incident on the surface of crystal at an angle θ. The scattered intensity can be measured as a function of scattering angle 2θ. An X-ray diffraction measurement the angle of incidence and detection was scanned. The X-ray diffraction pattern which is the characteristic for the sample material was obtained by plotting of the intensity of detected X-rays as a function of angle. The resulting XRD pattern efficiently determines the different phases present in the sample.

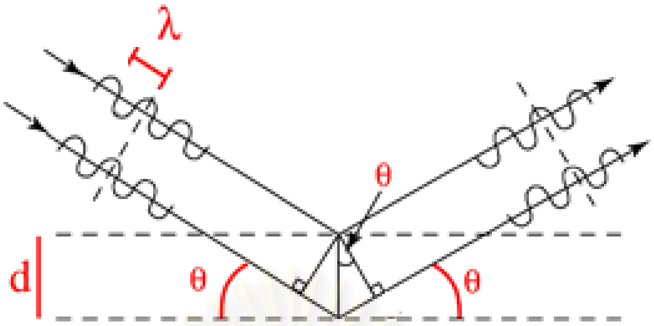

Figure 2.6 Diffraction of X-ray by regular planes of atoms.

Using this method, Bragg's law is able to determine the interplanar spacing of the samples, from diffraction peak according to Bragg angle.

$$n\lambda = 2 d \sin\theta$$

Where n = an integer of order of the diffracted beam
λ = wavelength of the X-ray
d = a distance between adjacent planes of atoms (*d*-spacing)
θ = an angle between the incident beam and the scattering planes

2.10.2 Nitrogen adsorption-desorption isotherm

The N_2 adsorption method is an important analysis technique and widely used to measurement the physical properties of porous materials such as the specific surface area, pore diameter, pore size distribution and pore volume of a variety of different solid materials. An adsorption isotherm can be described the adsorption of gas by porous materials. IUPAC classifying gas adsorption isotherms and pore sized have been suggested that indicate the relationship between adsorption and porosity. The types of adsorption isotherms are shown in Fig 2.7. The adsorption isotherms are divided the six types. The six types of isotherms are microporous materials [type I], nonporous materials or macroporous materials [types II, III, and VI] and mesoporous materials [types IV and V] [19].

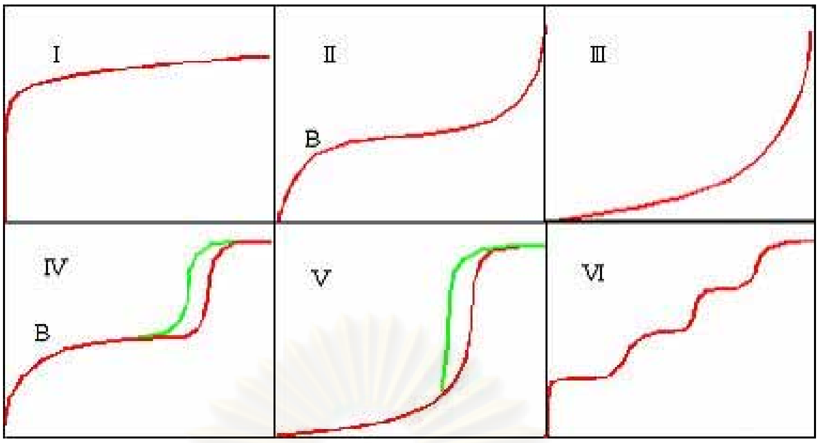

Figure 2.7 The types of adsorption isotherms.

Adsorption isotherms are described as shown in Table 2.1 based on the strength of the interaction between the sample surface and gas adsorbate, and the existence or absence of pores.

Table 2.1 Features of adsorption isotherms

Type	**Features**	
	Interaction between sample surface and gas adsorbate	**Porosity**
I	Relatively strong	Micropores
II	Relatively strong	Nonporous
III	Weak	Nonporous
IV	Relatively strong	Mesopore
V	Weak	Micropores or Mesopore
VI	Relatively strong sample surface has an even distribution of energy	Nonporous

The IUPAC classification of pore types is shown in Table 2.2. The use of nitrogen adsorption/desorption isotherm can be measured the pore size distribution. The classification of pore types according to their sizes are divided the three types: (1)

the macropores have pores diameter about 50 nm, (2) the mesopores have pore diameter between 2 nm and 50 nm and (3) the micropores have pores diameter not exceeding about 2 nm [20].

Table 2.2 IUPAC classification of pores

Pore Type	Pore diameter (nm)
Micropore	Up to 2
Mesopore	2 to 50
Macropore	50 to up

The most widely used technique to measure the surface area is BET method (Brunauer, Emmett and Teller, (BET)). Thus, analogously to the Langmuir isotherm obtains the BET isotherm:

$$\frac{1}{W[(P_0/P) - 1]} = \frac{1}{W_m C} + \frac{C-1}{W_m C}\left(\frac{P}{P_0}\right)$$

Where W = weight of nitrogen adsorbed at a given P/P_0
W_m = weight of gas to give monolayer coverage
C = a constants that is related to the heat of adsorption.
P = the equilibrium pressure
P_0 = the saturation pressure

The quantity of nitrogen adsorbed was obtained by a required of linear relationship between P/P_0 and $1/W[(P/P_0)-1]$. The quantity of nitrogen adsorbed in the monolayer of the slope and intercept of isotherm was used to calculate the surface area. The intercept was taken as zero or a small positive value for a single point method. The surface area could be calculated from the slope of BET plot [20].

2.10.3 Temperature programmed desorption (TPD) of ammonia

Temperature programmed desorption of ammonia is the most important and widely used technique to measure the acidic properties (weak acid sites and strong acid sites) of mesoporous materials. In various solid acid catalysts, the equilibrium between the gaseous and adsorbed ammonia can control desorption of ammonia. The acid-site concentration can be given by the amount of ammonia desorbing above some characteristic temperature. The heats of adsorption can be calculated by the peak desorption temperature. The acidity of pillared interlayered clays (iron oxide-pillared clays) samples has been measured by adsorption-desorption of ammonia. It is well known that desorption temperature of the ammonia molecule can be related to the strength of acidity of the materials tested. The bond formed between the acid site and the ammonia is broken by an energy supply. Thus, the maximum temperature in the NH_3 desorption process is a qualitative indication of the strength of the acid sites. It has been reported that in the NH_3-TPD one or more broad peaks of desorption at 150-400°C can be observed [21].

Principle of the measurement

TPD is the method to measure the status of physical adsorption and chemisorptions. It can be obtained by measuring desorption of the decomposition of adsorption molecules from the surface while continually heated. TPD can determine the number of desorption peaks (type of adsorption active sites) from the spectrum of desorbed molecules, desorption temperature (activation energy of desorption), and volume of desorption (number of adsorption active sites).

Method of the measurement

Adsorption of probe molecules to the sample is generally done by pulse injection method, volumetric method under the vacuum, or flow method. For the probe molecules, NH_3 can be used to measure the volume and distribution of acidic points. In order to measure basic points, CO_2 can be used. Also, chemisorptions gases (CO, H_2, hydrocarbon, *etc*.) can be used to obtain the information about the characteristics of adsorption during the reaction.

Although the condition of measurement varies the ambient pressure, desorption measurement can be basically done by heating under the carrier gas flow. Desorbed gas can be detected by Thermal Conductivity Detector (TCD) or mass analyzer (Q-mass) [21].

2.10.4 Inductively coupled plasma-optical emission spectroscopy (ICP-OES)

The ICP is a type of plasma source. The energy of plasma source is supplied by electromagnetic induction as shown in Fig 2.8. The plasma can be created by the argon gas. The sample is nebulized within the nebulizer. The nebulizer is introduced directly inside the plasma flame and break up into their several atoms. The plasma torch is composed of a coil of the RF (radio frequency) generator (essentially 1-5 kW at 27 MHz) and three concentric quartz tubes. An extreme magnetic field from the radio frequency generator is turned on when the plasma torch is turned on. The plasma can be created by the argon gas which it flowing through is ignited (a Tesla unit) and ionized in those fields. The stable high temperature plasma can be generated by the results of the inelastic collisions of create ions, the argon atoms and free electrons [22].

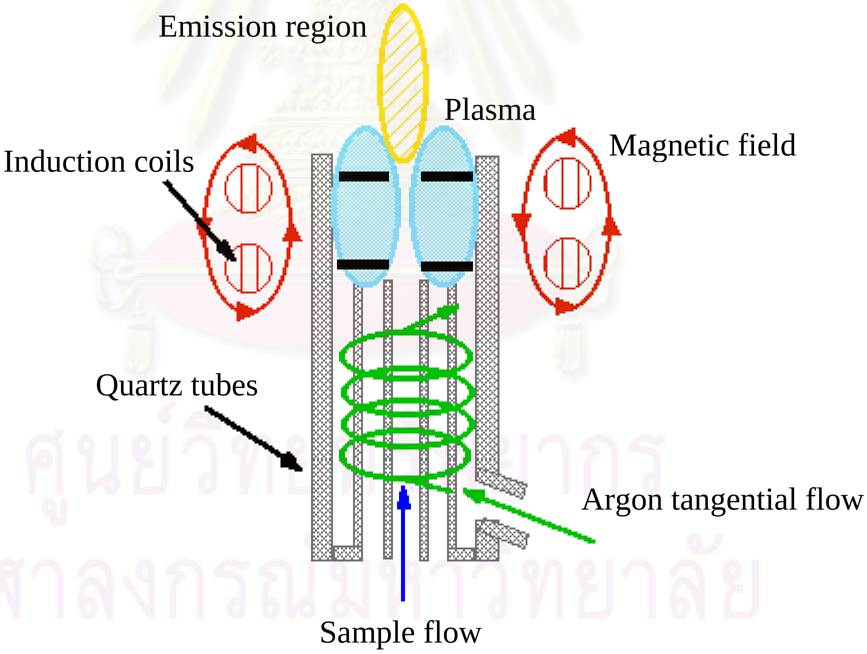

Figure 2.8 A typical plasma source [23].

ICP-OES is an emission spectroscopy (emission spectrophotometric) technique to select a single wavelength specific light for elemental analysis. ICP-OES spectroscopy used an ICP to produce excited atoms. When electrons of element are excited, they adsorb energy then when they return to ground state, each electrons of element will emit electromagnetic radiation energy at multiple wavelength characteristic of a particular element. The concentration of the element within the sample is obtained from the intensity of this electromagnetic radiation emission. Therefore the analyst could compare quantify concentration and composition of the element of the sample with reference standard by determining their intensities and determining emitted electromagnetic radiation energy wavelengths of the sample.

2.11 Literature reviews on clay catalysts

Many organic reactions use clays as efficient heterogeneous catalysts. The acidities as both Brønsted and Lewis types of clay catalysts have also been exploited for catalytic applications. Clay catalysts are gaining importance for organic reactions due to its advantages such as better yield and selectivity, easy work-up (separation of the catalyst simply by filtration or centrifugation), easy reusability and recovery of the catalysts, mild reaction conditions and shorter reaction times. The variety of reactions were successfully performed on clay catalysts including substitution, elimination, addition, oxidation-reduction, rearrangement, Diels-Alder reaction, ring opening reaction, esterification, dehydration, Friedal-Crafts reactions, condensation, and isomerization [14,24].

Reaction of alcohols with ketones and aldehydes

The reaction of alcohols to carbonyl compounds catalyzed by montmorillonite clays can be easily carried out. The montmorillonite K10 clay could be catalyzed the reaction of homoallyl alcohols with aldehydes to lead hemiacetal intermediates. The Prins-type cyclization products are obtained by intramolecular transformation of hemiacetal intermediates [24].

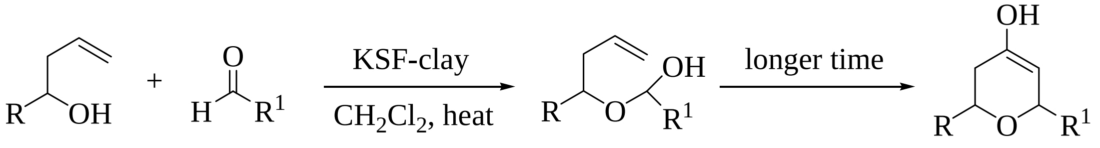

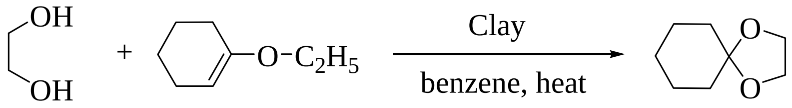

Oxidation-reduction reaction

The both synthesized Claycop and Clayfen K-10 clay supported iron(III) nitrate or copper(II) nitrate reagent were oxidizing agents for thio-compounds and alcohols [24].

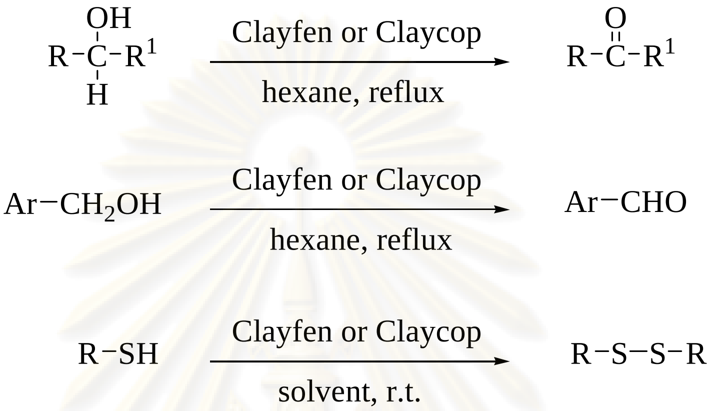

$$R\text{-}\overset{OH}{\underset{H}{C}}\text{-}R^1 \xrightarrow[\text{hexane, reflux}]{\text{Clayfen or Claycop}} R\text{-}\overset{O}{\overset{\|}{C}}\text{-}R^1$$

$$Ar{-}CH_2OH \xrightarrow[\text{hexane, reflux}]{\text{Clayfen or Claycop}} Ar{-}CHO$$

$$R{-}SH \xrightarrow[\text{solvent, r.t.}]{\text{Clayfen or Claycop}} R{-}S{-}S{-}R$$

Formylation of phenols

Phenols could be formylated by the reaction of phenol with formaldehyde using KSF clay catalyst and Et_3N in tolune at 100°C for 4 h [24].

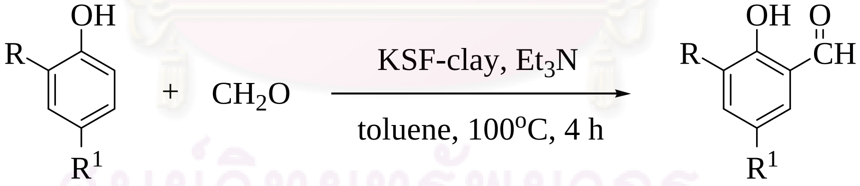

Ether formation

The reaction of olefin and alcohol using Al^{3+}-exchanged montmorillonite as a catalyst in *n*-hexane to prepare unsymmetrical ethers were carried out. In the case of primary alcohols, the yields of product were good but secondary alcohols gave low yields. The tertiary alcohols did not yield to ethers [14].

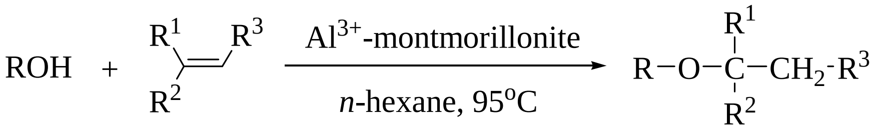

Addition reaction

The reaction of thiol and hydrogen sulfide with alkenes catalyzed by Al^{3+}-exchanged montmorillonite affording the corresponding dialkyl sulfides in good to high yields [14].

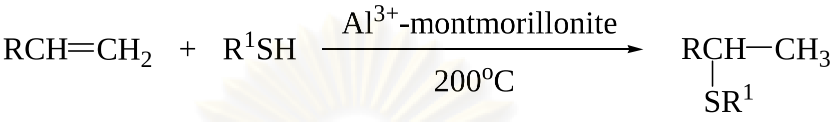

$$RCH{=}CH_2 + R^1SH \xrightarrow[200^oC]{Al^{3+}\text{-montmorillonite}} \underset{SR^1}{RCH}{-}CH_3$$

A microwave assisted montmorillonite K10 clay could be catalyzed the addition of aniline derivatives to cinnamaldehyde *via* Michael addition as the first step of a domino process involving cyclization in the second step followed by dehydration and oxidation in the final step to deliver quinolines. Reactions were completed and provided good to high yields and selectivities in short period of times. The reaction is carried out under solvent-free condition and with the assistance of microwave radiation [25].

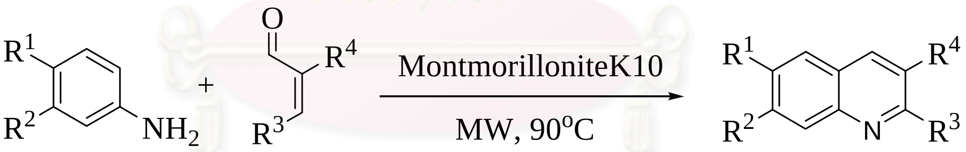

Condensation reaction

The chiral diphenylbis(oxazoline)-Cu^{2+} complex immobilized on laponite clay has proved to be an effective catalyst in bringing about Mukaiyama aldol reaction between 2-(trimethylsilyloxy)furan and α-ketoesters to give the aldols *syn* and *anti* isomers with the *anti*-isomers as major products [26].

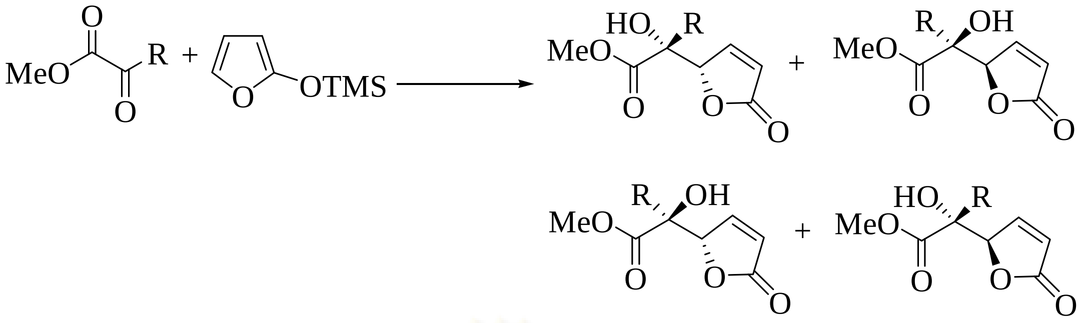

β-carbolines were efficiently prepared by the condensation of tryptamines and aromatic aldehydes dispersed in combined 10% Pd/C/K10 catalyst under microwave irradiation. The result showed that the condensation of tryptamines and aromatic aldehydes dispersed in combined 10% Pd/C/K10 catalyst under microwave irradiation method at 130°C to furnish the corresponding β-carbolines in good to excellent yields and 100% selectivity [27].

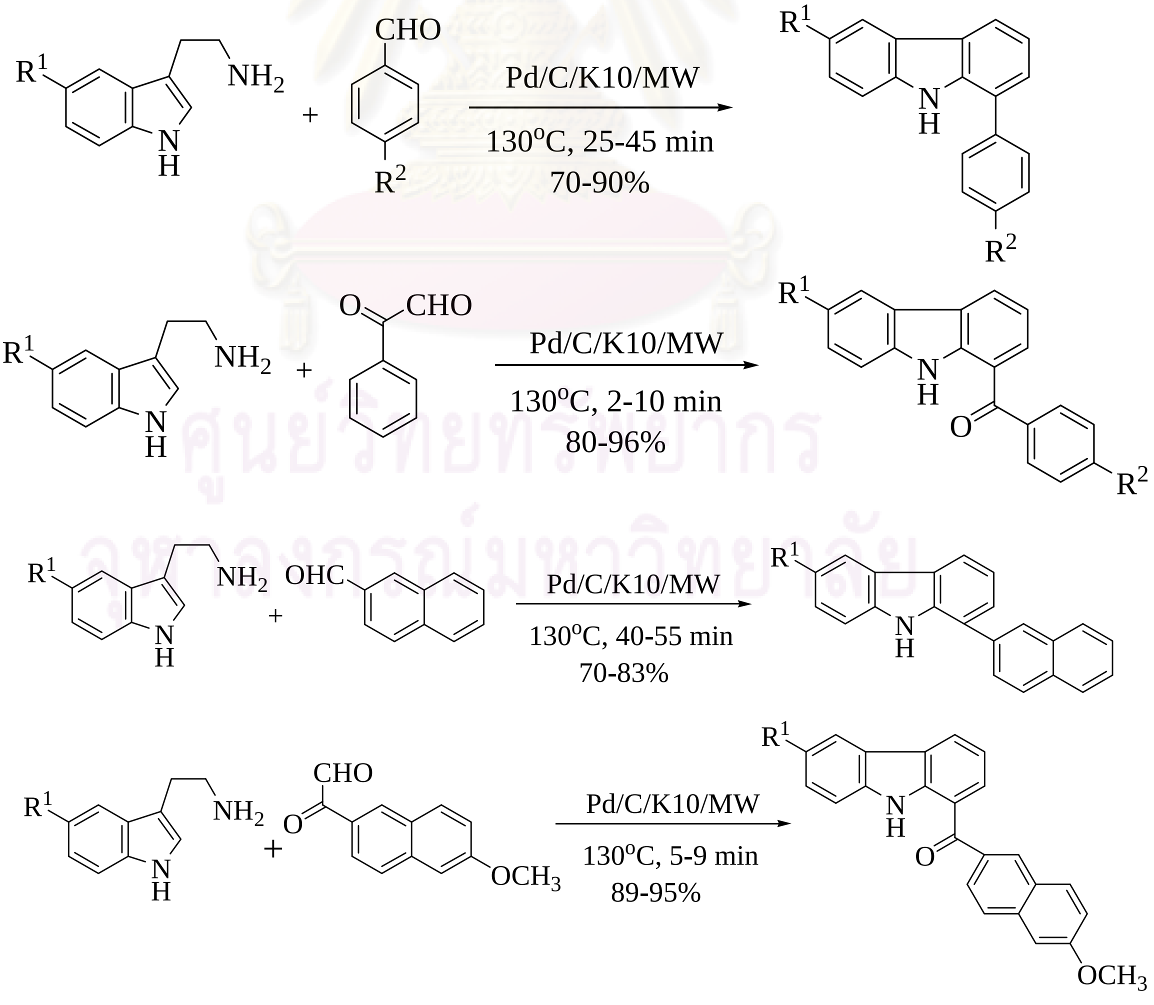

Diels-Alder reaction

The Diels-Alder reaction was carried out by using Fe^{3+}-exchanged montmorillonite and Cr^{3+}-exchanged montmorillonite clay as catalysts under very mild conditions. The study of endo:exo ratio was important and useful for this reaction. It was observed that the ratio of endo to exo could be operated by varying the exchanged metal cations [24].

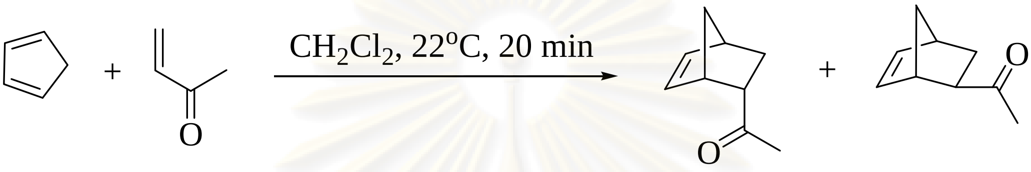

Fe^{3+}-montmorillonite K10	9	:	1 (97% yield)
Cr^{3+}-vermiculite	2.5	:	1 (47% yield)

Montmorillonite K10, filtrol-24, pyrophillite and bentonite clays were used as catalysts to bring about Diels-Alder addition of 1,4-naphthoquinone and *N*-phenyl maleimide. Filtrol-24 performed the best under this condition. Further, when montmorillonite K10 and bentonite were modified by impregnating with $AlCl_3$, $ZnCl_2$ and $FeCl_3$, the resulting modified K10 and bentonite catalysts performed as well as filtrol-24 [28].

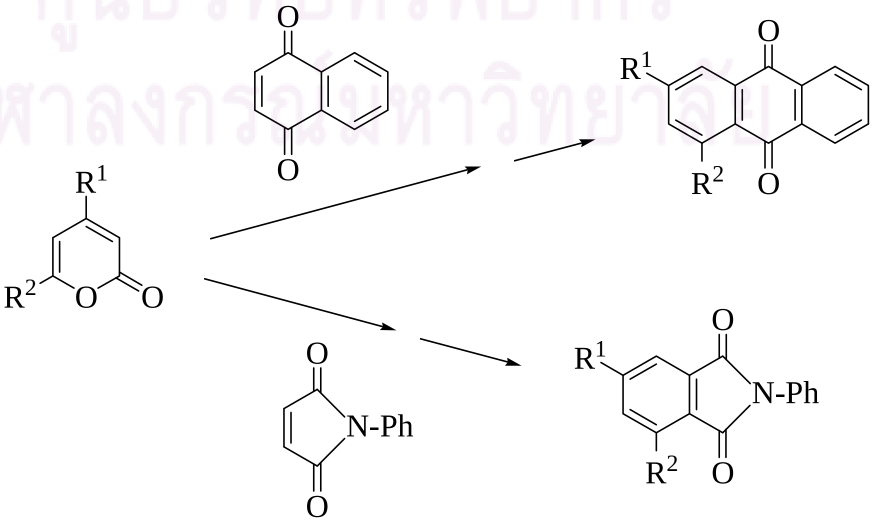

Esterification

The reaction of olefinic compound and carboxylic acid affording the corresponding ester product was performed in the presence of acid-activated montmorillonite clay.

$$H_3C-COOH + H_2C=CH_2 \xrightarrow{H^+\text{-montmorillonite}} H_3C-COOCH_2CH_3$$

The tosyl or sulfonyl esters could be prepared in high yields by refluxing alcohols with sulfonic acids in dichloromethane using Fe^{3+}-exchanged montmorillonite as a catalyst [24].

$$R-OH + R^1-SO_3H \xrightarrow[CH_2Cl_2,\ \text{reflux}]{\text{Montmorillonite}} R-O-SO_2R^1 + H_2O$$

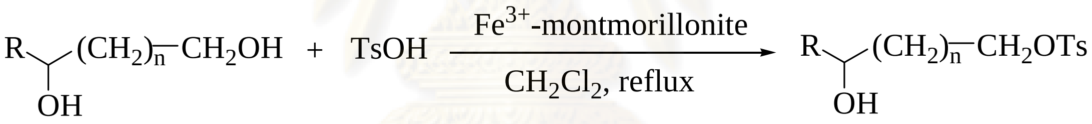

$$R-CH(OH)-(CH_2)_n-CH_2OH + TsOH \xrightarrow[CH_2Cl_2,\ \text{reflux}]{Fe^{3+}\text{-montmorillonite}} R-CH(OH)-(CH_2)_n-CH_2OTs$$

The esterification of methyl alcohol with mandelic acid was catalyzed by montmorillonite K10 supported dodecatungstophosphoric acid (DTP/K10) and its cesium salt (Cs-DTP/K10) affording the corresponding methyl mandelate in high yield. Methyl mandelate was used in artificial flavoring and perfumes industries [29].

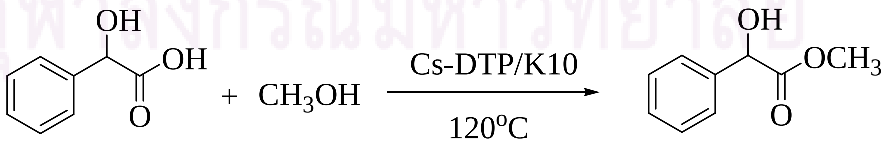

Hydroxybenzophenones is used in pharmaceutical industries and precursor for fine chemical. The esterification of benzoic acid with phenol, followed by the Fries rearrangement affording the corresponding hydroxybenzophenones in a one-pot synthesis were carried out by using montmorillonite K10 supported cesium dodecatungstophosphoric acid as a catalyst under solvent-free conditions [30].

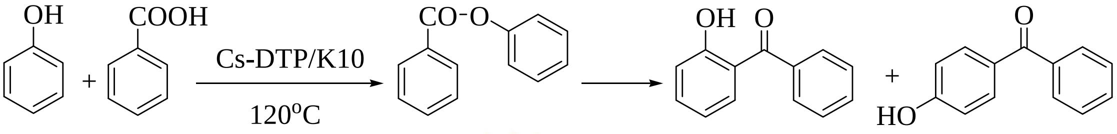

Isomerization reaction

The isomerization of allyl alcohols of the pinene series and their epoxides using askanite-bentonite clay (calcined at 110°C) as a catalyst in intra- and intermolecular reactions were studied. Treatment of (+)-*trans*-pinocarveol with askanite-bentonite at room temperature led to the formation of isomeric allyl alcohol (-)-myrtenol (**1**), and the dimeric ether (**2**), selectively. In contrast, the (+)-*trans*-pinocarveol gives Wagner-Meerwein rearrangement product (**3**), under homogeny eous acidic conditions, due to protonation of the exocyclic double bond. On the other hand, when (-)-myrtenol was kept on clay at room temperature for 1 h, (+)-*trans*-pinocarveol and the rearranged products **(4**) and (**5**) were obtained [31].

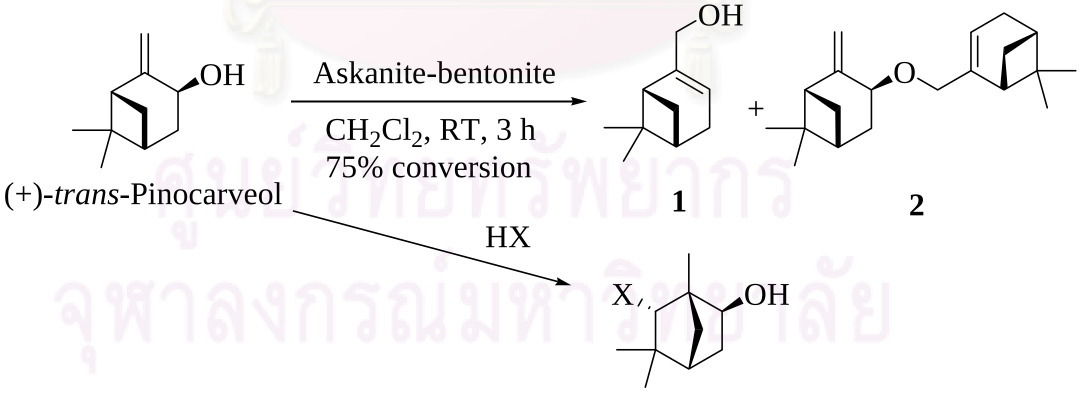

1 **2**

3

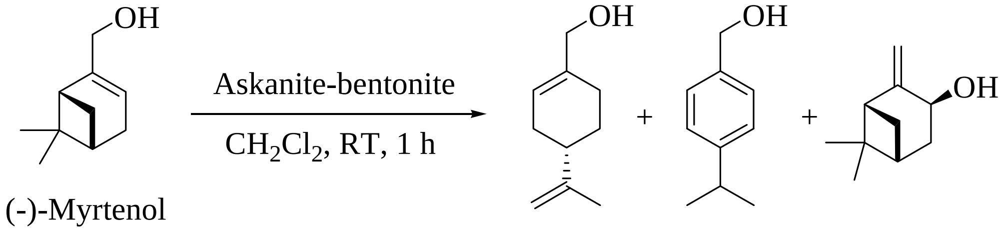

1 **4** **5**

A similar treatment of the pinocarpeol epoxide (**6**) and myrtenol epoxide (**7**) of these two allyl alcohols on askanite-bentonite clay yielded slightly differing results, though the two epoxides were visualized to give the same intermediate (**A**). The pinocarpeol epoxide yielded, among other unidentified products, the α,β-unsaturated ketone (**8**) and the monocyclic keto alcohol (**9**). Myrtenol epoxide produced the aromatic alcohol 4-isopropylbenzyl alcohol (**5**) and the hydroxy aldehyde (**9**) [31].

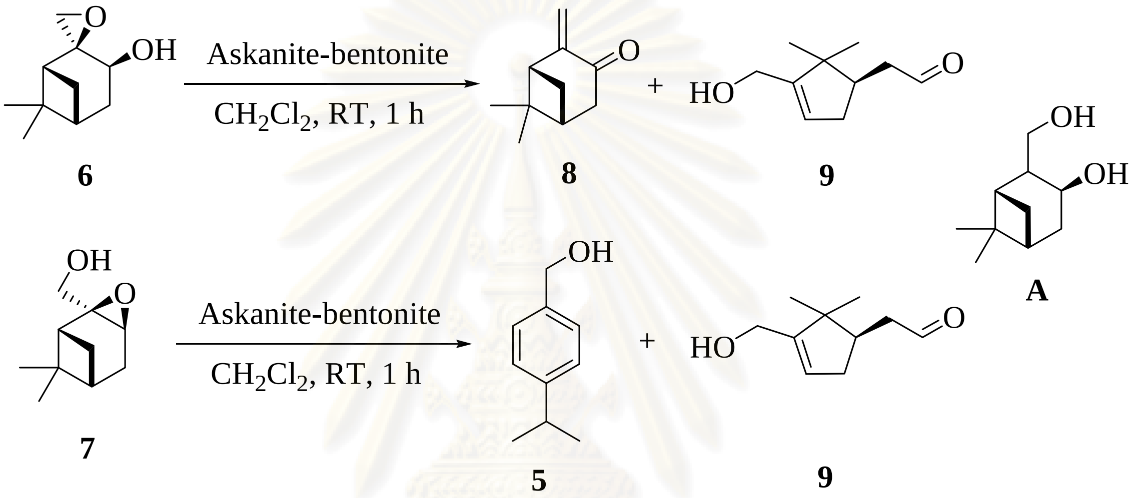

Prenylated phenolic compounds, such as prenylated xanthones have been synthesized hydroxyxanthones (**10a-c**) with prenyl bromide in chloroform solution catalyzed by montmorillonite K10 clay and montmorillonite K10 clay under microwave irradiation. The reaction of prenyl bromide with **10a** took just 20 minutes to give about 86% yield of the final dihydropyran product. The other two hydroxyxanthones (**10b**) and (**10c**) gave mixtures of products because two *ortho*-positions are available for cyclization in the prenyl ether intermediates [32].

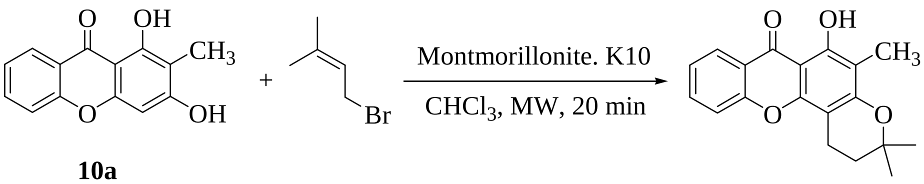

10a

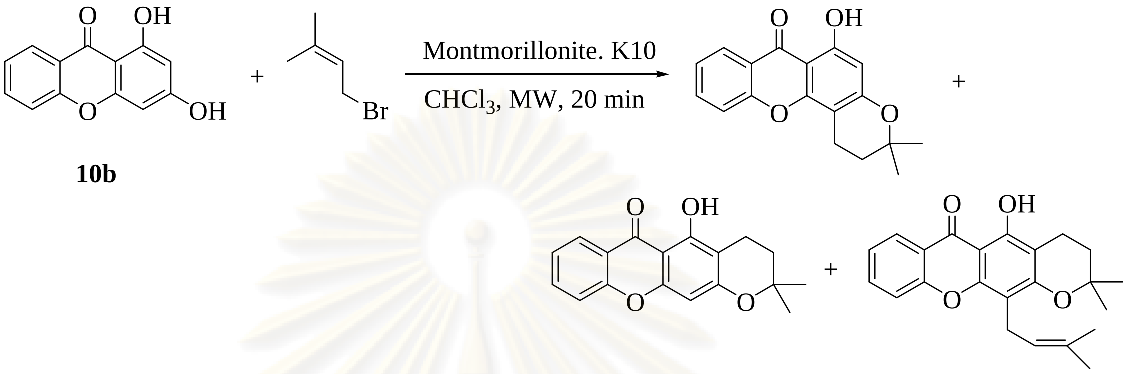

10b

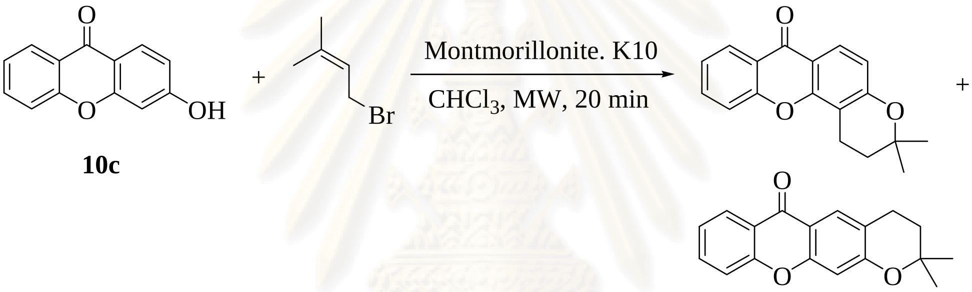

10c

Rearrangement reaction

The rearrangement reactions have been performed using modified clay catalysts. For example, pinacol-pinacolone rearrangement is a method for converting a 1,2-diol to a carbonyl compound. The reaction of tertiary 1,2-glycols have been performed in high yields in the presence of acid-treated montmorillonite clay [24].

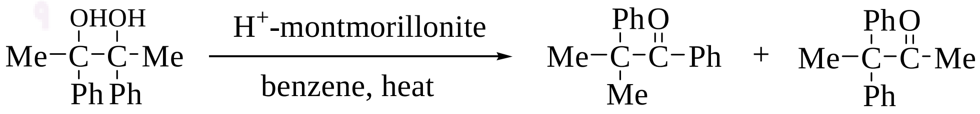

$$\mathrm{Me{-}\underset{Ph}{\overset{OH}{C}}{-}\underset{Ph}{\overset{OH}{C}}{-}Me} \xrightarrow[\text{benzene, heat}]{\text{H}^{+}\text{-montmorillonite}} \mathrm{Me{-}\underset{Me}{\overset{Ph}{C}}{-}\overset{O}{\overset{\|}{C}}{-}Ph} + \mathrm{Me{-}\underset{Ph}{\overset{Ph}{C}}{-}\overset{O}{\overset{\|}{C}}{-}Me}$$

For example, the isomerizations of α-pinene to camphene have been performed in high yields on acid-treated montmorillonite clay.

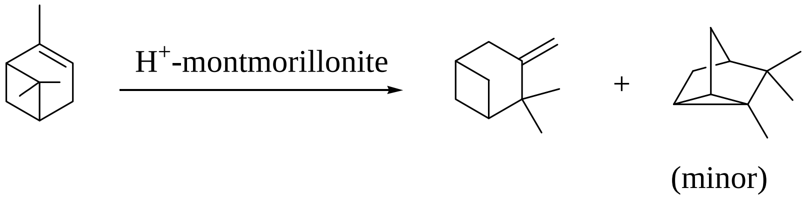

Petroleum cracking is an important industrial application in petrochemical processing. Pillared clays could be used in this process. These catalysts were more stable at high temperature. Catalytic reforming, the isomerization of *n*-alkanes to branches chain, the conversion of synthesis-gas to hydrocarbons and the conversion of methanol to alkanes have been carried out by using metal exchange montmorillonite and pillared clays as catalysts.

$$C_4\text{-to-}C_7 \xrightarrow{\text{Ni, Co-H}^+\text{-montmorillonite}} C_4\text{-to-}C_7 \quad \text{iso-alkanes}$$

(60% yield)

$$CH_3OH \xrightarrow[350^{\circ}C]{\text{Al}^{3+}\text{-montmorillonite}} C_2\text{-to-}C_4 \quad \text{alkanes}$$

$$CO + 2H_2 \xrightarrow[175^{\circ}C]{\text{Co}^{3+}\text{-montmorillonite}} C_5\text{-to-}C_{12} \quad \text{alkanes and alkenes}$$

Friedel-Crafts reaction (electrophilic aromatic substitution)

The Friedel-Crafts alkylation of cresols with suitable alkylating agents was catalyzed by montmorillonite K10 as a catalyst affording the corresponding three sesquiterpenes, elvirol, curcuphenol and sesquichemaenol [33].

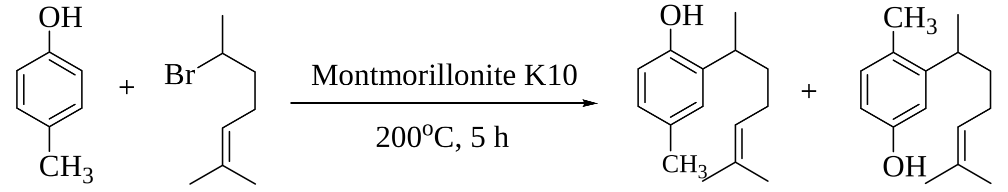

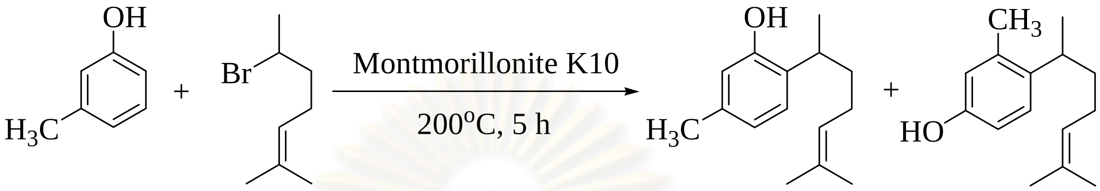

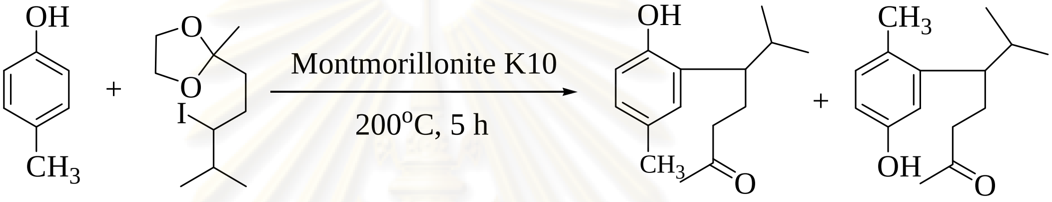

From these literature reviews, clay catalysts have been reported as an efficient catalyst in the acid catalyzed reactions. The importance in the acid catalyzed reaction involved the use of Brønsted and Lewis acid. The development of a more efficient heterogeneous catalyst for the acid catalyzed has been an important goal for organic synthesis and industrial point of view. Although there have been some investigation on the use of modified clays (iron oxide-pillared clays and metal chloride-impregnated aluminium oxide-pillared clays) for acid catalyzed reactions (isomerization reaction of α-pinene, the conversion of epoxides to acetonides and the Friedel-Crafts acylation). There is no report on the utilization of iron oxide-pillared clays and metal chloride-impregnated aluminium oxide-pillared clays as catalysts for these reactions.

2.12 The goal of this research

The aims of this research can be summarized as follows:

1. To synthesize the efficient iron oxide-pillared clays and metal chloride-impregnated aluminium oxide-pillared clays catalysts for the acid catalyzed reactions (the conversion of epoxides to acetonides, Friedel-Crafts acylation and isomerization).

2. To study the optimum conditions for the acid catalyzed reactions (the conversion of epoxides to acetonides, Friedel-Crafts acylation and isomerization) and the selected iron oxide-pillared clays and metal chloride-impregnated aluminium oxide-pillared clays as catalysts.
3. To apply the optimum conditions for
   - The conversion of epoxides to acetonides was conducted using selected epoxides and carbonyl compounds.
   - Friedel-Crafts acylation was selected using aromatic compounds and acid chlorides

2.13 Experimental

2.13.1 Instrument, apparatus and analytical measurement

2.13.1.1 Centrifuge

The purification of clays and the collection of the synthesized catalysts were processed by centaur 2, Sanyo centrifuge. The purification of clays is aimed for removing quartz and other impurities.

2.13.1.2 Oven and furnace

Raw clays and all synthesized catalysts were dried in a Memmert UM-500 oven at 100°C. The calcination was performed on a carbolite RHF 1600 muffle furnace in air. Calcination of assynthetic clays catalysts was conducted in order to convert metal precursors in the interlayer of clays into metal oxides. The heating program used for the calcination of synthesized catalysts is shown in Scheme 2.4.

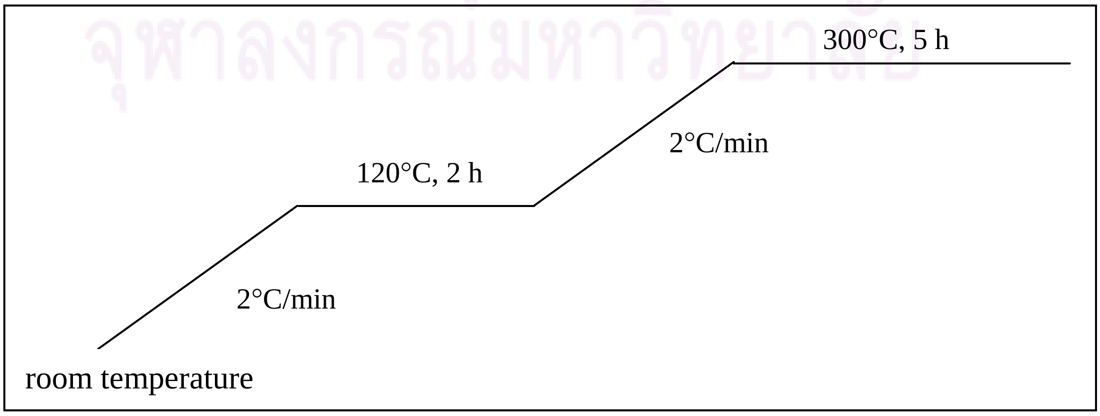

Scheme 2.4 The heating program used for the calcination of synthesized catalysts.

2.13.1.3 X-ray diffractometer (XRD)

The XRD patterns and consequence the basal spacings of catalysts (raw clays, synthetic clays catalysts) were determined using a Rigaku, Dmax 2200/utima+ X-ray powder diffractometer (XRD) with a monochromater and Cu K_{α} radiation (40 Kv, 30 mA). The 2-theta angle was ranged from 2 to 30 degree with scan speed of 3 degree/min and scan step of 0.02 degree. The scattering slit, divergent slit and receiving slit were fixed at 0.5 degree, 0.5 degree and 0.15 mm, respectively.

2.13.1.4Nitrogen adsorption/desorption (Brunauer-Emmett-Teller method, BET)

The BET specific surface area of raw clays and all synthesized catalysts were measured by the Quantachrome Autosorb-1 nitrogen adsorptometer.

2.13.1.5 Temperature Programmed Desorption (TPD) of Ammonia

The NH_3-TPD of raw clays and all synthesized catalysts were measured by the BEL Japan, BELCAT.

2.13.1.6 Inductively coupled plasma-optical emission spectroscopy (ICP-OES)

The amount of iron in the iron oxide pillared clays were analyzed using the Perkin Elmer PLASMA-1000 inductively couple plasma optical emission (ICP-OES) spectrometer at the Scientific and Technological Research Equipment Centre of Chulalongkorn University.

2.13.2 Starting materials

2.13.2.1 Clays

Clays (bentonite, hectorite and taeniolite) were used as a raw material. Bentonite was kindly supported by Cernic International Co., Ltd. Hectorite was kindly supported by Volclay Siam Limited. Taeniolite was kindly supported by Professor Shogo Shimazu at Chiba University, Japan. The compositions of bentonite, hectorite and taeniolite are summarized in Table 2.3

Table 2.3 Bentonite, hectorite and taeniolite compositions

	Bentonite[a]	Hectorite[b]	Taeniolite[c]
SiO_2	63.60	61.78	57.93
Al_2O_3	17.60	1.58	0.55
MgO	-	20.32	20.40
K_2O	0.50	0.33	10.61
F	-	-	9.00
Fe_2O_3	3.10	1.23	0.40
CaO	3.00	10.07	0.36
Na_2O	3.40	2.80	0.05
Li_2O	-	-	3.30
FeO	-	-	0.38
Rb_2O	-	-	0.14
MnO	-	-	0.11
TiO_2	-	-	0.11

[a] information from Cernic International Co., Ltd.

[b] information from Volclay Siam Limited.

[c] Geochemistry International, **2009**, *47*, 831-834.

2.13.2.2 Chemicals

1. Sodium hydroxide (Merck, reagent grade)
2. Iron (III) chloride anhydrous (Riedel-de Haën)
3. Aluminium (III) chloride hexahydrate (Ajax Finechemical, AR grade)
4. Cerium (III) chloride heptahydrate (Aldrich, AR grade)
5. Gadolinium (III) chloride hexahydrate (Aldrich, AR grade)
6. Neodynium (III) chloride hexahydrate (Aldrich, AR grade)
7. Ytterbium (III) chloride hexahydrate (Aldrich, AR grade)
8. Dysprosium (III) chloride hexahydrate (Aldrich, AR grade)
9. Lanthanum (III) chloride hydrate (Fluka, AR grade)
10. Hydrochloric acid (Merck, analysis grade)
11. Hydrofluoric acid (Merck, analysis grade)
12. Nitric acid (Merck, analysis grade)

2.13.3 Homoionic clays

Homoionic clays were prepared by purification and then ion exchange following the previous work by Kanjanaboonmalert [34].

2.13.3.1 Purification of bentonite

Bentonite was purified by fractionated sedimentation. 30 g of Bentonite were dispersed in 1,000 mL of deionized water under vigorous stirring at room temperature for 3 h. The colloid bentonite was collected and separated from quartz sediments by centrifugation. The colloid clay was centrifuged at 4,000 rpm and dried at 100°C. The purified bentonite was characterized by XRD technique.

2.13.3.2 Na-ion exchange

Na-clays (Na-bentonite, Na-hectorite and Na-taeniolite) were prepared by cation exchange. Na-ions were intercalated between the clay layers. The purified bentonite, raw hectorite or Li-taeniolite was suspended in 5 M NaOH with the ratio of clay to Na-solution as 1 g: 50 mL for 1 day at room temperature. Then the products were washed with deionized water until hydroxide anions were eliminated, and then the products were collected by centrifugation. The above process was repeated three times for Na-exchanged bentonite and Na-exchanged taeniolite, five times for Na-exchanged hectorite. The Na-exchanged clays were characterized using XRD technique.

2.13.4 Synthesis of metal oxide-pillared clays

2.13.4.1 Synthesis of iron oxide-pillared clays

Iron oxide-pillared clays (Fe-pillared clays) were synthesized according to Kanjanaboonmalert [34] by intercalation of iron precursors, following by calcinations at high temperature. Na-clays were dispersed in deionized water (10% w/w) by vigorous stirring for 1 day at room temperature. Then 1 M $FeCl_3$ solution, by the ratio of Fe^{3+} to clay of 10 meq per gram, was slowly added in the suspended Na-clay under stirring at room temperature for 24 h. The products were collected by centrifugation and then washed with deionized water until chloride ions were eliminated. The as-synthesized products, Fe-intercalated bentonite (as-BFe), Fe-intercalated hectorite (as-HFe) and Fe-intercalated taeniolite (as-TFe) were dried at 100°C for 24 h, followed by calcined at 300°C for 5 h in a muffle furnace. For denotion, B, H and T are bentonite, hectorite and taeniolite, respectively. The calcined products obtained were designated as BFe-PLC, HFe-PLC and TFe-PLC. The obtained products were characterized using XRD technique.

2.13.4.2 Synthesis of aluminium oxide-pillared clay

2 g of Na-montmorillonite was dispersed in 100 mL of deionized water under stirring at room temperature for 48 h. The Al-pillar agent was prepared by adding 0.2 M NaOH to 0.2 M $AlCl_3$ with the ratio of OH/Al was 1.9 and stirring at room temperature for 24 h. The Al-pillar agent was then slowly added to the prepared clay suspension with the ratio of Al/clay of 3.8 mol/kg. The mixture was stirred for at room temperature 24 h. After that, the precipitates were collected by centrifugation at 4,000 rpm and washed with distilled water until free of chloride ion. The as-synthesized product, Al-intercalated bentonite was dried at 100°C for 24 h, followed by calcined at 500°C for 1 h in a muffle furnace. The obtained products were characterized using XRD technique.

2.13.5 Synthesis of metal chloride-impregnated aluminium oxide-pillared clays

Metal trichloride ($LaCl_3$, $CeCl_3$, $NdCl_3$, $GdCl_3$, $DyCl_3$ and $YbCl_3$) impregnated aluminium oxide-pillared clays were synthesized by following the previous work of Masaleh [35]. The aluminium oxide-pillared clay was impregnated using a solution of 2% metal trichloride in ethanol. The slurry mixture was dried at 60°C and calcined with the rate 5°C/min and holding at 450°C for 4 h. The products were named ($LaCl_3$/Al-PLC, $CeCl_3$/Al-PLC, $NdCl_3$/Al-PLC, $GdCl_3$/Al-PLC, $DyCl_3$/Al-PLC and $YbCl_3$/Al-PLC). The obtained products were characterized using XRD technique.

2.13.6 Sample preparation for ICP

The 0.0400 g of a calcined catalyst, placed in a 100 mL Teflon beaker, was soaked with 10 mL concentrated HCl and subsequently with 10 mL of 48% HF in order to remove silica in the form of volatile SiF_4 species. The mixture was heated but not boiled to dryness on a hot plate. The removal of silica was repeated three times.

Then, 10 mL of 6 M HCl: 6 M HNO_3 mixtures in the ratio of 1:3 was added and further heated to dryness. 5 mL of 6 M HCl was added and the mixture was warmed for 5 min to complete dissolution. The solution was transferred to 50 mL polypropylene volumetric flask and made up its volume by adding deionized water. If the sample was not analyzed immediately, the solution was then transferred into a plastic bottle with a treated cap underlined with a polypropylene seal.

2.14 Results and discussion

2.14.1 The characterization of raw clays

Clay minerals (bentonite and hectorite) and synthetic clay (taeniolite) were characterized by X-ray diffraction (XRD). This technique was used to investigate the changes of clay structure, emphasizing on a basal spacing and the intensity of d_{001} reflection.

2.14.1.1 X-ray diffraction (XRD)

The characteristic structures of raw clays were characterized by XRD technique. The analysis of the X-ray diffraction patterns of raw bentonite, raw hectorite and Li-taeniolite are shown in Figs 2.9-2.11.

Bentonite is phyllosilicate-typed clay, generally containing montmorillonite and impurities such as calcite, quartz, feldspars, crystobalite and humic acids. Quartz is the major impurity of clay minerals that causes clays having low surface area and acidic site, which reduce the catalytic efficiency of clays. In Fig 2.9, raw bentonite shows the characteristic peak of montmorillonite at 2θ of 6° and 19°, corresponding to the 001 and 100 planes of montmorillonite, respectively [36]. The d_{001} basal spacing is 14.22 Å. The peaks at 2θ of 22°, 24° and 27° were assigned to quartz (SiO_2). The main impurity was quartz (SiO_2), which gave the sharp peak at 26.7°.

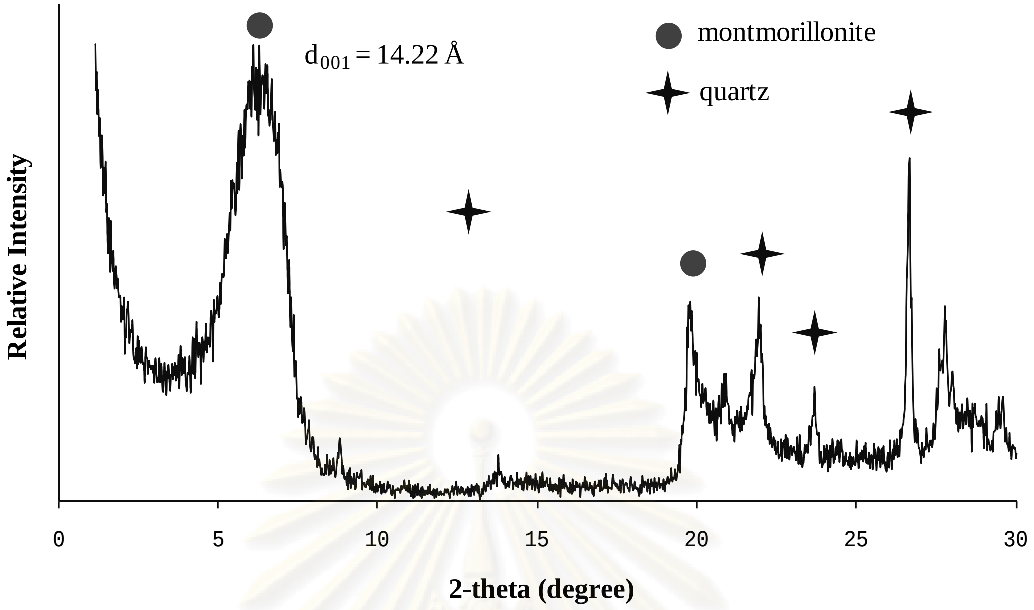

Figure 2.9 XRD patterns of raw bentonite (● represents bentonite peaks and ✦ represents impurity quartz peak).

In Fig 2.10, raw hectorite shows the characteristic peaks at 2θ of 7° and 19°, corresponding to the 001 and 100 planes, respectively. None of other crystalline phases was presented. The d_{001} basal spacing is 12.69 Å.

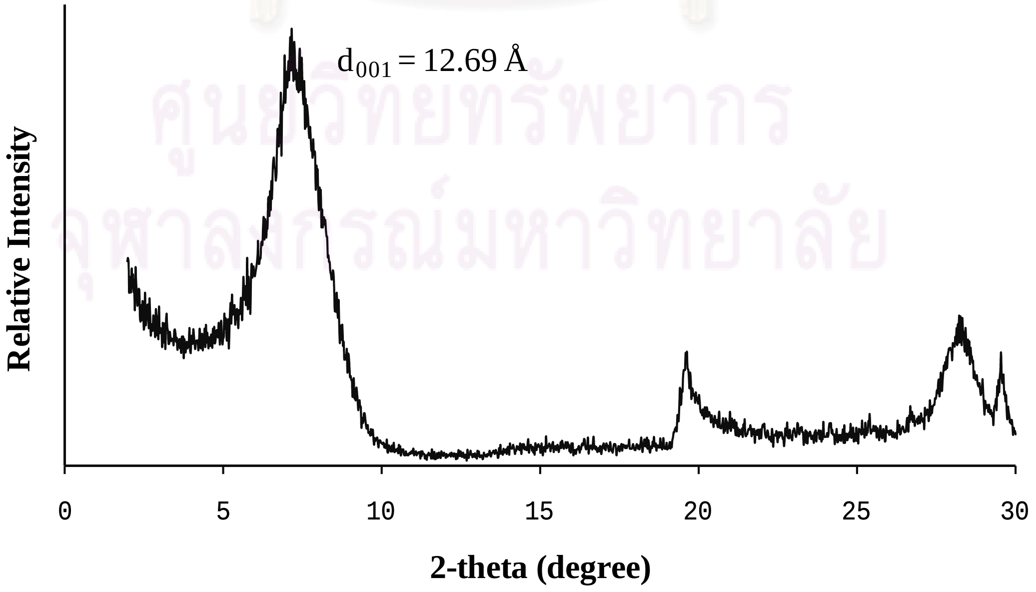

Figure 2.10 XRD patterns of raw hectorite.

In Fig 2.11, Li-taeniolite (synthetic clay) shows the characteristic peak at 2θ of 6° corresponding to the 001 planes of taeniolite. None of other crystalline phases was presented. The d_{001} basal spacing is 12.17 Å.

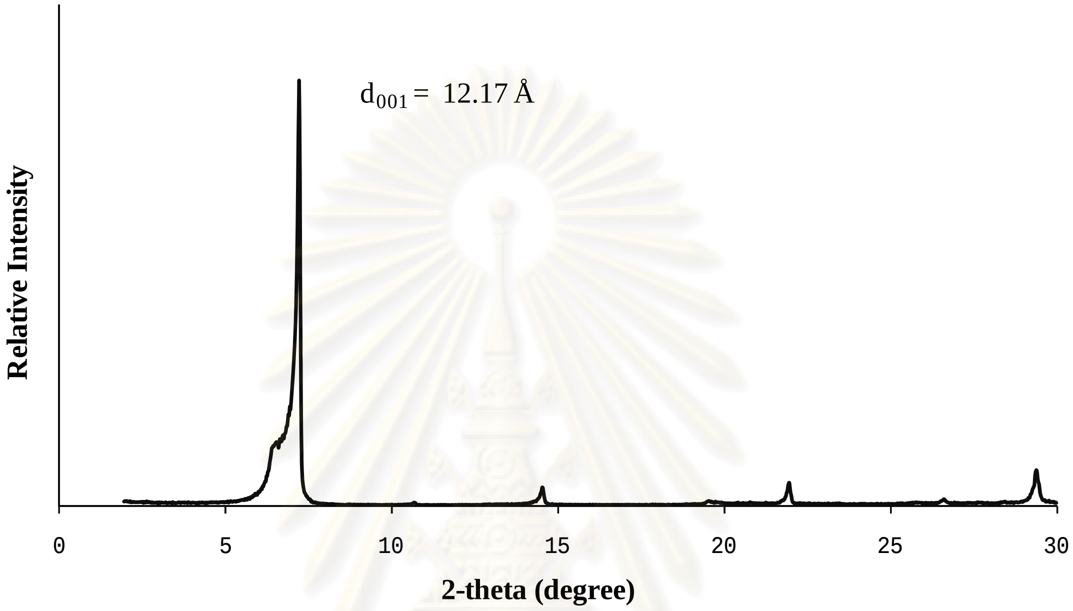

Figure 2.11 XRD patterns of Li-taeniolite.

2.14.2 The synthesis and characterization of homoionic clays

Homoionic hectorite was prepared by ion exchange method. Homoionic bentonite was purified prior to ion exchange. In the purification process, quartz and other impurities were removed from bentonite by dispersion and centrifugation process. The Na ions were intercalated between the clay layers in order to obtain homoionic clays that were used as the starting materials for synthesis of the clay catalysts.

2.14.2.1 The purification of bentonite

Mineral bentonite contains montmorillonite as main constituent and other impurities. These impurities could be removed from bentonite by dispersion and centrifugation processes. The quartz peak disappeared in purified bentonite collected from the centrifugal speed of 4,000 rpm, suggesting quartz and other impurities were removed from raw bentonite. Only montmorillonite was left in a solid residue and the residue was designated as montmorillonite. The X-ray diffraction patterns of raw bentonite and montmorillonite (purified bentonite) are shown in Figure 2.12. The quartz peak at 2θ of 22°, 24° and 27° disappeared in the XRD patterns of montmorillonite. The structure of montmorillonite clay was still remained and the (001) peak was found at the 2θ of 7Å, corresponding to the d_{001} basal spacing of 12.37 Å.

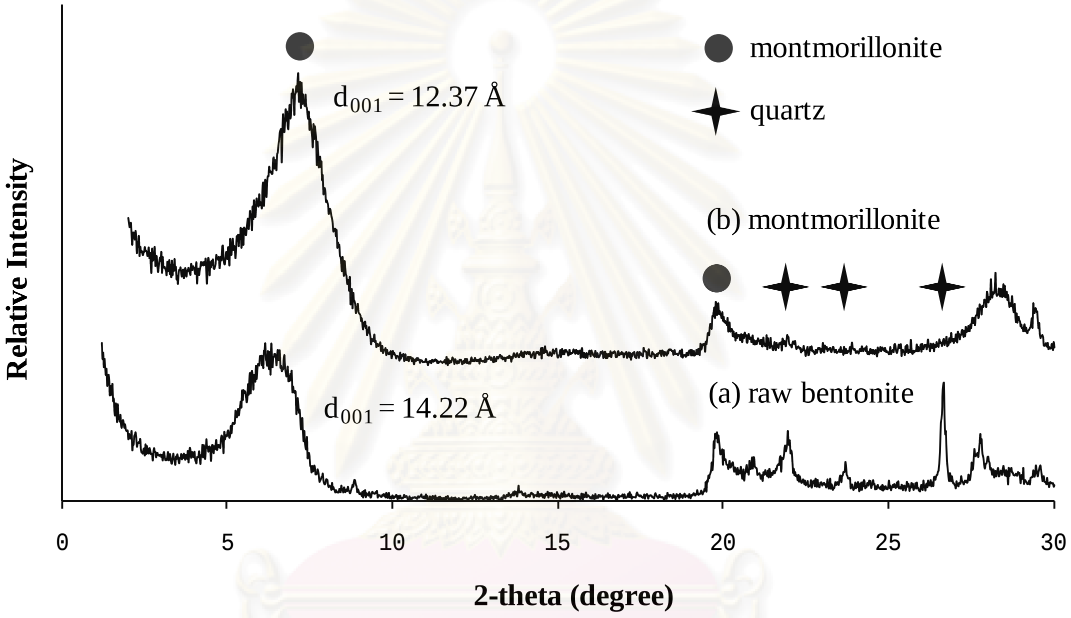

Figure 2.12 XRD patterns of (a) raw material bentonite and (b) montmorillonite (purified bentonite) obtained at the centrifugal speed of 4,000 rpm (● represents the peaks of montmorillonite and ✦ represents impurity quartz peak).

2.14.2.2 Na-ion exchange of clays

Layer structure of clays posses a net negative charge, which balanced with interlayer cations, such as Na or K ions. The predominant exchangeable cation in the clay swelling is sodium ion due to the large solvation energy (98 kcal/mol) [37] and its small electrostatic interaction between monovalent cation and negatively charged layer.

X-ray diffraction of Na-montmorillonite

Na-ions were intercalated between the clay layers by ion-exchange process. Montmorillonite were treated with 5 M NaOH for three times, and the obtained solid was designated as Na-montmorillonite. The X-ray diffraction patterns of Na-montmorillonite and montmorillonite are shown in Fig 2.13. The d_{001} basal spacing in Na-montmorillonite is 15.39 Å which is higher than that of the untreated montmorillonite, suggesting Na^+ ions intercalate into the clay layers. As previously mentioned that Na^+ ion has large solvation energy, more water molecules were solvated sodium interlayer cations, causing the larger d-spacing of Na-montmorillonite.

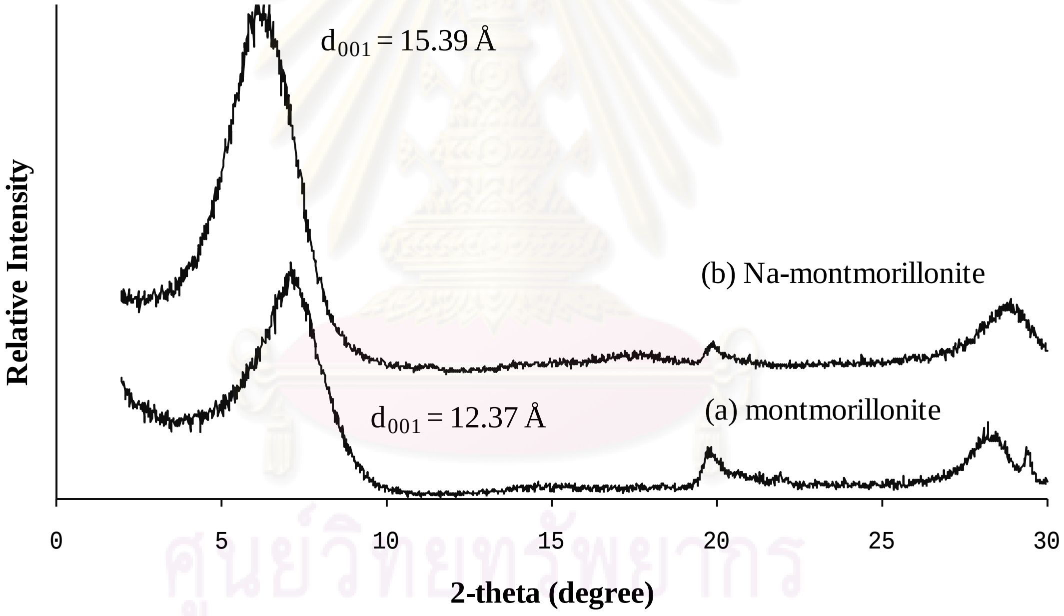

Figure 2.13 XRD patterns of (a) montmorillonite and Na-montmorillonite.

X-ray diffraction of Na-hectorite

Na-ions were intercalated between the clay layers by ion-exchange process. Raw hectorite was treated with 5 M NaOH for five times, and the obtained solid was designated as Na-hectorite. The X-ray diffraction patterns of Na-hectorite and raw hectorite are shown in Fig 2.14. The d_{001} basal spacing in Na-hectorite is 15.33 Å which is higher than that of the untreated raw hectorite, suggesting Na^+ ions intercalate into the clay layers. As previously mentioned that Na^+ ions has large solvation energy, more water molecules were solvated sodium interlayer cations, causing the larger d-spacing of Na-hectorite.

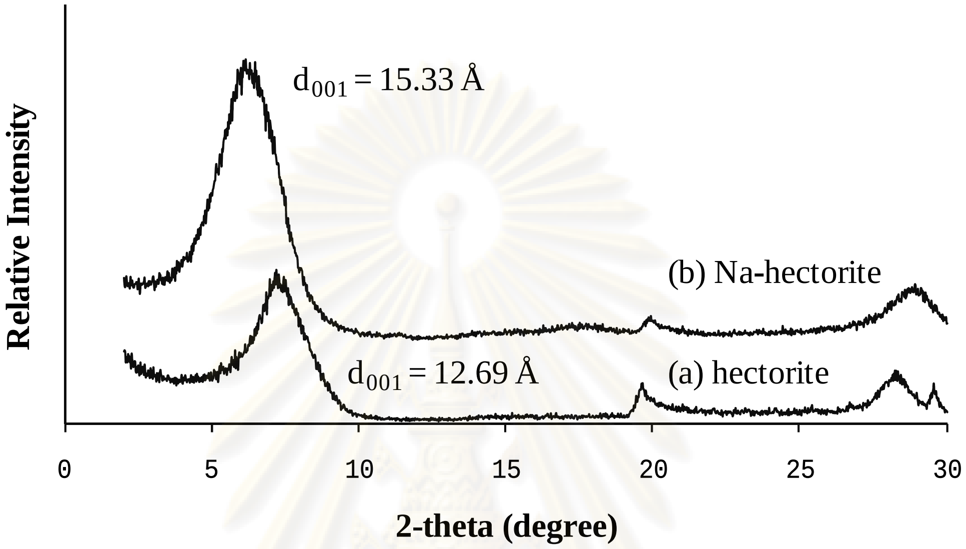

Figure 2.14 XRD patterns of (a) raw hectorite and (b) Na-hectorite.

2.14.3 The synthesis and characterization of iron oxide-pillared clays (Fe-PLC) and aluminium oxide-pillared clay (Al-PLC)

Iron oxide-pillared clays (such as iron oxide-pillared bentonite, iron oxide-pillared hectorite and iron oxide-pillared taeniolite) and aluminium oxide-pillared bentonite were synthesized by intercalation of iron and aluminium precursors between the clay layers, following by calcinations at high temperature. Iron oxide-pillared bentonite (BFe-PLC), iron oxide-pillared hectorite (HFe-PLC), iron oxide-pillared taeniolite (TFe-PLC) and aluminium oxide-pillared bentonite (Al-PLC) were successfully synthesized. BFe-PLC and HFe-PLC are red brown solids, and TFe-PLC and Al-PLC are yellow brown solids

2.14.3.1 X-ray diffraction of iron oxide-pillared clays (Fe-PLC)

As-synthesized products (as-HFe, as-BFe and as-TFe), the products after intercalation, were calcined at 300°C for 5 h. The X-ray diffraction patterns of Na-montmorillonite and BFe-PLC are shown in Fig 2.15, the X-ray diffraction patterns of

Na- hectorite and HFe-PLC are shown in Fig 2.16 and the X-ray diffraction patterns of Li-taeniolite and TFe-PLC are shown in Fig 2.17. The d_{001} basal spacing of BFe-PLC and HFe-PLC were found as a broad peak and smaller d-spacing, compared which those of Na-montmorillonite and Na-hectorite, respectively. During the process of calcination, excess water molecules adsorbed between clay layers were removed and iron precursors were converted to iron oxide at the calcined condition. In the case of TFe-PLC, the d_{001} basal spacing of TFe-PLC was found as a broad peak and higher d-spacing, compared which those of Li-taeniolite, because of iron precursors may associated to produce iron oligomers that bigger than iron oxide and enlarged d-spacing.

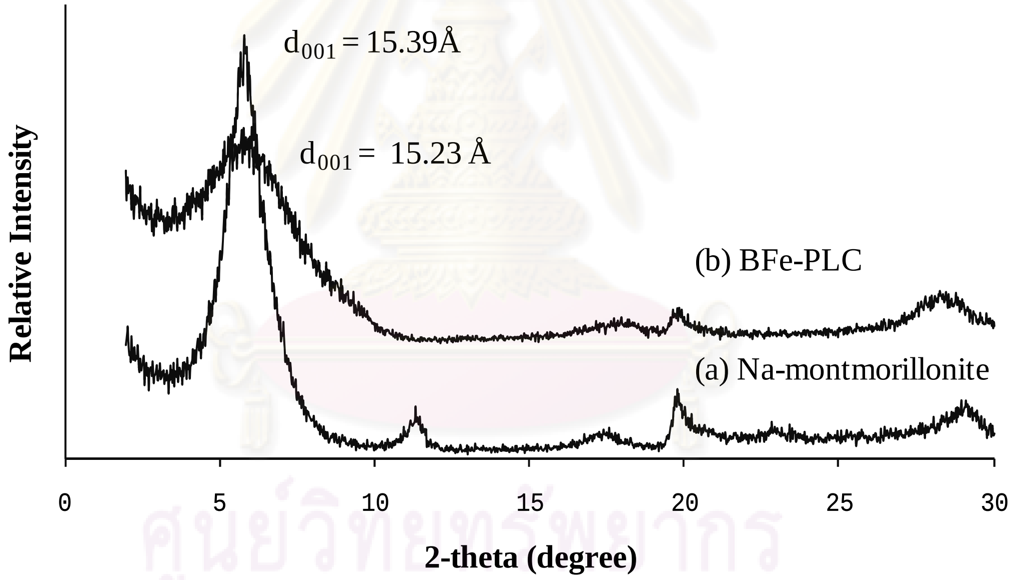

Figure 2.15 XRD patterns of (a) Na-montmorillonite and (b) BFe-PLC.

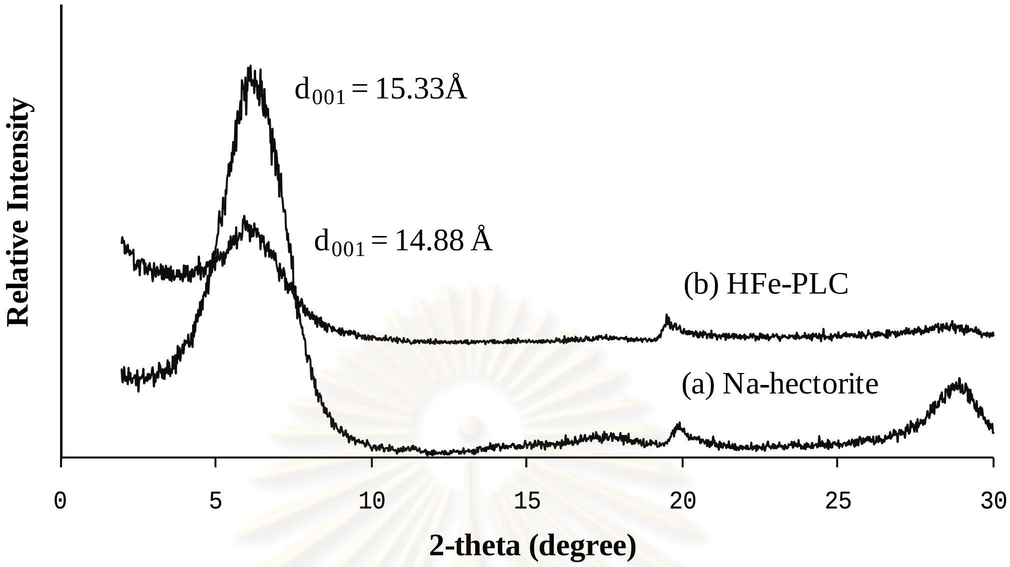

Figure 2.16 XRD patterns of (a) Na- hectorite and (b) HFe-PLC.

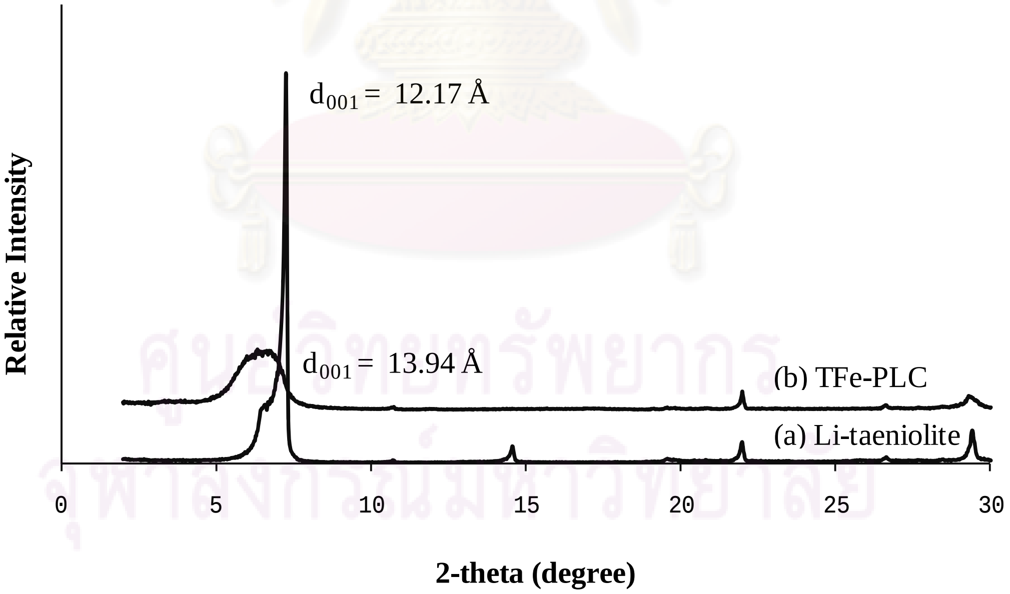

Figure 2.17 XRD patterns of (a) Li-taeniolite and (b) TFe-PLC.

2.14.3.2 X-ray diffraction of aluminium oxide-pillared bentonite (Al-PLC)

The XRD patterns of Al-PLC and Na-montmorillonite are shown in Fig 2.18. The d_{001} basal spacing of Al-PLC was found as a broad peak with the high intensity at

16.36 Å. The 2θ peak of Al-PLC was shifted slightly to the left as compared to that of Na-montmorillonite, indicating that the sodium ions within the layer of montmorillonite were exchanged by aluminium polyoxocations. The aluminium polyoxocations $[Al_{13}O_4(OH)_{24}\ (H_2O)_{12}]^{7+}$ [38], prepared by adding 0.2 M NaOH to 0.2 M $AlCl_3$ with the ratio of OH/Al was 1.9, intercalated into the clay layer and were converted to the aluminium oxide-pillars during calcinations process. The transformation of aluminium polyoxocations into rigid aluminium oxide-pillars, tightly bound to the clay layer, increased the disordering within interlayer spacing of clay structure, resulting to the broader peak with lower intensity.

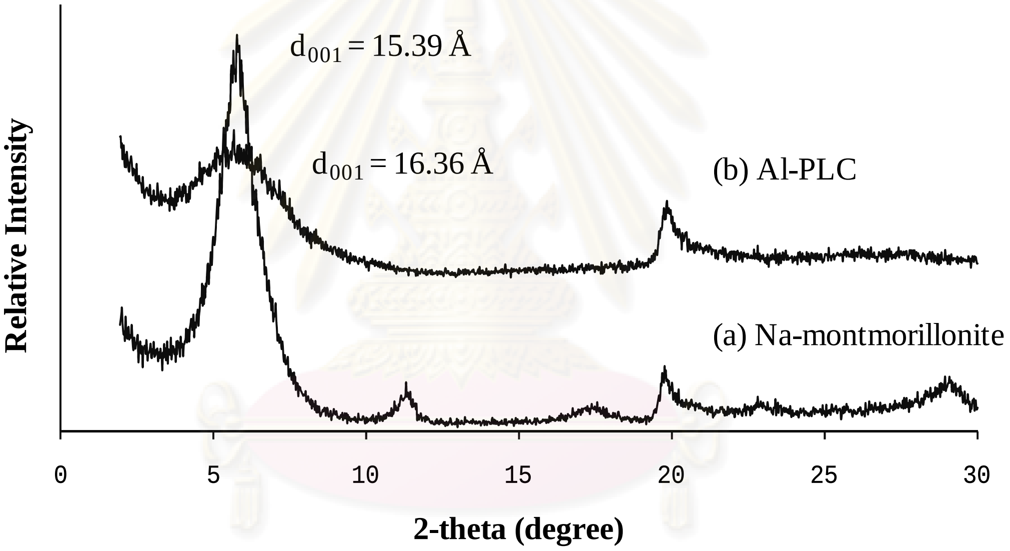

Figure 2.18 XRD patterns of (a) Na-montmorillonite and (b) Al-PLC.

2.14.4 The synthesis and characterization of metal chloride-impregnated aluminium oxide-pillared clay

The XRD patterns of metal chloride ($LaCl_3$, $CeCl_3$, $NdCl_3$, $GdCl_3$, $YbCl_3$ and $DyCl_3$) impregnated aluminium oxide-pillared clay ($LaCl_3$/Al-PLC, $CeCl_3$/Al-PLC, $NdCl_3$/Al-PLC, $GdCl_3$/Al-PLC, $YbCl_3$/Al-PLC and $DyCl_3$/Al-PLC) are compared as presented in Fig 2.19. The d_{001} basal spacings of metal chloride-impregnated aluminium oxide-pillared clay (MCl_3/Al-PLC) are about 14-15 Å which are a little bit lower than that of Al-PLC, but the d_{001} peaks are a lot broader, indicating that the recalcination process caused the pillared structure collapse slightly and the impregnation of metal chloride increased the disordering between the interlayer spacing of clay.

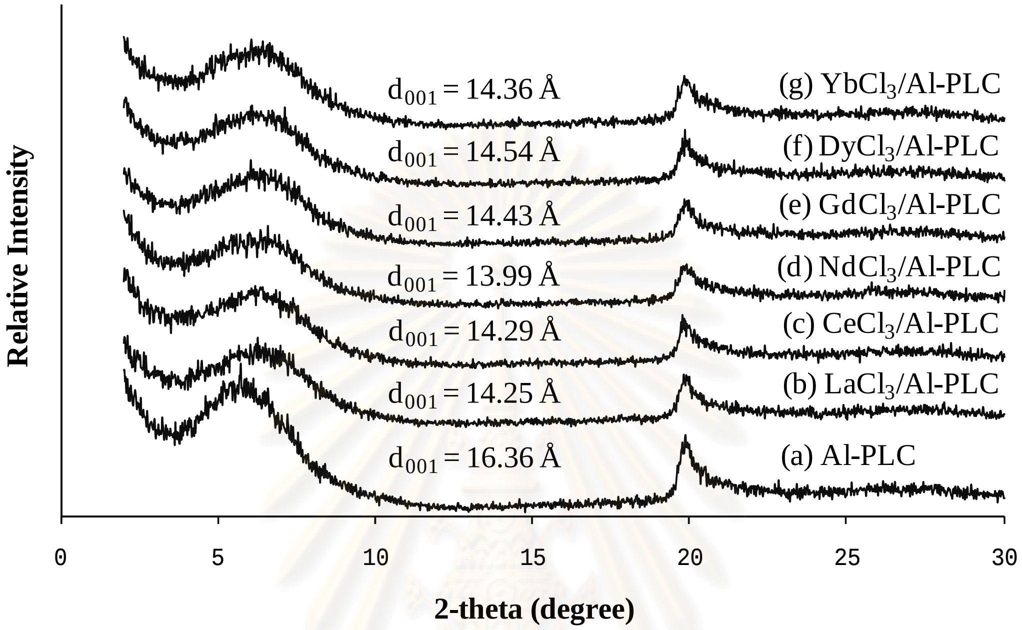

Figure 2.19 XRD patterns of (a) Al-PLC, (b) LaCl$_3$/Al-PLC, (c) CeCl$_3$/Al-PLC, (d) NdCl$_3$/Al-PLC, (e) GdCl$_3$/Al-PLC, (f) DyCl$_3$/Al-PLC and (g) YbCl$_3$/Al-PLC.

2.14.5 Temperature Programmed Desorption (TPD)

The most widely used procedure for the determination of the acidity of porous materials is NH$_3$-TPD analysis. The total amount of acidity (mmol/g) of montmorillonite, raw hectorite, Li-taeniolite, BFe-PLC, HFe-PLC, TFe-PLC, Al-PLC and metal chloride-impregnated aluminium oxide-pillared clay (LaCl$_3$/Al-PLC, CeCl$_3$/Al-PLC, NdCl$_3$/Al-PLC, GdCl$_3$/Al-PLC, YbCl$_3$/Al-PLC and DyCl$_3$/Al-PLC) are compared in Table 2.4.

Table 2.4 The total amount of acidity of clay catalysts

Entry	Samples	acidity (mmol/g)		Total amount of acidity (mmol/g)
		weak acid sites	strong acid sites	
1	Montmorillonite	0.14	1.12	1.26
2	BFe-PLC	0.62	3.11	3.73
3	Raw hectorite	0.04	0.51	0.55
4	HFe-PLC	0.73	1.43	2.16
5	Raw taeniolite	0.43	-	0.43
6	TFe-PLC	0.61	0.91	1.52
7	Al-PLC	0.43	1.24	1.67
8	$LaCl_3$/Al-PLC	0.72	1.45	2.17
9	$CeCl_3$/Al-PLC	0.89	2.17	3.06
10	$NdCl_3$/Al-PLC	0.60	2.90	3.50
11	$GdCl_3$/Al-PLC	0.45	1.38	1.83
12	$DyCl_3$/Al-PLC	0.65	1.47	2.12
13	$YbCl_3$/Al-PLC	0.56	1.41	1.97

Table 2.4 shows the acidity of all clays catalysts. In the case of iron oxide-pillared clays group, the acidity of iron oxide-pillared clays is higher than raw clays. BFe-PLC exhibited the highest acidity followed by HFe-PLC, TFe-PLC, montmorillonite, raw hectorite and raw taeniolite, respectively. The total numbers of acidic sites were 3.73 mmol/g for BFe-PLC, 2.16 mmol/g for HFe-PLC and 1.52 mmol/g for TFe-PLC. The acidic character of pillared clays derives from either Brønsted or Lewis site. Weak acid site appears to be associated with the coordination of water molecule with iron in pillars, while strong acid site is attributed from the Fe_2O_3 in pillars. The nature and strength of acid site were related to the types of clays and pillared species. From these results, it could be concluded that type of clays affects on the acidity of synthesized catalysts. The pillaring process enhanced the acidity in iron oxide-pillared clays compared to that of the raw clays.

In the case of aluminium oxide-pillared bentonite (Al-PLC), higher acidity could be measured than that of montmorillonite. All metal chloride-impregnated aluminium oxide-pillared bentonite ($LaCl_3$/Al-PLC, $GdCl_3$/Al-PLC, $DyCl_3$/Al-PLC, $YbCl_3$/Al-PLC, $CeCl_3$/Al-PLC and $NdCl_3$/Al-PLC) exhibited higher acidity than pristine montmorillonite and Al-PLC. The total number of acidic sites was 3.50 mmol/ g for $NdCl_3$/Al-PLC which is the highest among metal chloride-impregnated catalysts. This indicated that type of metal chlorides greatly affected on the acidity of synthesized clays catalysts [39].

2.14.6 Nitrogen adsorption-desorption (Brunauer-Emmett-Teller method, BET)

The BET specific surface area of montmorillonite, raw hectorite, Li-taeniolite, BFe-PLC, HFe-PLC, TFe-PLC, Al-PLC, $LaCl_3$/Al-PLC, $CeCl_3$/Al-PLC, $NdCl_3$/Al-PLC, $GdCl_3$/Al-PLC, $YbCl_3$/Al-PLC and $DyCl_3$/Al-PLC are compared in Table 2.5.

Table 2.5 The BET specific surface area of clay catalysts

Entry	Samples	BET specific surface area (m^2/g)
1	Montmorillonite	65.05
2	BFe-PLC	155.52
3	Raw hectorite	57.11
4	HFe-PLC	122.30
5	Raw taeniolite	3.53
6	TFe-PLC	20.33
7	Fe_2O_3	10.28
8	Al-PLC	145.70
9	$LaCl_3$/Al-PLC	117.40
10	$NdCl_3$/Al-PLC	127.25
11	$CeCl_3$/Al-PLC	122.40
12	$GdCl_3$/Al-PLC	121.10
13	$DyCl_3$/Al-PLC	113.50
14	$YbCl_3$/Al-PLC	121.60

Table 2.5 shows the BET specific surface area of all clays catalysts (raw clays and synthesized clays). In the case of iron oxide-pillared clays group, the nitrogen adsorption-desorption isotherms are the distorted reversible type IV isotherm,

indicating that Fe_2O_3 in calcined samples converted clay-layered structure (2-dimensional structure) to mesoporous structure (3-dimensional structure). Therefore, the BET specific surface areas of BFe-PLC and Al-PLC, HFe-PLC and TFe-PLC were higher than those of montmorillonite, raw hectorite and raw taeniolite, respectively. The pore size distribution of iron oxide-pillared clays except TFe-PLC from BJH analysis was in the range of 50 to 70 Å. In the case of TFe-PLC, the pore size distribution from BJH analysis was in the range of 130 to 140 Å, Therefore, all could be indicated as mesoporous materials (a diameter of 20-500 Å).

Aluminium oxide-pillared clays displayed higher specific surface area (m^2/g) than that of montmorillonite. The increase of surface area related to the increase of the d_{001} basal spacing from 12.37 to 16.36 Å. Aluminium oxide pillars popped up the clay gallery height and allowed more access of nitrogen probe molecules. Furthermore, the clay-layered structure (2-dimensional structure) was converted to mesoporous structure (3-dimensional structure) by connecting the adjacent aluminosilicate layers with the aluminium oxide pillars in the interlayered region. This result also confirmed the XRD results that Al_2O_3 in the prepared aluminium oxide-pillared clay distributed inside the interlayer of montmorillonite instead of aggregated outside the clay structure. If Al_2O_3 was presented as a bulk Al_2O_3 outside the clay structure, the surface area would be similar to or lower than that of montmorillonite because Al_2O_3 possesses a dense structure.

All metal chloride-impregnated aluminium oxide-pillared bentonite ($LaCl_3$/Al-PLC, $CeCl_3$/Al-PLC, $NdCl_3$/Al-PLC, $GdCl_3$/Al-PLC, $DyCl_3$/Al-PLC and $YbCl_3$/Al-PLC) showed higher specific surface area than montmorillonite but lower than Al-PLC. The pore size distribution of all metal chloride-impregnated aluminium oxide-pillared bentonite from BJH analysis was in the range of 50 to 70 Å, indicating the mesoporous material. This could be explained that metal trichloride (MCl_3) deposited on the pore wall of the aluminium oxide-pillared clay and occupied the void in mesoporous structure, resulting to the decrease in specific surface area.

2.14.7 Determination of iron contents

The iron content was also analyzed by inductively coupled plasma-optical emission spectroscopy. The total amount of acidity (mmol/g) of montmorillonite, raw hectorite, taeniolite, BFe-PLC, HFe-PLC and TFe-PLC are compared in Table 2.6.

Table 2.6 The iron contents in clays sample

Entry	Samples	Wt% of Fe content[a]
1	Montmorillonite	3.49
2	BFe-PLC	10.14
3	Hectorite	0.95
4	HFe-PLC	9.54
5	Taeniolite	0.35
6	TFe-PLC	4.22

[a] The iron content was analyzed by ICP.

Table 2.6 shows the iron contents in iron oxide-pillared clay catalysts in all type of clays. The iron content was also analyzed by ICP. The iron content in iron oxide-pillared bentonite was 10.14 wt%, which is the highest among iron oxide-pillared clay.

2.15 Conclusion

Iron oxide-pillared clays (BFe-PLC, HFe-PLC, TFe-PLC and Al-PLC) were synthesized by intercalation method, followed by calcination at 300°C for 5 h. Metal chloride-impregnated aluminium oxide-pillared bentonites ($LaCl_3$/Al-PLC, $CeCl_3$/Al-PLC, $NdCl_3$/Al-PLC, $GdCl_3$/Al-PLC, $DyCl_3$/Al-PLC and $YbCl_3$/Al-PLC) were synthesized by the impregnation method of metal chloride ($LaCl_3$, $CeCl_3$, $NdCl_3$, $GdCl_3$, $YbCl_3$ and $DyCl_3$) on Al-PLC, followed by calcination at 450°C for 4 h. In the case of metal oxide-pillared clays, the d_{001} basal spacings of BFe-PLC, HFe-PLC, TFe-PLC and Al-PLC were 15.23, 14.88, 13.94 and 16.36 Å, respectively, whereas the d_{001} spacings of all metal chloride-impregnated aluminium oxide-pillared bentonites are about 14-15 Å. The layered characteristics of clay starting materials still remained in all obtained clay catalysts. The nitrogen adsorption-desorption isotherms of all synthesized clays catalysts revealed the type IV isotherm, indicating their micro-mesoporous structure. The BET specific surface area of BFe-PLC, HFe-PLC, TFe-PLC were higher than montmorillonite, raw hectorite and Li-taeniolite respectively, and the BET specific surface area of $LaCl_3$/Al-PLC, $CeCl_3$/Al-PLC, $NdCl_3$/Al-PLC, $GdCl_3$/Al-PLC, $DyCl_3$/Al-PLC and $YbCl_3$/Al-PLC showed higher than montmorillonite but lower than Al-PLC. The acidity of BFe-PLC showed the highest acidity among all synthesized catalysts.

CHAPTER III

FRIEDEL-CRAFTS ACYLATION BY CLAY CATALYSTS

3.1 Introduction

Fundamentally, the most important and efficient procedure for synthesizing aryl ketones is Friedel-Crafts acylation by reacting aromatic compounds with acylating agents (acid chlorides, esters, acid anhydrides or carboxylic acids). Aryl ketones are valuable intermediates for the production of fine chemical in cosmetics, pharmaceuticals, colorants, perfumery chemicals, agrochemicals and other chemical industries. For instance, 4-methoxybenzophenone, a precursor for antioxidant used in alkylated resins, oil paints, cosmetics and valuable perfumery intermediate could be prepared from Friedel-Crafts acylation of anisole with benzoyl chloride using homogeneous catalysts [40].

Friedel-Craft acylation is an electrophilic aromatic substitution of aromatic compounds with acylating agent catalyzed by acid catalyst. However, common used homogeneous catalysts such as $AlCl_3$, BF_3, $FeCl_3$, $TiCl_4$ and $SnCl_4$ and protic acid (such as HF, H_2SO_4) posses several problems including high refluxing temperature, highly moisture sensitivity, the use of toxic and expensive catalysts, long reaction time, difficulty of separation from the reaction products. Therefore, there is a need to find newer catalysts for Friedel-Crafts acylation. Inorganic solid acid catalysts are gaining importance for organic reactions due to the advantage of heterogeneous catalysts such as better yield and selectivity, easy work-up (separation of the catalyst simply by filtration or centrifugation), easy reusability and recovery of the catalysts, mild reaction conditions and shorter reaction times. The solid acid catalysts such as zeolite [41], heteropoly acid [42], sulfated zirconia [43], and clay minerals [44] have been reported on their catalytic efficiencies in Friedel-Crafts acylation.

3.1.1 Literature review on Friedel-Crafts acylation

Friedel-Crafts acylation is typically more popular method than others for preparation of aryl ketones since the synthesis of aryl ketones using organometallic reagents sometimes suffers from drawback such as competition between nucleophilic addition and nucleophilic substitution and difficulty of separation and purification [45]. Friedel-Crafts acylation is affected by the formation of active electrophilic carbon (acylium ion). The reactive acylium ion is generated from an acid anhydride, acyl halide or carboxylic acid catalyzed by Lewis acid such as $AlCl_3$. The carbonyl group in aryl ketone is polarized (δ^+) and is attacked directly to the aromatic ring. The aryl ketone is deactivated relative to the starting material (aromatic compound) and the further reaction given a polyacylated derivative. It is not a major problem since acylium ion is less reactive than aromatic compound.

The general reaction was simply formulated using aromatic compound, $AlCl_3$ and acid chloride. The electrophilic aromatic substitution of acetyl chloride with benzene catalyzed by $AlCl_3$ would furnish acetophenone in good yields [46].

In 2000, Baudry and co-workers reported the use of uranyle salts as catalysts for Friedel-Crafts acylation. The results showed that Friedel-Crafts benzoylation of mesitylene with benzoyl chloride catalyzed by 1% UO_2Cl_2 at reflux for 1 h affording the corresponding mesityl phenylmethanone in high yield. The monoacylation and bisacylation products are obtained in high yield under dry air [47].

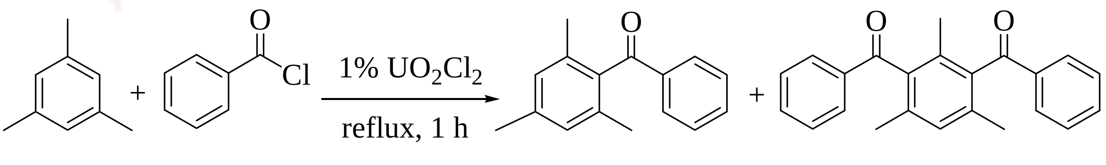

In 2000, Hwang and co-workers reported the new route to synthesize aryl ketones using a highly reactive benzoylating reagent produced by activating methyl benzoate with trifluoromethanesulfonic acid (CF_3SO_3H). Benzophenone derivatives could be obtained in good to excellent yields. On the other hand, benzoic acid esters were more reactive than aliphatic esters under the same conditions.

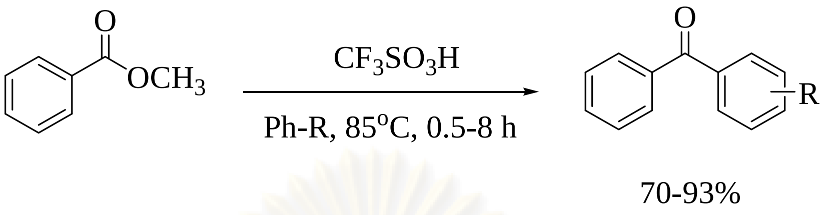

The methyl benzoate reacted with benzene catalyzed by CF_3SO_3H under reflux for three days giving benzophenone as a major product in 54% yield [48].

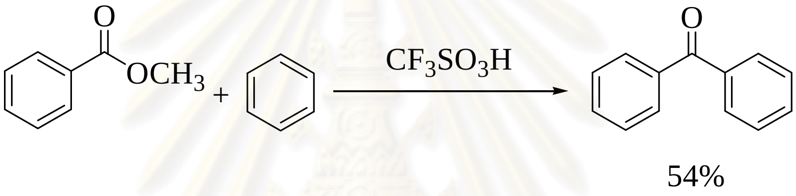

In 2001, Laidlawa and co-workers studied Friedel-Crafts benzoylation using Fe-exchanged zeolites and Zn-exchanged zeolites (mordenite, zeolite Y and H-ZSM-5) as catalysts. Friedel-Crafts benzoylation of toluene with benzoyl chloride could be catalyzed by Zn- and Fe-exchanged zeolites at 110°C for 24 h affording the corresponding 4-methylbenzophenone in high conversion. All zeolites could be catalyzed toluene benzoylation. In the case of zeolite Y, when using Fe-Na-Y as a catalyst, the product selectivity of 2-, 3-, 4-methylbenzophenones was 17, 3 and 80%, respectively. The Fe-Na-Y was more active than Zn-Na-Y; however, the same product selectivity was observed [49].

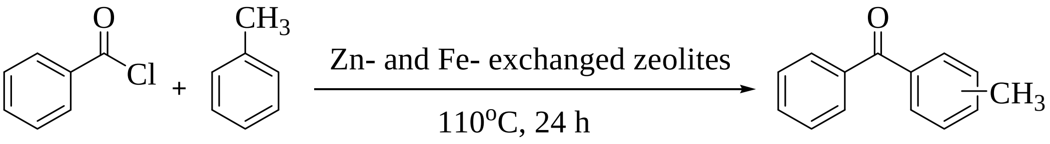

In 2002, Patil and co-workers reported the use of borate zirconia as a catalyst for Friedel-Crafts benzoylation of anisole with benzoyl chloride in nitrobenzene at

150°C for 22 h. The 91% conversion of anisole and the 93.6% selectivity to 4-methoxybenzophenone were obtained [50].

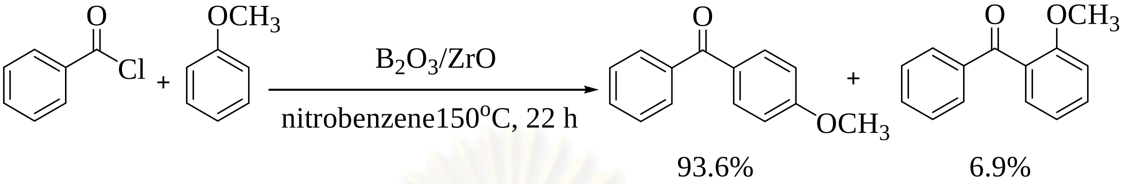

In 2002, Choudhary and Jana addressed Friedel-Crafts acylation using Ga_2O_3 or In_2O_3 supported on Si-MCM-41 catalyst (Ga_2O_3/Si-MCM-41 and In_2O_3/Si-MCM-41) of toluene with benzoyl chloride. Using In_2O_3/Si-MCM-41, the reaction time was 2.47 h which is less than 3.42 h when Ga_2O_3/Si-MCM-41 was used [51].

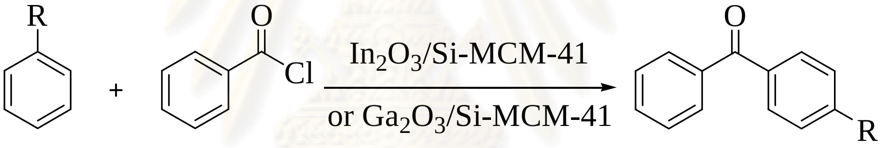

In 2002, Duris and co-workers reported the use of 1 mol% of neodymium *bis*(trifluoromethylsulfonyl)amides named neodymium triflimidates ($Nd(NTf_2)_3$) as an efficient catalyst for Friedel-Crafts benzoylation of diphenylether with benzoyl chloride at 197°C for 4 h. This reaction gave a mixture of monosubstituted and disubstituted products in the ratio of mono/di = 20/80 [52].

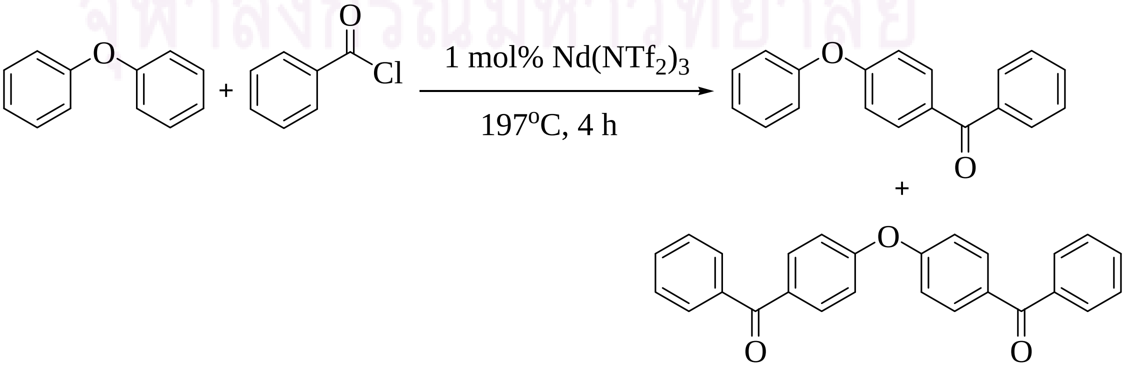

In 2003, Kawamura and co-workers reported the synthesis of aryl ketones using rare-earth metal Lewis acids ($Eu(NTf_2)_3$) as an efficient catalyst for Friedel-Crafts acylation of *p*-xylene with aliphatic and aromatic carboxylic acids at high temperature. $Eu(NTf_2)_3$ revealed as the best catalyst for Friedel-Crafts acylation of *p*-xylene with heptanoic acid in 78% yield [53].

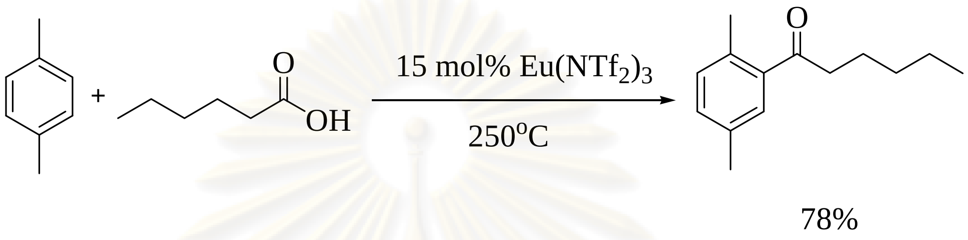

In 2003, Sheemol and co-workers addressed Friedel-Crafts acylation of toluene with acetic anhydride in nitrobenzene by various rare earth metal cations exchanged zeolite β as catalysts. The regioselectivity for the *p*-isomer product was >95%. The order of catalytic activity of various rare earth metal cations exchanged zeolite β is La-β >H-β=Ce-β >Dy-β >Eu-β >Sm-β >Gd-β >Nd-β >Pr-β [54].

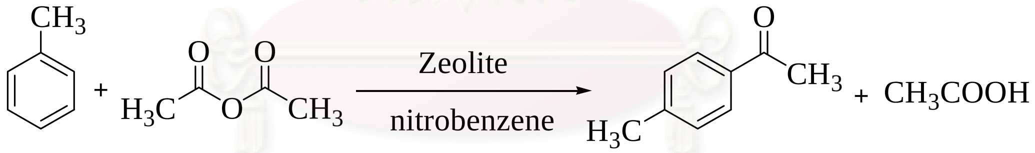

In 2004, Sawant and co-workers reported the new route to synthesize aryl ketones using 12-tungstophosphoric acid supported on zirconia (TPA/ZrO_2) as an efficient catalyst for Friedel-Crafts benzoylation of diphenyl oxide with benzoyl chloride at 120°C for 3 h. TPA/ZrO_2 catalyst showed good catalytic activity for this reaction. The conversion of benzoyl chloride was 39.3% and the selectivity to 4-(benzoyl)-diphenyl oxide was 97.4% [55].

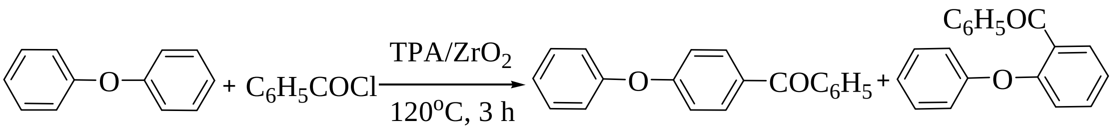

In 2004, Deutsch and co-workers reported the use of sulfated zirconia as a catalyst for Friedel-Crafts benzoylation. Friedel-Crafts benzoylation of anisole with benzoyl chloride was catalyzed by 0.2 g sulfated zirconia at 50°C for 3 h affording the corresponding 4-methoxybenzophenone in high yield. The reactivity order of the aromatics was anisole > mesitylene > 3-chloroanisole ~ *m*-xylene ~ 2-chloroanisole > toluene [56].

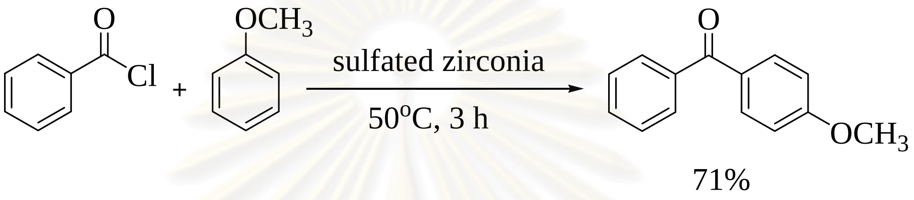

In 2004, Melero and co-workers synthesized the arenesulfonic acid modified mesostructured SBA-15 (Ar-SO_3H) as an active catalyst for Friedel-Crafts acylation of various aromatic compounds with acetic anhydride. Friedel-Crafts benzoylation of anisole with acetic anhydride catalyzed by 0.5 g of Ar-SO_3H at 125°C for 3 h afforded the corresponding *p*-methoxyacetophenone in good yield and the selectivity to *p*-methoxyacetophenone was higher than 95%. As expected, when using pure silica SBA-15, no product was observed [57].

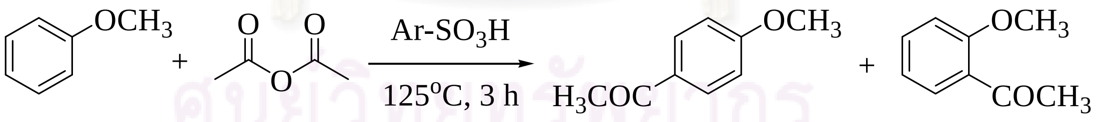

In 2006, Gopalakrishnan and co-workers reported that microwave assisted Friedel-Crafts acylation of aromatic compounds with acetyl chloride or benzoyl chloride catalyzed by aluminium metal powder furnished the corresponding acylated products in good to excellent yields. Moreover, the major product of this reaction was *p*-isomer. The advantages of this procedure were short reaction time, simple operation and environmentally friendly. Moreover, this catalyst could be reused and recovered for several times [58].

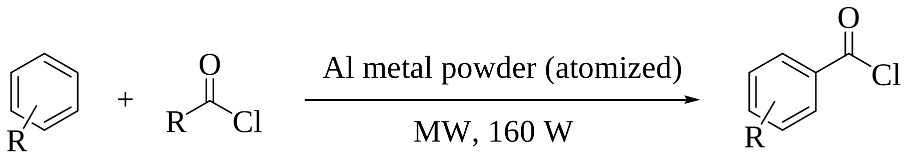

In 2006, Jana experimented Friedel-Crafts acylation using $InCl_3$ supported on Si-MCM-41($InCl_3$/Si-MCM-41). The benzoylation of 2-methoxynaphthalene with benzoyl chloride catalyzed by 20 wt% $InCl_3$/Si-MCM-41 at 80°C for 3 h affording the corresponding 1-benzoyl-2-methoxylnaphthalene in high yield [59].

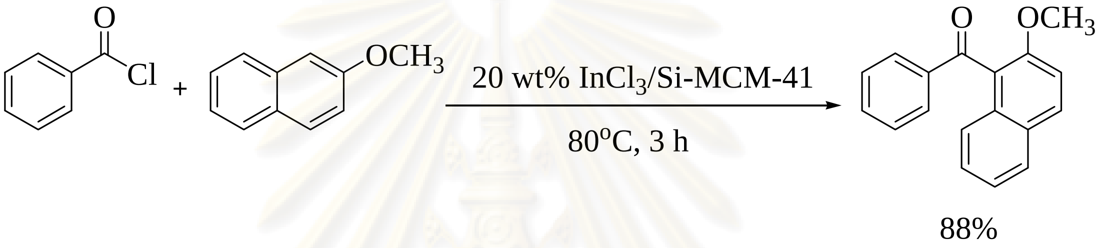

In 2008, Yadav and Badure conducted the comparative study of Friedel-Crafts acylation of 1,3-dibenzyloxybenzene with acetic anhydride by UDCaT-5 (modified zirconia), sulfated zirconia, 20 wt% Cs-DTP/K-10 (cesium modified dodecatungstophosphoric acid (DTP) on clay), amberlyst-36 (acidic ion exchange resin) and Indion-130 (ion exchange resin) affording the corresponding 3,5-di-benzyloxyacetophenone. The catalytic result of 20 wt% Cs-DTP/K-10 showed the highest selectivity and the catalyst could be reused for several times. The Cs-DTP/K-10 showed the best catalyst. The selectivity to 3,5-dibenzyloxyacetophenone of the catalysts was in order of Cs-DTP/K-10 > Indion-130 > sulfated zirconia > amberlyst-36 > UDCaT-5 [60].

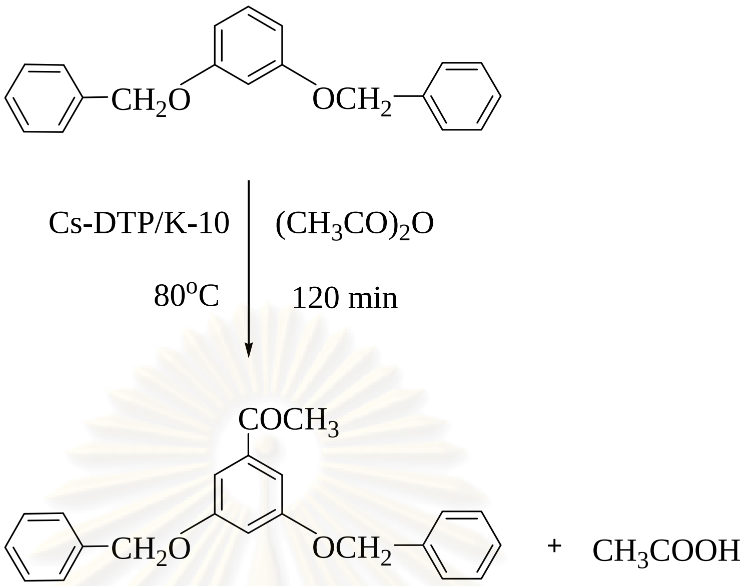

In 2008, Tamilselvan and co-workers reported Friedel-Crafts acylation of toluene, anisole and thioanisole with a variety of acyl chlorides catalyzed by cobalt(II) acetylacetonate in nitromethane under milder conditions affording the corresponding *p*-acylated products in excellent yields [61].

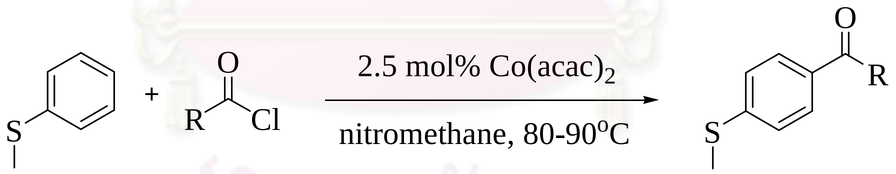

The mechanism for Friedel-Crafts acylation catalyzed by cobalt(II) acetylacetonate was proposed in scheme 3.1. Mechanistically, the formation of [I] and [II] must require for this reaction. The selectivity for *p*-position in anisole and thioanisole was occurred.

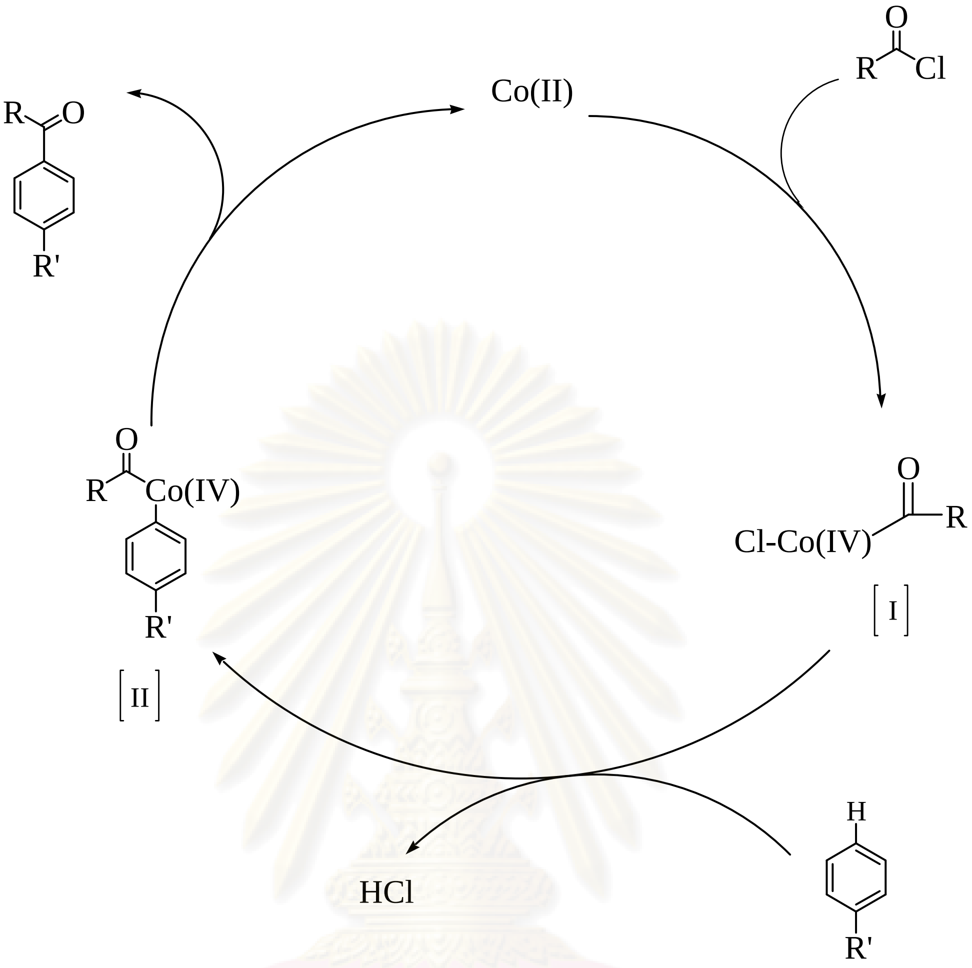

Scheme 3.1 Proposed mechanism for the cobalt (II) acetylacetonate catalyzed Friedel-Crafts acylation

3.1.2 Literature review on clay catalysts used in Friedel-Crafts reactions

In 2000, Fargas and co-workers reported the use of Fe^{3+}-exchange in K10 as a catalyst for Friedel-Crafts reaction of resorcinol with phenylacetyl chloride. The reaction proceeded smoothly to give 1-(2,4-dihydroxyphenyl)-2-phenylethanone [62].

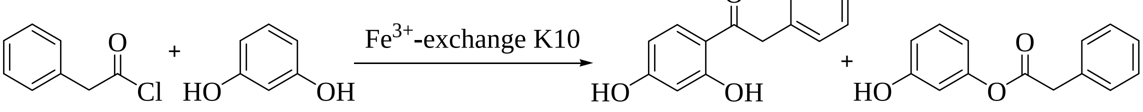

In 2001, Choudhary and co-workers reported the use of Ga-Mg hydrotalcite-derived anionic clay as catalyst for Friedel-Crafts acylation (by benzoyl chloride) and benzylation (by benzyl chloride) and reactions with toluene and benzene in good to excellent yields. Fresh hydrotalcite (basic anionic clay) showed no catalytic activity for both Friedel-Crafts acylation and benzylation, even for a long period of time [63].

In 2003, Yadav and co-workers synthesized the cesium-substituted dodecatungstophosphoric acid ($Cs_{2.5}H_{0.5}PW_{12}O_{40}$) supported on K10 clay for Friedel-Crafts benzoylation. Friedel-Crafts benzoylation of anisole with benzoyl chloride catalyzed by 20 wt% $Cs_{2.5}H_{0.5}PW_{12}O_{40}$/K10 at 70°C for 2 h afforded the corresponding 4-methoxybenzophenone in high yield with 100% selectivity for the formation of 4-methoxybenzophenone. This catalyst can be reused and recovered several times [64].

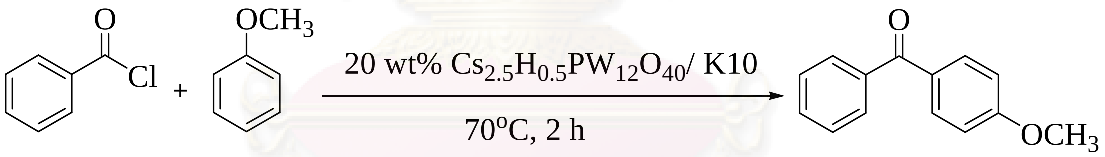

In 2004, Choudhary and co-workers reported that montmorillonite K10 clay supported $InCl_3$ was an efficient catalyst for Friedel-Crafts acylation of phenols with a variety of acyl chlorides. For instance, Friedel-Crafts benzoylation of 2-naphthol with benzoyl chloride yielded the target product 90% [65].

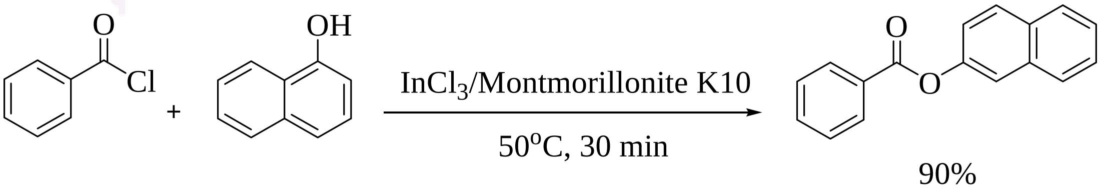

In 2004, Singh and Samant investigated Friedel-Crafts benzylation of benzene with benzyl chloride by ion-exchanged montmorillonite K10, impregnated pillared montmorillonite K10 and metal oxide pillared bentonite clays under milder conditions. The pillaring solutions of Al, Fe or Zr impregnated montmorillonite K10 were prepared and calcined at 120°C (K10-MPLS120) and 550°C (K10-MPLS550). The results showed that impregnated pillared montmorillonite K10 was more active than pillared bentonite and ion-exchanged montmorillonite K10. The K10-FePLS120 catalyst showed good selectivity and activity for this reaction [66].

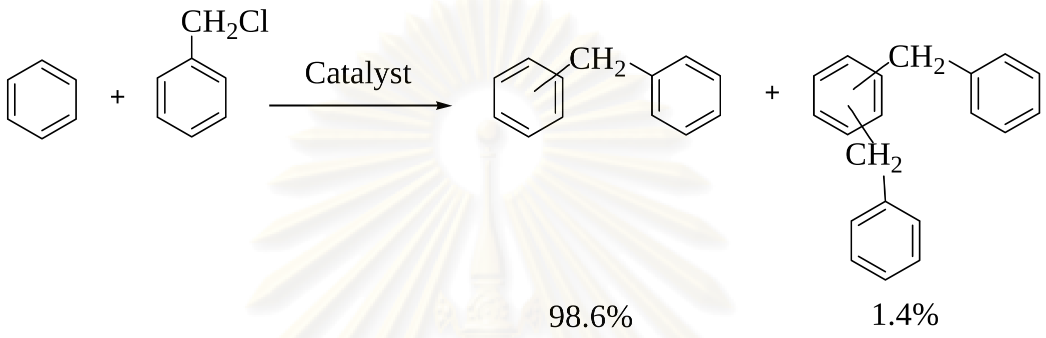

In 2008, Choudhary and Jha reported the use of $GaAlCl_x$-grafted montmorillonite K10 clay catalyst for Friedel-Crafts benzoylation with naphthalene affording the corresponding naphthalen-2-yl(phenyl)methanone in excellent yields. It was observed that the catalyst was highly stable and no leaching of Al and Ga from the catalyst during Friedel-Crafts benzoylation reactions [67].

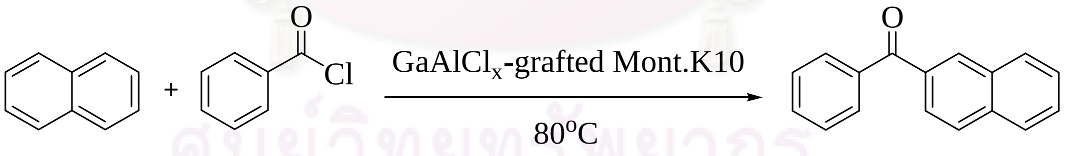

3.2 Scope of this work

From the literature reviews, homogeneous catalysts and some heterogeneous catalysts could be employed as good catalysts for Friedel-Crafts reaction. However, the disadvantage of some catalysts is their toxicity and expensiveness, long reaction time and difficulty in separation from the reaction products. The main features of this research focused on the development of a new and efficient methodology for Friedel-Crafts acylation using iron oxide-pillared clays and metal chloride-impregnated aluminium oxide-pillared clay catalysts.

3.3 Experimental

3.3.1 General procedure:

This section provides general information of general and/or specific reaction conditions and spectral data for compounds along with a representative ^{1}H NMR. The reactions were monitored by TLC on aluminium sheets precoated with silica gel (Merck's, Kieselgel 60 PF_{254}). *Buchi* rotary evaporator connected to a vacuum pump was used for removal of solvents.

Chromatography: Gas chromatographic analysis was carried out on a Shimadzu gas chromatography instrument equipped with a flame ionization detector (FID) with N_2 as a carrier gas and a 30-m long HP-5 column (0.25-mm outer diameter, 0.25 µm film thickness). Column chromatography was performed on silica gel (Merck's, kieselgel 60 G Art 7754 (70-230 mesh)).

^{1}H-NMR spectra were recorded at 400 MHz on a Varian spectrometer. Chemical shifts are reported in ppm from tetramethylsilane with the solvent residue of $CDCl_3$ (7.26 ppm)

Chemicals: All solvents in this research were purified according to the procedures described in the standard methodology except for reagents and solvents that are reagent grade.

1. anisole (Laboratory reagent)
2. benzoyl chloride (Sigma-Aldrich, 99%)
3. benzene (Carlo Erba)
4. toluene (Lab-Scan, reagent grades)
5. 1,3-dimethoxybenzene (Fluka Chemika, 98%)
6. 1,4-dioxane (Carlo Erba)
7. ethyl acetate (Lab-Scan, reagent grades)
8. 1,2-dichloroethane (Laboratory reagent)
9. dichloromethane (Lab-Scan, reagent grades)
10. acetonitrile (Merck, analysis grade)
11. *n*-hexane (Lab-Scan, reagent grades)
12. acetone (commercial grade)
13. butyric acid (Fluka Chemika, analysis grade)
14. 4-ethylbenzoic acid (Fluka Chemika, analysis grade)

15. acetic acid (Merck, analysis grade)

3.3.2 Syntheses

3.3.2.1 The general procedure for Friedel-Crafts acylation of anisole with benzoyl chloride

A typical reaction: a mixture of anisole (1 mmol), benzoyl chloride (3 mmol) and 1,4-dioxane (0.5 mL) was added to a round bottom flask with 30 wt% of catalyst to anisole, connected with a condenser for refluxing. The solution was continuous stirred for desired time and temperature. After the specific time or the reaction was finished, the catalyst was simply filtered out of the mixture, and washed the product out with EtOAc. The solvent was evaporated to dryness under reduced pressure. The obtained product was analyzed by ^{1}H NMR with the addition of an exact amount of an appropriate internal standard (toluene).

3.3.2.2 Optimum condition study on Friedel-Crafts acylation of anisole with benzoyl chloride

Effect of mole ratio of anisole to benzoyl chloride

Friedel-Crafts benzoylation was carried out according to the general procedure, but the mole ratio of anisole to benzoyl chloride was changed to 1:1, 1:2, 1:3, 1:4 and 1:5 mmol.

Effect of the amount of catalyst

Friedel-Crafts benzoylation was performed according to the general procedure, but the amount of catalyst was changed to 10, 20 and 30 wt% of catalyst to anisole.

Effect of the reaction time

Friedel-Crafts benzoylation was carried out according to the general procedure, but the reaction time was changed to 30 min, 1, 2 and 4 h.

Effect of type of organic solvent

Friedel-Crafts benzoylation was performed according to the general procedure, but using different organic solvents including 1,4-dioxane, 1,2-DCE, CH_2Cl_2, EtOAc and CH_3CN.

3.3.2.3 Study on the scope of Friedel-Crafts acylation for other aromatic compounds

The general procedure using iron oxide-pillared bentonite and 1,4-dioxane at reflux temperature for 2 h was carried out. Anisole, 1,3-dimethoxybenzene, toluene and benzene were tested.

3.3.2.4 Study on the scope of Friedel-Crafts acylation for other acid chlorides

The general procedure using iron oxide-pillared bentonite and 1,4-dioxane at reflux temperature for 2 h was carried out. The types of acid chlorides were varied as following: benzoyl chloride, acetyl chloride, butyryl chloride and 4-ethylbenzoyl chloride.

3.3.2.5 Reuse of catalysts

The used iron oxide-pillared bentonite was regenerated by calcinations at 300°C for 5 h. The structural characterization of the regenerated iron oxide-pillared bentonite catalyst was characterized using XRD, N_2-adsorption/desorption and NH_3-TPD technique. The regenerated iron oxide-pillared bentonite was reused as a catalyst in Friedel-Crafts acylation.

3.4 Results and discussion

3.4.1 Catalytic activities of iron oxide-pillared clay and metal chloride-impregnated aluminium oxide-pillared clays for Friedel-Crafts acylation

The Friedel-Crafts acylation of anisole with benzoyl chloride to produce 4-methoxybenzophenone (**11**) was selected for testing the catalytic activity of synthesized iron oxide-pillared clay and metal chloride-impregnated aluminium oxide-pillared clays catalysts. In this research, various factors were carefully scrutinized to optimize the conditions for the preparation of aryl ketone. The mole ratio of anisole to benzoyl chloride, reaction time, the amount of catalyst and type of organic solvent were varied to search for the optimal conditions.

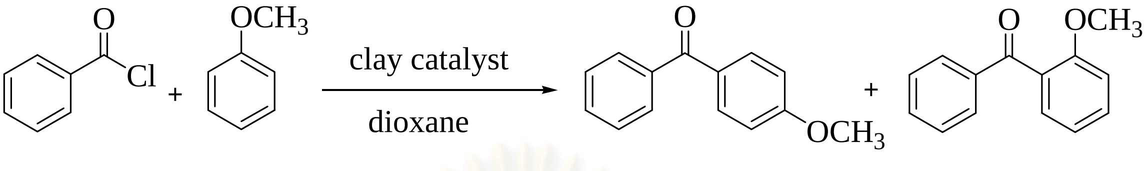

11 **12**

Generally in Friedel-Crafts acylation, two main possible isomers were produced: *o*- and *p*-isomers. Under the particular conditions studied, 4-methoxy-benzophenone (**11**) was detected as a sole product from the reaction while none of 2-methoxybenzophenone (**12**) was observed. The product was identified by ^{1}H NMR compared with authentic specimen synthesized [64].

Other aromatic compounds utilized to examine the scope of the catalytic activity for Friedel-Crafts acylation including 1,3-dimethoxybenzene, toluene and benzene. Other acid chlorides are 4-ethylbenzoyl chloride, acetyl chloride and butyryl chloride.

3.4.1.1 Effect of raw hectorite clay, montmorillonite and iron oxide-pillared clays on the reactivity of Friedel-Crafts acylation

The goal of this study was to screen for suitable catalysts that could provide aryl ketones in high yield with good selectivity. The catalytic activity of iron oxide-pillared clays such as iron oxide-pillared bentonite and iron oxide-pillared hectorite were compared with montmorillonite, raw hectorite and iron oxide (Fe_2O_3, hematite). Conditions investigated were 30 wt% catalysts to anisole at refluxing 1,4-dioxane for 2 and 4 h. The results are shown in Table 3.1. All iron oxide-pillared clays gave much higher %yield than pure clays and Fe_2O_3.

Table 3.1 The effect of raw hectorite clay, montmorillonite, and iron oxide-pillared clays on the reactivity of Friedel-Crafts acylation

Entry	**Catalysts**	**BET Surface area (m^2/g)**	**Acidity (mmol/g)**	**% Yield**[a]
1	none	-	-	0[b]
2	Montmorillonite	65.05	1.26	trace[b]
3	Raw hectorite	57.11	0.55	trace[b]
4	Fe_2O_3	-	-	21[b]
5	Fe-pillared bentonite	155.52	3.73	quant[b], quant[c]
6	Fe-pillared hectorite	122.30	2.16	quant[b], 65[c]

[a] The yield was quantified by ^{1}H NMR using toluene as an internal standard.

Reaction conditions: anisole 1 mmol, benzoyl chloride 3 mmol, 30 wt% catalyst to anisole at refluxing 1,4-dioxane for [b] 4 h; [c] 2 h.

When the reaction was performed without catalyst, no product was observed. Raw hectorite clay, montmorillonite and Fe_2O_3 showed lower activity than iron oxide-pillared clays (entries 2-6). This result corresponds with the temperature programmed desorption experiment to determine acidity and nitrogen adsorption-desorption experiment to observe surface area. The iron oxide-pillared bentonite and iron oxide-pillared hectorite have acidity and BET surface area higher than montmorillonite, raw hectorite, respectively. Iron oxide-pillared bentonite revealed the highest acidity and BET surface area resulting in the most activity in Friedel-Crafts acylation. It should be mentioned at this point that all iron oxide-pillared clays afforded good yield of Friedel-Crafts acylation product without contamination of undesired product.

3.4.1.2 Effect of metal chloride-impregnated aluminium oxide-pillared clays on the reactivity of Friedel-Crafts acylation

The goal of this study was to screen for suitable catalysts that could synthesize aryl ketones in high yield with good selectivity. The catalytic activity of metal chloride-impregnated aluminium oxide-pillared bentonite ($LaCl_3$/Al-PLC, $NdCl_3$/Al-PLC, $CeCl_3$/Al-PLC, $GdCl_3$/Al-PLC, $YbCl_3$/Al-PLC and $DyCl_3$/Al-PLC) was observed. Conditions for this reaction are 30 wt% catalysts to anisole at refluxing 1,4-dioxane for 4 h. The results are presented in Table 3.2.

Table 3.2 Effect of metal chloride-impregnated aluminium oxide-pillared bentonite on the reactivity of Friedel-Crafts acylation

Entry	Catalysts	% Yield[a]
1	Al-PLC	14
2	$LaCl_3$/Al-PLC	16
3	$NdCl_3$/Al-PLC	21
4	$CeCl_3$/Al-PLC	15
5	$GdCl_3$/Al-PLC	15
6	$DyCl_3$/Al-PLC	18
7	$YbCl_3$/Al-PLC	17

Reaction conditions: anisole 1 mmol, benzoyl chloride 3 mmol, 30 wt% catalyst to anisole at refluxing 1,4-dioxane for 4 h.

[a] The yield was quantified by ^{1}H NMR using toluene as an internal standard.

Table 3.2 displays the catalytic activity of metal chloride-impregnated aluminium oxide-pillared bentonite (MCl_3/Al-PLC) comparing to Al-PLC. All MCl_3/Al-PLC and Al-PLC showed low catalytic activity around 14-21% yield. This observation was directly related to the fact that there was no significantly difference of BET surface area and acidity of MCl_3/Al-PLC and Al-PLC. $NdCl_3$/Al-PLC had the highest acidity, but still cannot show the high activity in Friedel-Crafts acylation of anisole and benzoyl chloride to furnish the desired product. This can be concluded that these synthesized catalysts are not suitable for this reaction.

3.4.2 Optimum conditions for Friedel-Crafts acylation of anisole with benzoyl chloride by iron oxide-pillared bentonite

Since iron oxide-pillared bentonite showed good activity for Friedel-Crafts acylation of anisole with benzoyl chloride, further investigation on the mole ratio of anisole to benzoyl chloride, the amount of catalyst, reaction time and type of organic solvents was varied to search for the optimized conditions.

3.4.2.1 Effect of the mole ratio of anisole to benzoyl chloride on Friedel-Crafts acylation

The effect of the mole ratio of anisole with benzoyl chloride for Friedel-Crafts acylation was carried out. The reaction of anisole with various amounts of benzoyl chloride with the fixed amount (1 mmol) of anisole was experimented. The results are shown in Table 3.3.

Table 3.3 Effect of the mole ratio of anisole to benzoyl chloride on Friedel-Crafts acylation

Entry	anisole:benzoyl chloride (mmol)	%Yield[a]
1	1:1	56
2	1:2	64
3	1:3	72
4	1:4	73
5	1:5	75

Reaction conditions: anisole 1 mmol, benzoyl chloride (varied), 30 wt% catalyst to anisole at refluxing in dioxane for 1 h.

[a] The yield was quantified by ^{1}H NMR using toluene as an internal standard.

From table 3.3, the yield of **11** was increased with increasing the amount of benzoyl chloride (entries 1-3). The highest yield was detected around 72% even the amount of anisole:benzoyl chloride was raised up to 1:4 and 1:5 (entries 4-5). The higher amount of benzoyl chloride increased the number of acylium ion that might attack anisole at several positions and generated by product. Therefore, the mole ratio of 1:3 was chosen for further experiments.

3.4.2.2 Effect of the amount of catalyst on Friedel-Crafts acylation

The amount of catalyst normally influenced the performance of the reaction. The variation of the amount of iron oxide-pillared bentonite: 10, 20 and 30 wt% was used to search for the appropriate amount of catalyst for Friedel-Crafts acylation. The effect of the amount of iron oxide-pillared bentonite for Friedel-Crafts acylation was examined. The results are presented in Table 3.4.

Table 3.4 Effect of the amount of iron oxide-pillared bentonite on Friedel-Crafts acylation

Entry	**iron oxide-pillared bentonite (wt%)**	**% Yield**[a]
1	10	76
2	20	89
3	30	92

Reaction conditions: anisole 1 mmol, benzoyl chloride 3 mmol, wt% catalyst to anisole at refluxing 1,4-dioxane for 2 h.

[a] The yield was quantified by ^{1}H NMR using toluene as an internal standard.

Table 3.4 shows that the amount of iron oxide-pillared bentonite profoundly affected the reaction yield. When the amount of iron oxide-pillared bentonite increased, the yield of 4-methoxybenzophenone (**11**) was significantly increased. The amount of iron oxide-pillared bentonite of 30 wt% was chosen for further experiments.

3.4.2.3 Effect of the reaction time on Friedel-Crafts acylation

The effect of the reaction time on Friedel-Crafts acylation catalyzed by iron oxide-pillared bentonite was carried out and the results are presented in Table 3.5.

Table 3.5 Effect of the reaction time on Friedel-Crafts acylation catalyzed iron oxide-pillared bentonite

Entry	**Time**	**% Yield**[a]
1	30 min	51
2	1 h	72
3	2 h	92
4	4 h	93

Reaction conditions: anisole 1 mmol, benzoyl chloride 3 mmol, 30 wt% catalyst to anisole at refluxing 1,4-dioxane.

[a] The yield was quantified by ^{1}H NMR using toluene as an internal standard.

The result from table 3.5 demonstrated that the reaction time profoundly affected the reaction yield. The optimal reaction time was 2 h affording the target molecule in 92% (entry 3).

3.4.2.4 Effect of type of organic solvents on Friedel-Crafts acylation

To observe the effect of type of organic solvents for Friedel-Crafts acylation, five diverse solvents including 1,4-dioxane, 1,2-DCE, CH_2Cl_2, EtOAc and CH_3CN were investigated. The effect of organic solvents on Friedel-Crafts acylation was performed using 1:3 mmol of anisole to benzoyl chloride and 30 wt% iron oxide-pillared bentonites to anisole at refluxing conditions for 2 h. The results are presented in Table 3.6.

Table 3.6 Effect of type of organic solvents on Friedel-Crafts acylation

Entry	Organic solvent	Dipole moment	% Yield[a]
1	1,4-dioxane	0.45	92
2	1,2-DCE	1.50	74
3	CH_2Cl_2	1.60	62
4	EtOAc	1.78	44
5	CH_3CN	3.92	25

Reaction conditions: anisole 1 mmol, benzoyl chloride 3 mmol, 30 wt% catalyst to anisole at refluxing solvent for 2 h.

[a] The yield was quantified by ^{1}H NMR using toluene as an internal standard.

The synthesis of 4-methoxybenzophenone (**11**) was fruitfully performed in 1,4-dioxane (entry 1) with almost quantitative yield within 2 h. Other solvents: 1,2-DCE, CH_2Cl_2 and EtOAc provided the target molecule in moderate yield (entries 2-4), while CH_3CN gave low yield (entry 5). This result may be derived from the effect of dipole moment of the solvent. 1,4-Dioxane possesses the lowest polarity among these solvents. The more polar solvent, the stronger its coordination with the generated acylium ion intermediate. The stronger coordination would block the access of nucleophile to attack the formed intermediate [28]. Therefore, in this work, 1,4-dioxane was the most suitable solvent.

It could be summarized the standard conditions for Friedel-Crafts acylation catalyzed by iron oxide-pillared bentonite as follows: anisole 1 mmol, benzoyl chloride 3 mmol, 30 wt% iron oxide-pillared bentonite to anisole, reaction temperature at refluxing 1,4-dioxane and reaction time for 2 h.

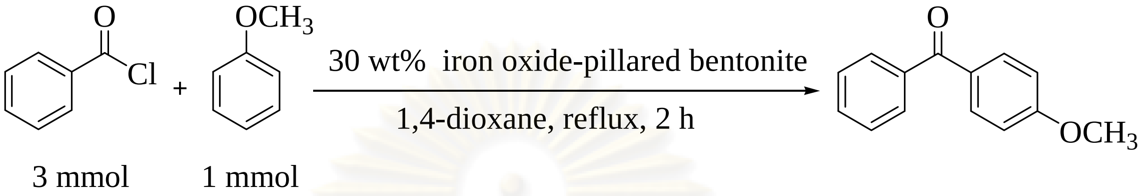

3.4.3 The scope of the reaction

Utilizing the optimal conditions for Friedel-Crafts acylation of anisole and benzoyl chloride, various aromatic compounds and acid chlorides were examined to observe the scope of this developed reaction.

3.4.3.1 Type of aromatic compounds

Various aromatic compounds including 1,3-dimethoxybenzene, toluene and benzene were selected to perform Friedel-Crafts acylation catalyzed by iron oxide-pillared bentonite under standard conditions. The variation of aromatic compounds under optimized conditions was carried out and the results are presented in Table 3.7.

Table 3.7 Synthesis of aromatic ketones from various aromatic compounds under the optimal conditions

Entry	**Aromatic compounds**	**% Yield**[a]
1	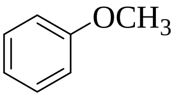	92
2	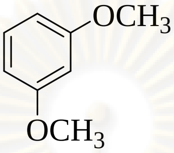	70
3	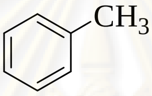	55
4	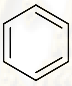	25

Reaction conditions: aromatic compound 1 mmol, benzoyl chloride 3 mmol, 30wt% catalyst to anisole at refluxing in 1,4-dioxane for 2 h.

[a]The yield was quantified by ^{1}H NMR using toluene as an internal standard.

Friedel-Crafts acylation of benzoyl chloride with aromatic compounds such as anisole and 1,3-dimethoxybenzene gave high yield of aryl ketones (entries 1-2), while the reactions with toluene and benzene gave moderate and low yield, respectively (entries 3-4). The reaction of 1,3-dimethoxybenzene gave slightly lower activity than that of anisole, possibly caused by its steric effect. For the moderate activity in the case of toluene, it probably results from the methyl group which is considered as the weakly electron donating group. In the case of benzene with no activating group, the acylation was difficult to accomplish and led to the poor yield of the desired product because the lack of an electron donating group. The electron donating group released the electron density to the aromatic ring, making it more nucleophilic aromatics which strongly attack to the acylium ion intermediate.

3.4.3.2 Type of acid chlorides

Various acid chlorides including 4-ethylbenzoyl chloride, acetyl chloride and butyryl chloride were selected to perform Friedel-Crafts acylation catalyzed by iron oxide-pillared bentonite under optimized conditions. The results are presented in Table 3.8.

Table 3.8 Synthesis of aromatic ketones from various acid chlorides under the optimal conditions

Entry	Acid chloride	% Yield[a]
1	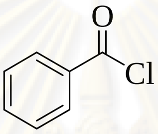	92
2	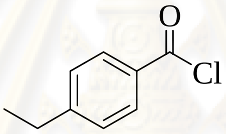	85
3	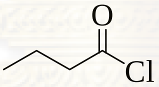	89
4	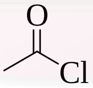	91[b]

Reaction conditions: anisole 1 mmol, acid chloride 3 mmol, 30wt% catalyst to anisole at refluxing 1,4-dioxane for 2 h.

[a]The yield was quantified by ^{1}H NMR using toluene as an internal standard.

[b]The yield was quantified by ^{1}H NMR using CH_3CN as an internal standard.

From Table 3.8, various acid chlorides could be employed to synthesize aromatic ketones in high yields.

To compare this protocol with other previous reported methods, this method provided aryl ketones in excellent yield under mild conditions whereas most of prior reports presented the manipulation of aryl ketones under severe conditions [68].

Additionally, this optimized conditions required shorter reaction time to complete the reactions comparing with many procedures [50, 51, 69]

All products presented in Figure 3.1 were verified their identities by ^{1}H NMR spectroscopy.

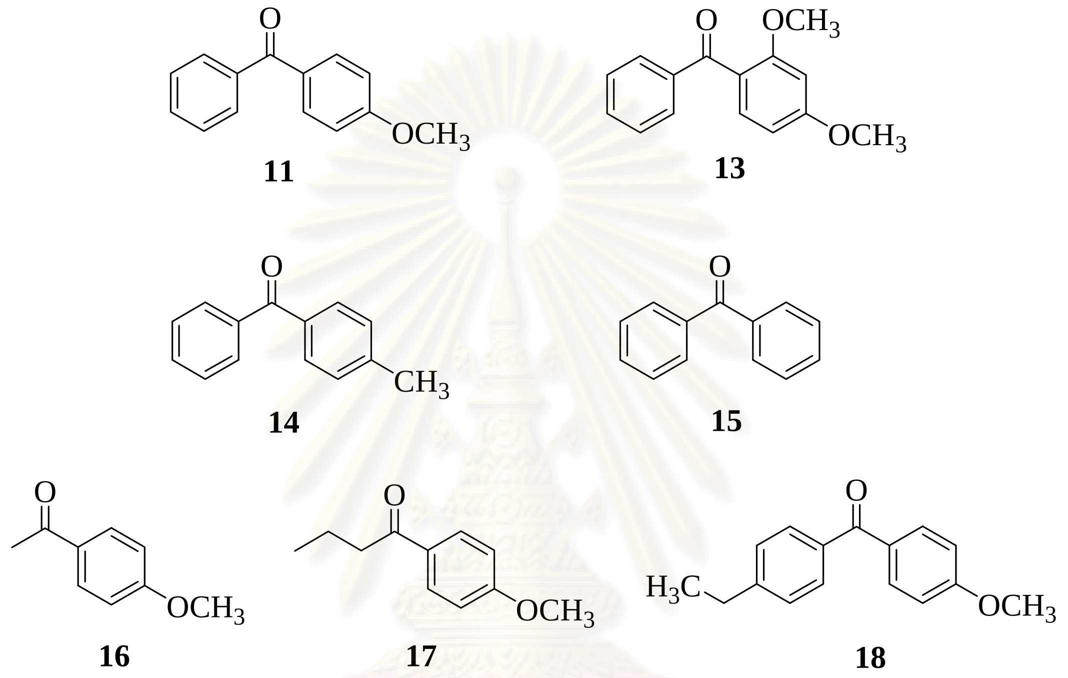

Figure 3.1 Products obtaining from various aromatic compounds and acid chlorides.

4-methoxybenzophenone (11): ^{1}H NMR (CDCl$_3$) δ (ppm): 3.84 (3H, s, ArOC**H$_3$**), 6.93 (2H, d, *J* = 8.67 Hz, Ar**H**), 7.45 (2H, t, *J* = 7.37 Hz, Ar**H**), 7.53 (1H, t, *J* = 7.26 Hz, Ar**H**), 7.69 (2H, d, *J* = 7.43 Hz, Ar**H**), 7.78 (2H, d, *J* = 8.72 Hz, Ar**H**).

2,4-dimethoxybenzophenone (13): ^{1}H NMR (CDCl$_3$) δ (ppm): 3.65 (3H, s, ArOC**H$_3$**), 3.82 (3H, s, ArOC**H$_3$**), 7.12 (1H, d, *J* = 7.83 Hz, Ar**H**), 7.45 (1H, d, *J* = 7.65 Hz, Ar**H**), 7.53 (3H, t, *J* = 7.26 Hz, Ar**H**), 7.60 (1H, s, Ar**H**), 7.78 (2H, d, *J* = 7.05 Hz, Ar**H**).

4-methylbenzophenone (14): ^{1}H NMR (CDCl$_3$) δ (ppm): 2.42 (3H, s, ArC**H$_3$**), 7.25 (2H, t, *J* = 7.84 Hz, Ar**H**), 7.44 (1H, t, *J* = 7.26 Hz, Ar**H**), 7.56 (2H, t, *J* = 7.43 Hz, Ar**H**), 7.70 (2H, d, *J* = 8.12 Hz, Ar**H**), 7.74 (2H, d, *J* = 6.95 Hz, Ar**H**).

benzophenone (15): ^{1}H NMR (CDCl$_3$) δ (ppm): 7.44 (2H, t, *J* = 7.12 Hz, Ar**H**), 7.56 (4H, t, *J* = 7.10 Hz, Ar**H**), 7.78 (4H, d, *J* = 8.12 Hz, Ar**H**).

4-methoxyacetophenone (16): ^{1}H NMR (CDCl$_3$) δ (ppm): 2.62 (3H, s, C$\mathbf{H_3}$C=O), 3.85 (3H, s, ArOC$\mathbf{H_3}$), 6.94 (2H, d, *J* = 8.62 Hz, Ar**H**), 7.85 (2H, d, *J* = 8.74 Hz, Ar**H**).

4-methoxybutyrophenone (17): ^{1}H NMR (CDCl$_3$) δ (ppm): 0.96 (3H, t, *J* = 7.41 Hz, CH$_2$C$\mathbf{H_3}$), 1.64 (2H, q, *J* = 7.32 Hz, CH$_2$C$\mathbf{H_2}$CH$_3$), 2.97 (2H, t, *J* = 7.37 Hz, CH$_2$C$\mathbf{H_2}$C=O), 3.85 (3H, s, ArOC$\mathbf{H_3}$), 6.93 (2H, d, *J* = 8.65 Hz, Ar**H**), 7.86 (2H, d, *J* = 8.70 Hz, Ar**H**).

4-ethyl-(4-methoxybenzophenone) (18): ^{1}H NMR (CDCl$_3$) δ (ppm): 1.24 (3H, t, *J* = 7.21 Hz, CH$_2$C$\mathbf{H_3}$), 2.62 (2H, q, *J* = 7.24 Hz, CH$_2$C$\mathbf{H_3}$), 3.85 (3H, s, ArOC$\mathbf{H_3}$), 6.94 (2H, d, *J* = 8.51 Hz, Ar**H**), 7.25 (2H, d, *J* = 8.23 Hz, Ar**H**), 7.66 (2H, d, *J* = 7.39 Hz, Ar**H**), 7.82 (2H, d, *J* = 8.21 Hz, Ar**H**).

3.4.4 The mechanism of Friedel-Crafts acylation

The mechanism of Friedel-Crafts acylation shown in scheme 3.3 was believed to occur by the same manner as that described for homogeneous reaction employing Lewis acid catalyst [70].

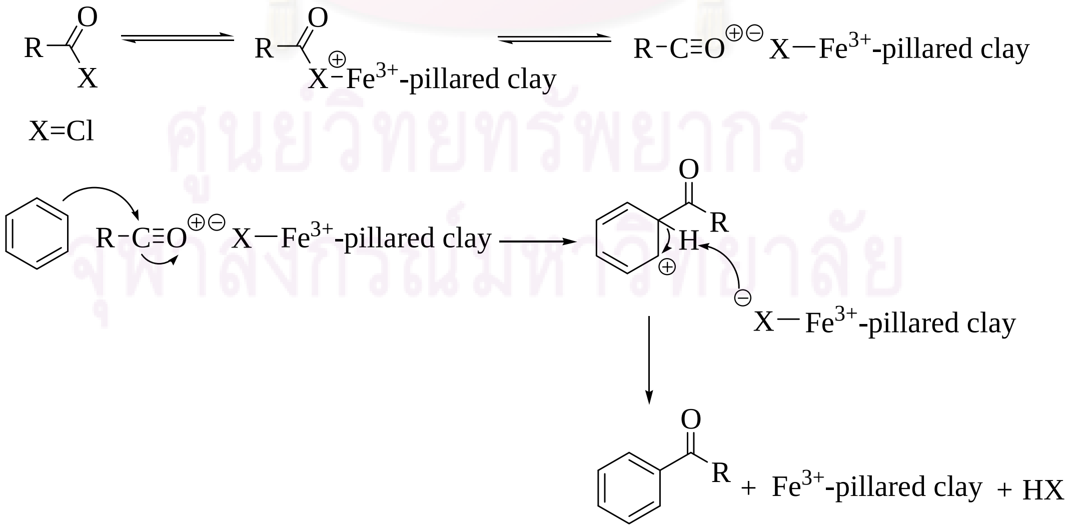

Scheme 3.3 The mechanism of Friedel-Crafts acylation of aromatic compounds on iron oxide-pillared bentonite

The first step, acyl chloride reacted with metal cation of the pillared clay catalyst to form a more electrophilic carbon. The electrophilic acylium ion was attacked by π electrons of aromatic compound. This step destroyed the aromaticity giving the cyclohexadienyl cation intermediate. Removal of the proton from the sp^3 carbon bearing the acyl-group reformed the π electrons of the aromatic C=C and the aromatic system, regenerating the active catalyst and generating HCl [70].

3.4.5 The direct methodology for one-pot synthesis of aryl ketones

The main purpose of this part is to develop a one-pot procedure to prepare aryl ketones from acid halide generated from carboxylic acid and combination of halogenating agent and PPh_3. In fact, the reaction is composed of two steps. The first step is the conversion of carboxylic acids to acid halides, while the second step is Friedel-Crafts acylation between aromatic compounds and acylating agent in the presence of common lewis acids such as $AlCl_3$, $FeCl_3$, *etc*. The general equation can be simplified as shown below.

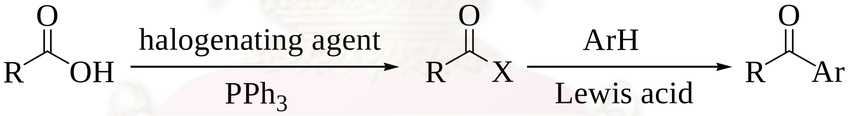

In this study, the optimum conditions for the preparation of aryl ketones were used following the previous work by Kasemsuknimit [71]. The optimum condition for the first step is benzoic acid (1 equiv), Cl_3CCN as halogenating agent (2 equiv) and PPh_3 (2 equiv) in CH_2Cl_2 at RT for 1 h and the optimum condition for the second step is anisole (1 equiv) and $AlCl_3$ (4 equiv) at reflux for 2 h. Under these optimum conditions, it could be applied for a one-pot synthesis of aryl ketones catalyzed by 30 wt% iron oxide-pillared bentonite at reflux for 2 h. A one-pot procedure to prepare aryl ketones is shown below.

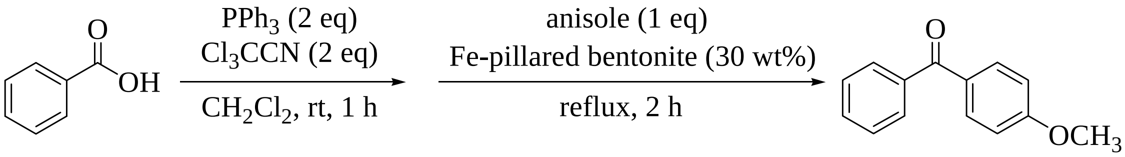

The reaction of benzoic acid with anisole in the presence of iron oxide-pillared bentonite was carried out to furnish the corresponding 4-methoxybenzophenone (**11**) in 78% under this particular condition.

3.4.6 Regenerated catalyst

3.4.6.1 The characterization of regenerated catalyst

The X-ray diffraction patterns of iron oxide-pillared bentonite and regenerated iron oxide-pillared bentonite from Friedel-Crafts acylation are shown in Figure 3.2.

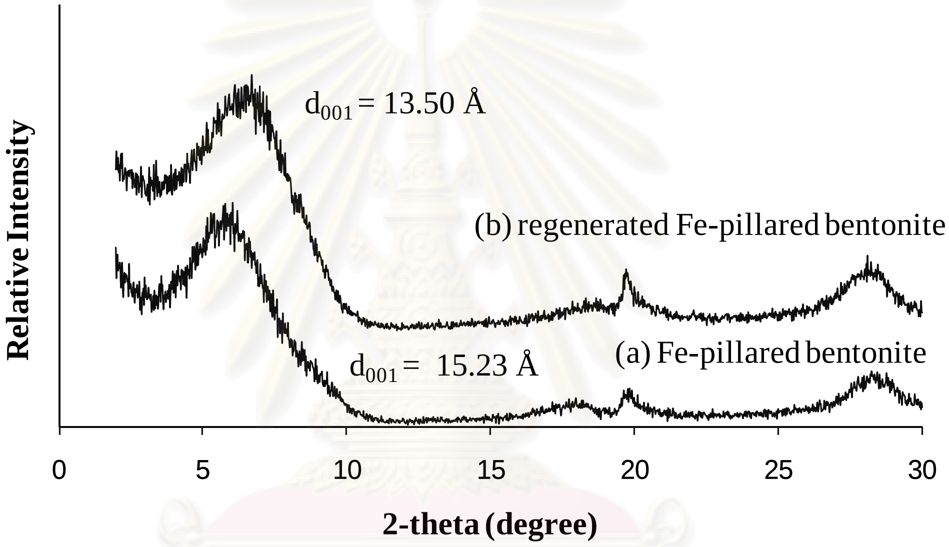

Figure 3.2 XRD patterns of (a) Fe-pillared bentonite and (b) regenerated Fe-pillared bentonite.

After Friedel-Crafts acylation was completed, the clay catalyst was filtered out of the reaction mixture, washed with EtOAc and calcined at 300°C for 5 h. The X-ray diffraction pattern of regenerated iron oxide-pillared bentonite was similar to that of iron oxide-pillared bentonite. The broad (001) peak appeared at the same range (2θ of 6°-8°) as that of fresh iron oxide-pillared bentonite, indicating that the structure of catalyst was preserved upon regeneration process. Although the hightest point of d_{001} was around 13.50 Å that was smaller than the d_{001} of fresh iron oxide-pillared bentonite. The collapse resulted from the re-calcination process and the local heat produced from decomposition of trapped organic species.

3.4.6.2 Nitrogen adsorption-desorption of regenerated catalyst

The nitrogen adsorption-desorption isotherms of iron oxide-pillared bentonite and regenerated iron oxide-pillared bentonite are shown in Table 3.9.

Table 3.9 The BET specific surface area of iron oxide-pillared bentonite and regenerated iron oxide-pillared bentonite for Friedel-Crafts acylation

Entry	Samples	BET specific surface area (m^2/g)
1	Fe-pillared bentonite	155.52
2	Regenerated Fe-pillared bentonite#1	71.87

Table 3.9 shows the BET specific surface area of iron oxide-pillared bentonite and regenerated iron oxide-pillared bentonite. The BET specific surface area of regenerated iron oxide-pillared bentonite was lower than the iron oxide-pillared bentonite. There are two reasons: (i) the re-calcination process at 300°C was not enough to remove all organic residues that could block the pores of the catalyst and (ii) the collapse of the d-spacing also caused the smaller pores; however, re-calcination process at higher 300°C caused the pillared structure change or collapse.

3.4.6.3 Temperature programmed desorption of regenerated catalyst

The total acidity (mmol/g) of iron oxide-pillared bentonite and regenerated iron oxide-pillared bentonite for Friedel-Crafts acylation are compared in Table 3.10.

Table 3.10 The acidity of iron oxide-pillared bentonite and regenerated iron oxide-pillared bentonite for Friedel-Crafts acylation

Entry	Samples	acidity (mmol/g)		Total acidity (mmol/g)
		Weak acid sites	Strong acid sites	
1	Fe-pillared bentonite	0.62	3.11	3.73
2	regenerated Fe-pillared bentonite#1	0.61	2.97	3.58

Table 3.10 exhibits the acidity of iron oxide-pillared bentonite and regenerated iron oxide-pillared bentonite. The acidity of regenerated iron oxide-pillared bentonite was lower than the iron oxide-pillared bentonite. This was due to the remaining organic residues in catalyst pores, possibly the regenerated process at 300°C may not completely destroy or decompose the organic compounds adsorbed on used catalyst.

3.4.6.4 Activity of regenerated iron oxide-pillared bentonite in Friedel-Crafts acylation of anisole with benzoyl chloride

For industrial economy, it is important to investigate the catalytic efficiency of reused catalyst. The regenerated iron oxide-pillared bentonite was used as a catalyst in Friedel-Crafts acylation of anisole with benzoyl chloride. The results are presented in Table 3.11.

Table 3.11 The results of regenerated iron oxide-pillared bentonite in Friedel-Crafts acylation

Entry	Run (times)	% Yield[a]
1	1	quant
2	2	93
3	3	88

Reaction conditions: anisole 1 mmol, benzoyl chloride 3 mmol, 30 wt% catalyst to anisole at refluxing 1,4-dioxane for 2 h.

[a] The yield was quantified by ^{1}H NMR using toluene as an internal standard.

The regenerated iron oxide-pillared bentonite was used for the next run. The regenerated iron oxide-pillared bentonite exhibited lower activity than the original iron oxide-pillared bentonite. This result was well corresponded to that of the collapse of d_{001} basal spacing, lower BET surface area and lower acidity.

3.4.7 Conclusion

The catalytic activities of iron oxide-pillared bentonite were performed for Friedel-Crafts acylation of anisole with benzoyl chloride. The optimized conditions were the mole ratio of anisole to benzoyl chloride of 1:3 and 30 wt% iron oxide-pillared bentonite to anisole in refluxing 1,4-dioxane for 2 h. The reaction could be performed to furnish 4-methoxybenzophenone (**11**) in almost quantitative yield with excellent selectivity. The optimized conditions were also applied for various aromatic compounds and acid chlorides. From the variation of aromatic compounds, the yields of aromatic ketones depended on the steric and electronic effects of starting aromatic compounds. From the variation of acid chlorides, the type of acid chlorides did not affect the yield. This catalytic system could be reused up to three times without appreciable loss of activity.

CHAPTER IV

THE CONVERSION OF EPOXIDES TO ACETONIDES BY CLAY CATALYSTS

4.1 Introduction

4.1.1 The importance of epoxides and acetonides

Acetalization, ketalization and thioacetalization are the most useful protecting methods for carbonyl functional groups of aldehydes and ketones. Among those mentioned protecting methodolies, acetonides (1,3-dioxolanes) are widely used in organic synthesis [72], natural product synthesis and synthesis of valuable fine chemicals for the production in fragrance, steroid, polymer and pharmaceutical industries [73-75].

4.1.2 Literature review on the synthesis of 1,3-dioxolanes

4.1.2.1 Reaction with homogeneous catalysts

Epoxides can be directly converted to 1,3-dioxolanes by the aids of Lewis acid catalysts. In 1993, Torok and co-workers reported the use of $BF_3.OEt_2$ for the reaction of ketones with epoxides yielding the corresponding 1,3-dioxalones. $BF_3.OEt_2$ was found to be the effective catalyst for the reaction of 4-*tert*-butylcyclohexanone with propylene oxide [76].

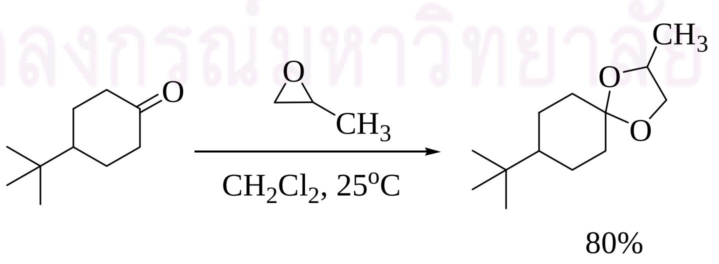

In 1998, Iranpoor and Zeynizadeh reported the use of $TiO(TFA)_2$ and $TiCl_3(OTf)$ for the conversion of epoxides to acetonides in excellent yields. These two known solid titanium(IV) compounds were stable and could be prepared from $TiCl_4$.

Epoxides with both electron withdrawing and electron-releasing groups were treated with these catalysts in acetone. $TiCl_3(OTf)$ was reported to be more efficient than $TiO(TFA)_2$ [77].

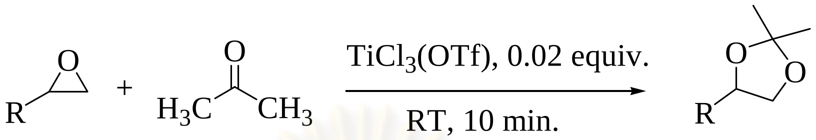

In the same year, Iranpoor and Kazemi addressed the conversion of epoxides using anhydrous $RuCl_3$ affording the corresponding 1,3-dioxolanes. For instance, the reaction of 2-(vinyloxymethyl)oxirane with acetone catalyzed by anhydrous $RuCl_3$ yielded 2,2-dimethyl-4-(vinyloxymethyl)-1,3-dioxolane in 87%. This catalytic procedure could be applied for various epoxides containing both electron withdrawing and electron releasing groups at refluxing acetone in high yields [78].

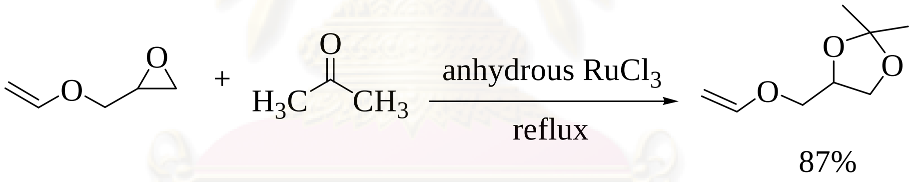

Recently, bismuth compounds have attracted the methodologists' attention due to their good stability, low cost and low toxicity. In 2001, Mohammadpoor and co-workers reported the synthesis of 1,3-dioxolanes from epoxides using bismuth(III) salts. An efficient method was performed for the reaction of styrene oxide with acetone using $BiCl_3$, $Bi(OTf)_3$ and $Bi(TFA)_3$ affording the corresponding 2,2-dimethyl-4-phenyl-1,3-dioxolanes in excellent yields. $Bi(OTf)_3$ showed better efficient catalytic activity than $Bi(TFA)_3$ and $BiCl_3$ [79].

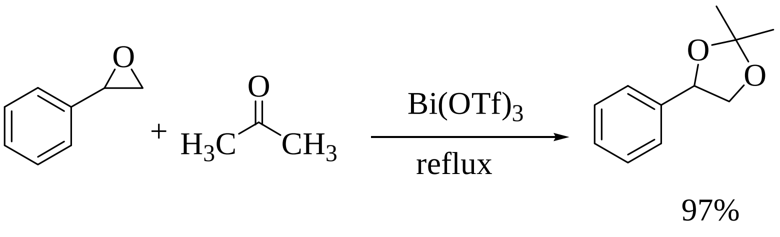

In 2003, Vyvyan and co-workers reported the synthesis of benzoxocane-containing natural products. The formation of 2,2-dimethyl-1,3-dioxolanes catalyzed by anhydrous $SnCl_2$ was performed in good to excellent yields. The 2-((*S*)-4-(2,2,5,5-tetramethyl-1,3-dioxolan-4-yl)butan-2-yl)phenol was formed when acetone was added to 2-((*S*)-4-(2,3,3-trimethyloxiran-2-yl)butan-yl)phenol and anhydrous $SnCl_2$ in chloroform [80].

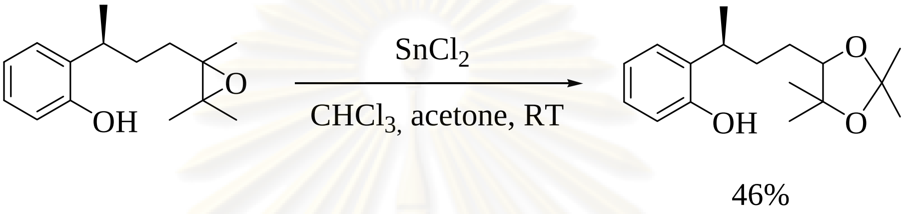

Recently, $Er(OTf)_3$ has been introduced due to its very environmentally friendly catalyst for acid-catalyzed reactions. In 2005, Procopio and co-workers reported the use of $Er(OTf)_3$ for the conversion of epoxides to acetonides in high yields. A mild and efficient procedure was successfully performed for the conversion of styrene oxide to 2,2 dimethyl-1,3-dioxolane catalyzed by the catalytic amount of $Er(OTf)_3$ (0.1 mol%) at room temperature for 30 min. The procedure could be applied for other epoxides and carbonyl compounds [81].

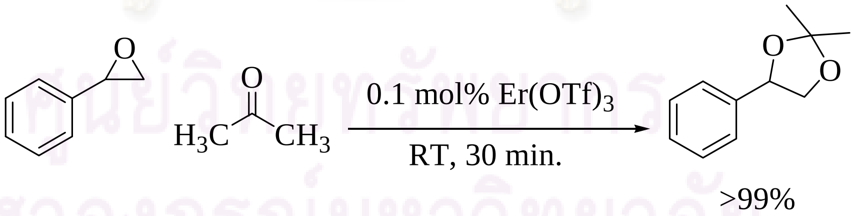

In 2008, Saha and co-workers reported that $FeCl_3$ catalyzed the synthesis of acetonides from epoxides. This communication described an efficient synthesis of acetonides [82].

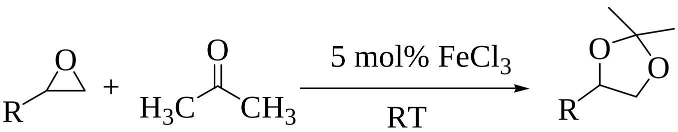

The reaction of 2-(phenoxymethyl)oxirane with acetone was screened utilizing 5 mol% of anhydrous $FeCl_3$ at room temperature for 4.5 h. The reaction proceeded smoothly to give 2,2-dimethyl-4-(phenoxymethyl)-1,3-dioxolane [82].

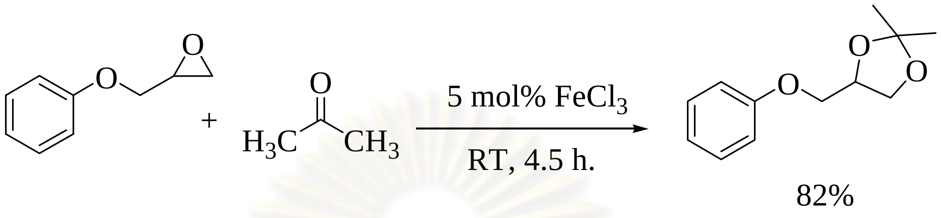

In 2008, Zeynizadeh and Sadighnia addressed the conversion of epoxides to acetonides using phosphomolybdic acid (PMA) as a catalyst. With 0.1-0.2 mol% of PMA, the reaction of styrene oxide with acetone was well proceeded affording the corresponding 2,2-dimethyl-1,3-dioxolanes in good to excellent yields. The reactions were successfully performed at room temperature for 2 min [83].

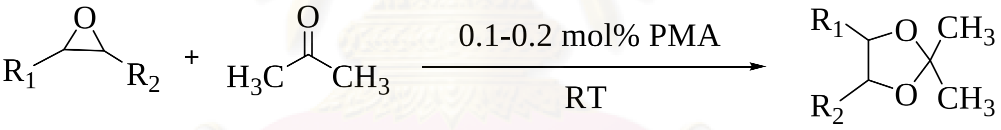

4.1.2.2 Reaction with heterogeneous catalysts

Heterogeneous catalysts are important in organic synthesis. The development of an efficient heterogeneous catalyst for the formation of 1,3-dioxolanes is another important goal for organic synthesis and industrial point of view.

In 1996, Ponde and co-workers reported an efficient reaction of various ketones and aldehydes with ethane-1,2-dithiol or ethane-1,2-diol by kaolinite clay affording the corresponding 1,2-dithioxolane or 1,3-dioxolane derivatives, respectively in high yields [84].

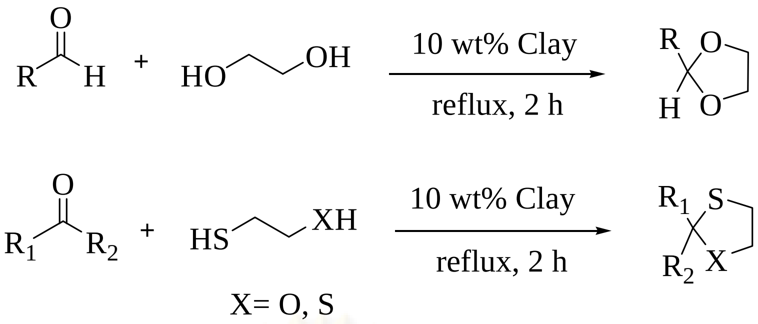

In 1998, Ballini and co-workers reported the conversion of epoxides to 1,3-dioxolanes using zeolite HSZ 360 and offered many advantages over the existing methodologies. For instance, the advantage of zeolite HSZ 360 catalyst is the ease of work up, easy reusable catalyst and mild reaction conditions. The reaction of cyclohexene oxide with ethylene glycol in toluene was screened utilizing 0.2 g of zeolite HSZ-360 as a catalyst. The reaction proceeded smoothly to give 1,3-dioxolane in high yield [85].

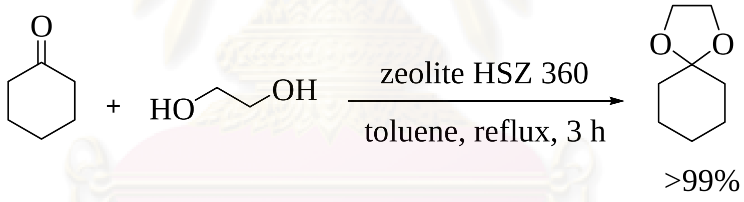

In 2001, Bucsi and co-workers tested the catalytic activity of various types of catalysts such as SiW: $H_4[SiW_{12}O_{40}]$, K10 montmorillonite and BF_3 for the synthesis of 1,3-dioxolanes from ketones and oxiranes. K10 montmorillonite showed the best catalyst for this reaction [86].

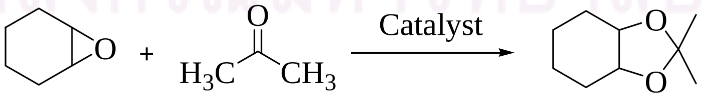

Catalyst	Reaction time (h)	Isolated yield (%)
SiW: $H_4[SiW_{12}O_{40}]$.	3	58
K 10 montmorillonite	2	75
BF_3	2	40

In 2005, Ledneczki and co-workers reported the use of SAC-13 solid superacid in the synthesis of cyclic acetals. High catalytic activity and selectivity in the synthesis of cyclic acetals was observed. Various types of carbonyl compounds could be reacted with propane-1,3-diol and ethane-1,2-diol to form 1,3-dioxanes and 1,3-dioxolanes, respectively in good to high yields [87].

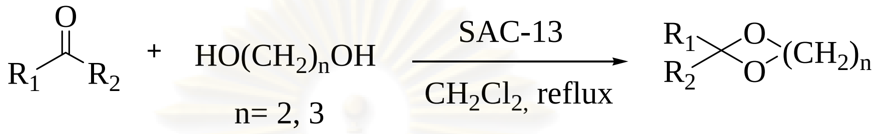

The reaction of pentanal and ethane-1,2-diol was catalyzed by SAC-13 solid superacid at reflux for 1 h affording the corresponding 2-butyl-1,3-dioxolane in excellent yield [87].

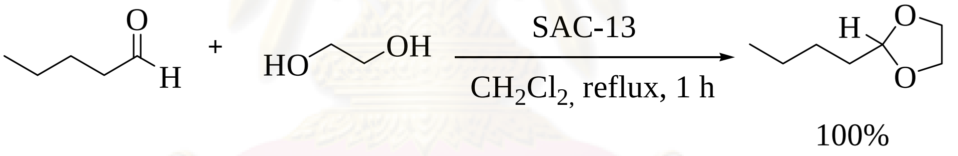

In 2004, Wu and co-workers reported the use of ionic liquid (*N*-methylimidazolium tetrafluoroborate ([Hmim]BF_4)) and Brønsted acid for protection of a variety of carbonyl compounds by the formation of ketals or acetals. [88].

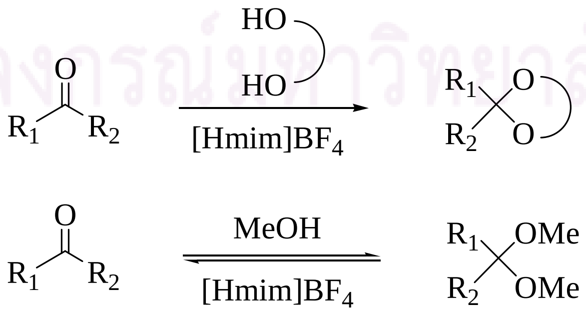

The use of ionic liquid ([Hmim]BF_4) for the reaction of *n*-hexanal with neopentyl glycol was successfully performed with quantitative yield and good selectivity.

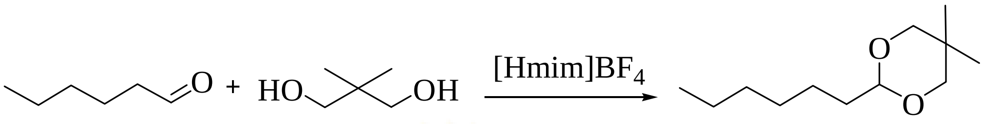

98%

The stable and inexpensive ionic liquids have been prepared from choline chloride and $ZnCl_2$. choline chloride. $xZnCl_2$ is moisture-stable, cheap and easy to handle. In 2006, Duan and co-workers reported that benzyltrimethylammonium chloride.$2ZnCl_2$ and choline chloride. $xZnCl_2$ (x=1-3) were very efficient catalysts for the synthesis of 1,3-dioxanes and 1,3-dioxolanes [89].

$Y = aZnCl_3^- + bZn_2Cl_5^- + cZn_3Cl_7^-, a + b + c = 1$

Choline chloride. $xZnCl_2$ Benzyltrimethylammonium chloride. $2ZnCl_2$

The reaction of neopentyl glycol and benzaldehyde catalyzed by choline chloride.$xZnCl_2$ (x=1-3) at 25°C for 10 h afforded the corresponding 5,5-dimethyl-2-phenyl-1,3-dioxane in high yield [89].

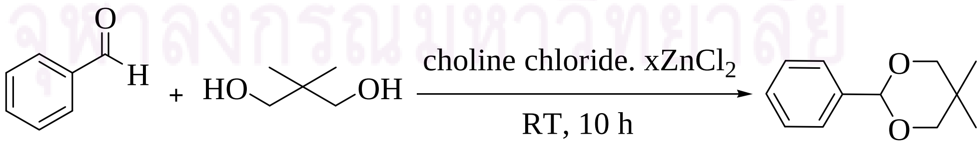

80-83%

In 2008, Srivastava and co-workers reported the use of Al-SBA-15 as a catalyst for the reaction of various carbonyl compounds with catechol. This procedure described an efficient synthesis of 1,3-benzodioxoles. An important molecule such as

2,2-disubstituted 1,3-benzodioxoles and 2-substituted 1,3-benzodioxoles were obtained from these reations [90].

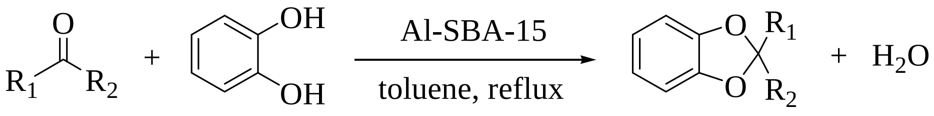

The reaction of catechol with hexane-2,5-dione was screened utilizing Al-SBA-15 as catalyst. The mono-benzodioxole product was obtained in 10 wt% Al-SBA-15 and 1:2 molar ratio hexane-2,5-dione to catechol. The reaction proceeded smoothly to give 60% of 2-methyl-2-(3-oxobutyl)-1,3-benzodioxole (mono benzodioxole product) and 40% of 2,2'-dimethyl-2,2'-ethylenebis(1,3-benzodioxole) (bi-benzodioxole product).

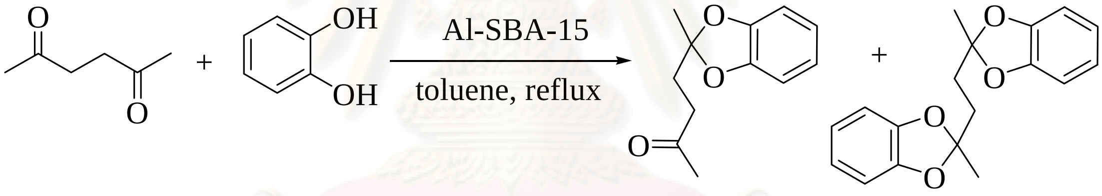

An efficient procedure for protecting *N-tert*-butoxy carbonyl [N(Boc)] amino alcohols as acetonides and the deprotection of acetonides using Al-SBA-15 and 2,2-dimethoxypropane (DMP) was successfully performed.

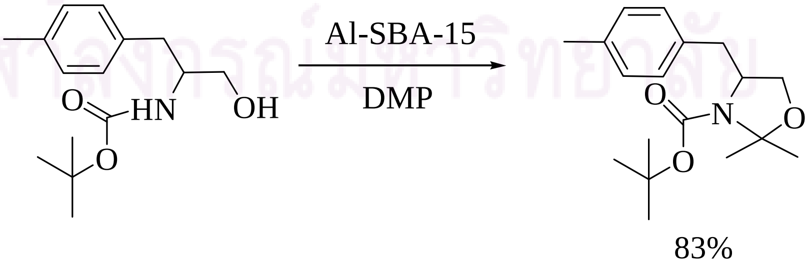

Oxathioacetalization has attracted intensive interests in organic synthesis due to their stabilities under reaction conditions, ease of formation and removal. In 2009, Shirini and co-workers reported the use of silica sulfuric acid (SSA) as an efficient catalyst in the oxathioacetalization of ketones and aldehydes with 2-mercaptoethanol affording the corresponding 1,3-oxathiolane products and the deprotection of the obtained products in excellent yields [91].

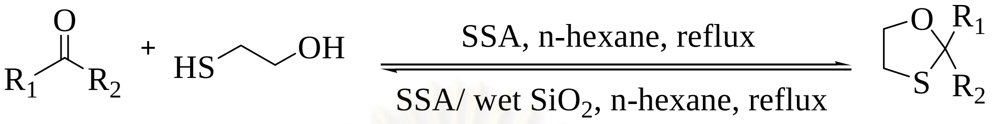

In 2009, Amrute and co-workers reported the successful synthesis of 1,3-dioxolane and 1,3-dioxane catalyzed by MoO_3/SiO_2. The advantages of MoO_3/SiO_2 catalyst are inexpensive, environmentally friendly and reusable without loss of activity and product selectivity [92].

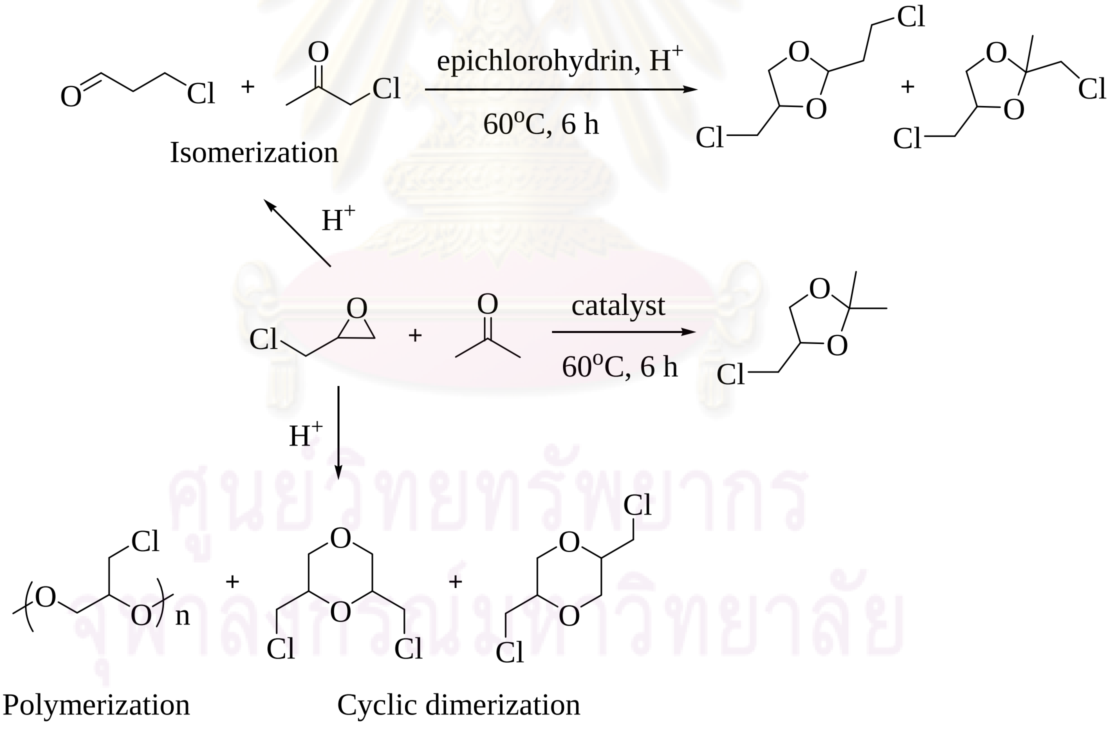

4.2 Scope of this study

Previous literature reviews revealed the evidence that homogeneous catalysts and some heterogeneous catalysts could be employed as a good catalyst for the conversion of epoxide to 1,3-dioxolanes. However, the disadvantages of some catalysts are air- and moisture-sensitive catalysts, high temperatures required, the use of expensive and toxic catalysts and long reaction time and difficulty of separation and recovery. The main features of this research focused on the methodology toward the conversion of epoxide such as cyclic epoxides, epoxides with ethereal linkage and terminal aliphatic epoxides to more valuable products catalyzed by the synthesized iron oxide-pillared clays and metal chloride-impregnated aluminium oxide-pillared clays catalysts.

4.3 Experimental

4.3.1 General procedure:

This section provides general information of general and/or specific reaction conditions and spectral data for compounds along with a representative ^{1}H NMR. The reactions were monitored by TLC on aluminium sheets precoated with silica gel (Merck's, Kieselgel 60 PF_{254}). *Buchi* rotary evaporator connected to a vacuum pump was used for removal of solvents.

Chromatography: Gas chromatographic analysis was carried out on a Shimadzu Gas Chromatography instrument equipped with a flame ionization detector (FID) with N_2 as a carrier gas and a 30-m long HP-5 column (0.25-mm outer diameter, 0.25 µm film thickness). Column chromatography was performed on silica gel (Merck's, kieselgel 60 G Art 7754 (70-230 mesh).

^{1}H NMR spectra were recorded at 400 MHz on a Varian spectrometer. Chemical shifts are reported in ppm from tetramethylsilane with the solvent residue of $CDCl_3$ (7.26 ppm).

Chemicals: All solvents were purified according to the procedures described in the standard methodology except for reagents and solvents that are reagent grade. The reagents are listed as follows:

1. Styrene oxide (Fluka Chemika, 97%)
2. 1-Dodecene oxide (Fluka Chemika, 95%)
3. Cyclohexene oxide (Fluka Chemika, 98%)
4. Butyl-glycidyl ether (Fluka Chemika, 95%)
5. *tert*-Butyl-glycidyl ether (Fluka Chemika, 97%)
6. 2,3-Epoxypropyl isopropylether (Merck, 98%)

7. 2,3-Epoxypropyl phenylether epoxy (Merck, 98%)
8. Acetone (commercial grade)
9. Ethyl acetate (Lab-Scan, reagent grades)
10. Diethyl ether (Merck, reagent grade)
11. Acetophenone (Fluka Chemika, 97%)
12. Benzaldehyde (Baker analyzed)

4.3.2 Syntheses

4.3.2.1 The general procedure for the conversion of styrene oxide to its acetonide

A typical reaction mixture of styrene oxide (1 mmol) and acetone (3 mL) was added to a round bottom flask with 10 wt% of catalyst to styrene oxide at room temperature. The solution was continuous stirred for desired time and temperature. After the specific time or the reaction was finished, the catalyst was simply filtered out of the mixture, and washed the product out with EtOAc. The solvent was evaporated to dryness under reduced pressure to afford the product. The product was analyzed by GC with the addition of an exact amount of an appropriate internal standard (cyclohexanone).

4.3.2.2 Optimum conditions for the conversion of styrene oxide to its acetonide

Effect of the amount of catalyst

The conversion of styrene oxide to acetonide was carried out according to the general procedure, but the amount of catalyst was changed to 2, 5, 10 and 30 wt% of catalyst to styrene oxide.

Effect of reaction time

The conversion of styrene oxide to acetonide was performed according to the general procedure, but the reaction time was changed to 1, 3 and 5 min.

Effect of reaction temperature

The conversion of styrene oxide to acetonide was carried out according to the general procedure, but the reaction temperature was changed to 30°C (RT) and 60°C.

Effect of the amount of acetone

The conversion of styrene oxide to acetonide was performed according to the general procedure, but the amount of acetone was changed to 0.5, 1 and 2 mmol.

Effect of type of organic solvents

The conversion of styrene oxide to acetonide was carried out according to the general procedure, but using different organic solvents including CH_2Cl_2, hexane, EtOAc, 1,4-dioxane, CH_3CN and DMF.

4.3.2.3 Study on the reaction of other epoxides with acetone to acetonides

1-Dodecene oxide, cyclohexene oxide, 2,3-epoxypropyl isopropylether or 2,3-epoxypropyl phenylether

According to the general procedure, the conversion of various epoxides such as 1-dodecene oxide, cyclohexene oxide, 2,3-epoxypropyl isopropylether or 2,3-epoxypropyl phenylether to the corresponding acetonides were experimented using iron oxide-pillared bentonite as catalyst at 60°C for 2 h.

Butyl glycidyl ether and *tert*-butyl glycidyl ether

According to the general procedure of the conversion of butyl glycidyl ether and *tert*-butyl glycidyl ether to acetonides using iron oxide-pillared bentonite as catalyst were examined. The reaction temperature (30°C and 60°C), reaction time (15 min, 30 min, 2 h and 4 h) and the amount of catalyst (10 wt% and 30 wt% of catalyst to styrene oxide) were varied.

4.3.2.4 Study on the conversion of styrene oxide with other carbonyl compounds to 1,3-dioxolanes

To observe the scope of the reaction, the conversion of styrene oxide with other carbonyl compounds such as acetophenone and acetaldehyde was conducted. The chosen conditions included using iron oxide-pillared bentonite as catalyst in and CH_2Cl_2 at refluxing CH_2Cl_2 (40°C) for 2 h.

4.3.2.5 Reuse of catalysts

The used iron oxide-pillared clays were regenerated by calcination at 300°C for 5 h. The structural characterization of the regenerated iron oxide-pillared bentonite was characterized using XRD, N_2-adsorption/desorption and NH_3-TPD technique. Then, the regenerated iron oxide-pillared bentonite was tested as a catalyst in the conversion of styrene oxide to acetonide.

4.4 Results and discussion

4.4.1 Catalytic activities of iron oxide-pillared clay and metal chloride-impregnated aluminium oxide-pillared clays for the conversion of epoxides to 1,3-dioxolanes

The synthesis of 2,2-dimethyl-4-phenyl-1,3-dioxolane (**19**) from styrene oxide with acetone was selected for testing the catalytic activity of catalysts (iron oxide-pillared clay and metal chloride-impregnated aluminium oxide-pillared clays). Various factors were carefully scrutinized to optimize the conditions for the preparation of 1,3-dioxolane. The reaction time, the amount of acetone, the amount of catalyst and type of organic solvents were varied to search for the optimal conditions.

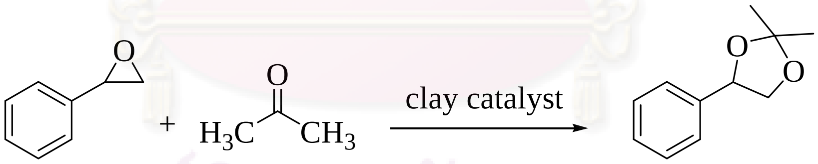

(19)

Compound **19** was identified by ^{1}H NMR spectroscopic data compared with authentic specimen synthesized. The preparation of authentic sample **19** involved the reaction of styrene oxide with acetone using $FeCl_3$ as a catalyst [81]. The characterization of conpound **19**; ^{1}H NMR ($CDCl_3$) δ (ppm): 1.48 (3H, s), 1.52 (3H, s), 3.67 (1H, t), 4.27 (1H, dd, J = 8.6, 6.4 Hz), 5.05 (1H, dd, J = 8.6 Hz), 7.31 (5H, m).

Other epoxides: cyclohexene oxide, 1-dodecene oxide, butyl glycidylether, *tert*-butyl glycidylether, 2,3-epoxypropyl isopropylether and 2,3-epoxypropylphenyl ether, and other carbonyl compounds: acetophenone, acetaldehyde and cyclohexanone were utilized in order to examine the scope of the catalytic activity of the reaction.

4.4.1.1 Effect of raw clays (bentonite, hectorite and taeniolite) and iron oxide pillared clays on the reactivity for the conversion of styrene oxide to acetonide

The catalytic activity of iron oxide-pillared clays (Fe-pillared clays): iron oxide-pillared bentonite, iron oxide-pillared taeniolite and iron oxide-pillared hectorite were compared with montmorillonite, Li-taeniolite, raw hectorite and iron oxide (Fe_2O_3, hematite) for the conversion of styrene oxide to acetonide. Conditions for this reaction were 30 wt% catalyst to styrene oxide at 60°C for 24 h. The results are shown in Table 4.1. All iron oxide-pillared clays gave much higher yield than pure clays and Fe_2O_3.

Table 4.1 Effect of raw clays, iron oxide-pillared clays on the reactivity for the conversion of styrene oxide to acetonide

Entry	**Catalysts**	**BET surface area** (m^2/g)	**Acidity (mmol/g)**	**% Yield**	**% Styrene oxide (recovered)**	**MB (%)**
1	None	-	-	0	99.9	99.9
2	montmorillonite	65.05	1.26	trace	97.5	97.5
3	Raw hectorite	57.11	0.55	trace	98.7	98.7
4	Li- taeniolite	3.53	0.43	trace	98.5	98.5
5	Fe_2O_3	-	-	22.5	76.2	98.7
6	Fe-pillared bentonite	155.52	3.73	quant	0	100.0
7	Fe-pillared hectorite	122.30	2.16	quant	0	100.0
8	Fe-pillared taeniolite	20.33	1.52	90.0	0	90.0

Reaction conditions: styrene oxide 1 mmol, acetone in excess (3 mL), 30 wt% catalyst to styrene oxide at 60°C for 24 h.

When the reaction was performed without catalyst, no product was observed. Three iron oxide-pillared clays were screened to observe their potentially catalytic ability. It was disclosed that all iron oxide-pillared clays afforded good yield for conversion of styrene oxide to acetonide at 60°C for 24 h without contamination of undesired products. Iron oxide-pillared clays gave much higher yield than pure clays of all types. This result well corresponded with the temperature programmed desorption experiment to determine acidity and nitrogen adsorption-desorption experiment to observe surface area. Iron oxide-pillared clays gave much higher acidity and BET surface area than pure clays. The amount of acidity and BET surface area of iron oxide-pillared bentonite, iron oxide-pillared hectorite and iron oxide-pillared taeniolite were higher than montmorillonite, raw hectorite and raw taeniolite, respectively. This manifestly revealed that types of clays greatly affected on the catalytic activity.

4.4.1.2 Comparative study on the effect of iron oxide-pillared bentonite, iron oxide-pillared hectorite and iron oxide-pillared taeniolite for the conversion of styrene oxide to acetonide

The comparative study on the effect of iron oxide-pillared clays was observed. The results are shown in Table 4.2.

Table 4.2 Comparative study on the effect of iron oxide-pillared bentonite, iron oxide-pillared hectorite and iron oxide-pillared taeniolite for the conversion of styrene oxide to acetonide

Entry	Time	% Yield of 1 using Fe-pillared bentonite	% Yield of 1 using Fe-pillared hectorite	% Yield of 1 using Fe-pillared taeniolite
1	5 min	94.1	35.2	11.2
2	15 min	-	65.6	52.7
3	30 min	-	83.3	77.4
4	2 h	-	89.6	86.2

Reaction conditions: styrene oxide 1 mmol, acetone in excess (3 mL), 10 wt% catalyst to styrene oxide at RT (30°C).

The comparative study on the effect of the reaction time of three catalysts (iron oxide-pillared bentonite, iron oxide-pillared hectorite and iron oxide-pillared taeniolite) for the conversion of styrene oxide to acetonide at RT (30°C) by 10 wt% catalyst to styrene oxide was conducted. The amount of the obtained product was increased when reaction time increased. Among those iron oxide-pillared clays examined, iron oxide-pillared bentonite provided the highest yield of **19**. The iron oxide-pillared bentonite provided the excellent yield within 5 min revealing its remarkably efficient catalyst for the conversion of styrene oxide to acetonide. These observed results were corresponded to the acidity and BET surface area. Iron oxide-pillared bentonite had the highest acidity and BET surface area (Table 4.1, entry 6). Therefore, the following study will concentrate on iron oxide-pillared bentonite as a catalyst for the conversion of epoxide to acetonide.

4.4.1.3 Effect of metal chloride-impregnated aluminium oxide-pillared bentonite on the reactivity for the conversion of styrene oxide to acetonide

The catalytic activity of metal chloride-impregnated aluminium oxide-pillared bentonites ($LaCl_3$/Al-PLC, $NdCl_3$/Al-PLC, $CeCl_3$/Al-PLC, $GdCl_3$/Al-PLC, $YbCl_3$/Al-PLC and $DyCl_3$/Al-PLC) was observed. Some metal chloride-impregnated aluminium oxide-pillared bentonite catalysts have been documented to be effective in conversion of styrene oxide to acetonide. Six synthesized metal chloride-impregnated aluminium oxide-pillared bentonite catalysts were explored for their capability on the conversion of styrene oxide to **19**. Conditions for this reaction were 30 wt% catalyst to styrene oxide at 60^{o}C for 24 h. The results are shown in Table 4.3.

Table 4.3 Effect of metal chloride-impregnated aluminium oxide-pillared bentonite on the reactivity for the conversion of styrene oxide to acetonide

Entry	**Catalysts**	**Acidity (mmol/g)**	**% Yield**	**% Styrene oxide (recovered)**	**MB (%)**
1	Al-PLC	1.67	trace	96.1	96.1
2	$NdCl_3$/Al-PLC	3.50	95.0	5.4	100.4
3	$CeCl_3$/Al-PLC	3.06	87.5	3.1	90.6
4	$YbCl_3$/Al-PLC	1.97	59.2	34.2	93.4
5	$DyCl_3$/Al-PLC	2.12	53.4	47.5	100.9
6	$GdCl_3$/Al-PLC	1.83	50.0	52.7	102.7
7	$LaCl_3$/Al-PLC	2.17	48.8	51.1	99.9

Reaction conditions: styrene oxide 1 mmol, acetone in excess (3 mL), 30 wt% catalyst to styrene oxide at 60°C for 24 h.

Table 4.3 demonstrates the comparative study on the effect of metal chloride-impregnated aluminium oxide-pillared bentonites. The yield of **19** obtained from the reaction catalyzed by $NdCl_3$/Al-PLC (entry 2) was more than those achieved by other metal chloride-impregnated aluminium oxide-pillared bentonite. This result was also well matched with the acidity, $NdCl_3$/Al-PLC exhibited the highest acidity; therefore expressing the highest activity. It could thus be concluded that types of rare earth metal chlorides affected on the catalytic activity in this reaction.

The results obtained from tables 4.2 and 4.3 clearly displayed the effect of iron oxide-pillared bentonite and $NdCl_3$/Al-PLC for the conversion of styrene oxide to **19**. The iron oxide-pillared bentonite provided excellent yield at RT by 10 wt% catalyst to styrene oxide for 5 min (Table 4.2, entry 1), whereas $NdCl_3$/Al-PLC showed good yield using 30 wt% catalyst to styrene oxide at 60°C at for 24 h (Table 4.3, entry 2). When other parameters (reaction temperature, reaction time and the amount of catalyst) for the preparation of acetonides were considered, It could be concluded that the iron oxide-pillared bentonite was much more efficient than $NdCl_3$/Al-PLC for the conversion of styrene oxide to **19**. Thus, the structure and component of clays markedly affected on the catalytic activity of this reaction. The following study will concentrate on iron oxide-pillared bentonite as a catalyst for the conversion of epoxide to acetonide.

4.4.2 Optimum conditions study on the conversion of styrene oxide to acetonide by iron oxide-pillared bentonite

Utilizing iron oxide-pillared bentonite as a catalyst, further investigation was focused on the amount of catalyst, the amount of acetone, the reaction time and types of organic solvents that may influence the reactivity of the reaction.

4.4.2.1 Effect of the amount of catalyst for the conversion of styrene oxide to acetonide

The amount of catalyst normally influenced the performance of the reaction. The variation of the amount of iron oxide-pillared bentonite: 2, 5, 10 and 30 wt% were used to search for the appropriate amount of catalyst in the conversion of styrene oxide to **19**. The results are presented in Table 4.4.

Table 4.4 Effect of the amount of iron oxide-pillared bentonite for the conversion of styrene oxide to acetonide

Entry	Fe-pillared bentonite	% Yield	% Styrene oxide (recovered)	MB (%)
1	2 wt%	83.1	17.2	100.3
2	5 wt%	90.5	7.6	98.1
3	10 wt%	94.1	0	94.1
4	30 wt%	94.8	0	94.8

Reaction conditions: styrene oxide 1 mmol, acetone in excess (3 mL), iron oxide-pillared bentonite varied at RT (30°C) for 5 min.

According to the results presented, when the amount of catalyst increased from 2 to 10 wt%, the yield of **19** was increased. Almost quantitative yield of **19** was achieved when 10 wt% of iron oxide-pillared bentonite to styrene oxide was employed. In addition, when the amount of catalyst was decreased from 10 wt%, the lower yield was detected. Using 30 wt% of catalyst, the yield of **19** was more or less the same as that using 10 wt% of catalyst. It could thus be summarized that the suitable amount of iron oxide-pillared bentonite was 10 wt%.

4.4.2.2 Effect of the reaction time for the conversion of styrene oxide to acetonide

The effect of the reaction time for the conversion of styrene oxide to acetonide catalyzed by iron oxide-pillared bentonite was varied from 1 to 5 min. The results are presented in Table 4.5.

Table 4.5 Effect of the reaction time for the conversion of styrene oxide to acetonide catalyzed by iron oxide-pillared bentonite

Entry	Time (min)	% Yield	% Styrene oxide (recovered)	MB (%)
1	1	65.4	21.4	86.8
2	3	92.0	10.6	102.6
3	5	94.1	0	94.1

Reaction conditions: styrene oxide 1 mmol, acetone in excess (3 mL), 10 wt% iron oxide-pillared bentonite to styrene oxide at RT (30°C).

The conversion of styrene oxide to **19** catalyzed by iron oxide-pillared bentonite could be accomplishly performed at RT as a single product in excellent yield. The suitable reaction time for the conversion of styrene oxide to **19** was 5 min.

4.4.2.3 Effect of the amount of nucleophile for the conversion of styrene oxide to acetonide

The variation of the amount of nucleophile was examined since some nucleophiles have high cost and toxic. Thus, it should avoid employing in an excess amount. The objective of this study was to try to minimize the amount of nucleophile while maintaining the efficiency of the reaction: CH_2Cl_2 was chosen as a reaction medium. The effect of the variation of the amount of acetone on the conversion of styrene oxide to **19** catalyzed by iron oxide-pillared bentonite was examined and the results are presented in Table 4.6.

Table 4.6 Effect of the amount of acetone for the conversion of styrene oxide to acetonide catalyzed by iron oxide-pillared bentonite

Entry	**Acetone (mmol)**	**% Yield**	**% Styrene oxide (recovered)**	**MB (%)**
1	0.5	34.8	65.5	100.3
2	1	39.0	62.4	101.4
3	2	quant	0	100.0

Reaction conditions: styrene oxide 1 mmol, 10 wt% iron oxide-pillared bentonite to styrene oxide, CH_2Cl_2 (3 mL), acetone (varied) at RT (30°C) for 5 min.

When acetone 2 mmol was used, the reaction gave almost quantitative yield. In addition, when the amount of acetone was decreased from 2 mmol, the yield was declined, possibly due to less amount of nucleophile present. Thus in this research, the amount of acetone 2 mmol was chosen for further study on the optimum conditions of this reaction.

4.4.2.4 Effect of solvent for the conversion of styrene oxide to acetonide

Solvent was another important factor influencing for conversion of styrene oxide to acetonide. Six diverse solvents investigated including CH_2Cl_2, hexane, EtOAc, 1,4-dioxane, CH_3CN and DMF. The results are shown in Table 4.7.

Table 4.7 Effect of solvent for the conversion of styrene oxide to acetonide catalyzed by iron oxide-pillared bentonite

Entry	**Solvent**	**% Yield**	**% Styrene oxide (recovered)**	**MB (%)**
1	CH_2Cl_2	quant	0	100.0
2	hexane	60.0	34.4	94.4
3	EtOAc	41.7	43.2	84.9
4	1,4-dioxane	66.3	30.3	96.6
5	CH_3CN	0	97.9	97.9
6	DMF	0	101.6	101.6

Reaction conditions: styrene oxide 1 mmol, 10 wt% iron oxide-pillared bentonite to styrene oxide, acetone (2 mmol), solvent (3 mL) at RT (30°C) for 5 min.

The conversion of styrene oxide to **19** was performed in various solvents at RT (30°C) for 5 min. The use of CH_2Cl_2 provided the highest yield of product (entry 1). Common solvents which were inexpensive and commercially available such as hexane, EtOAc and 1,4-dioxane provided the desired product in low to moderate yields (entries 2-4), whereas using CH_3CN or DMF, the products were not formed (entries 5-6). This could be explained that DMF with its high polarity may cause the stronger coordination with carbocation intermediate in more polar molecule. Therefore, the nucleophile could not attack at that intermediate. The yield of **19** was found to depend on type of solvent. In this research, CH_2Cl_2 was chosen as a solvent for studying the optimum conditions for screening substrates.

It could be summarized the standard conditions for the conversion of styrene oxide to acetonide catalyzed by iron oxide-pillared bentonite as follows: styrene oxide 1 mmol, acetone 3 mL, 10 wt% iron oxide-pillared bentonite to styrene oxide, reaction temperature at RT (30°C) and reaction time for 5 min.

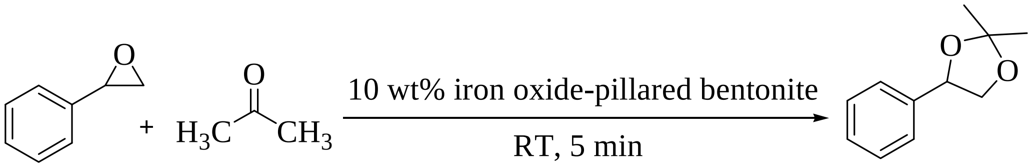

4.4.3 The conversion of other epoxides to acetonides catalyzed by iron oxide-pillared bentonite

Various epoxides including cyclohexene oxide, 1-dodecene oxide, butyl glycidyl ether, *tert*-butyl glycidyl ether, 2,3-epoxypropyl isopropylether and 2,3-epoxypropyl phenylether were chosen as substrates to observe the conversion of epoxides to acetonides catalyzed by 10 wt% iron oxide-pillared bentonite under standard conditions (30°C for 5 min). The results are summarized in Table 4.8.

Table 4.8 The conversion of epoxides to acetonides catalyzed by iron oxide-pillared bentonite under standard conditions

Entry	Epoxides	Acetonides	% Yield
1	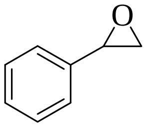	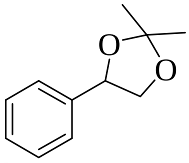	94.1
2	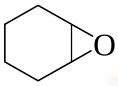	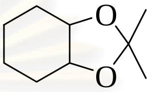	79.4
3	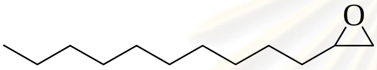	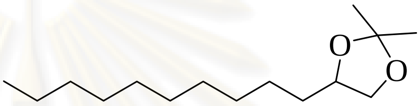	8.1
4	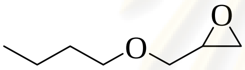	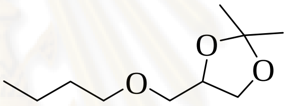	12.1
5	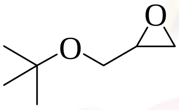	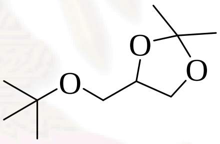	trace
6	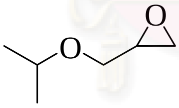	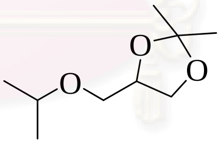	trace
7	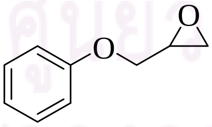	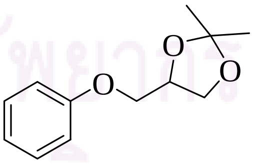	trace

Reaction conditions*:* epoxide (1 mmol), acetone in excess (3 mL), 10 wt% iron oxide-pillared bentonite to epoxide at RT (30°C) for 5 min.

According to the results from Table 4.8 demonstrates the styrene oxide was stirred in the presence of 10 wt% iron oxide-pillared bentonite to styrene oxide and acetone at RT for 5 min to produce the **19** in excellent yield. The reaction of cyclohexene oxide with acetone proceeded smoothly to give acetonide in high yields (entry 2). In the case of 1-dodecene oxide and butyl glycidyl ether, the reactions were performed in low yield (entries 3-4). Whereas the conversion of three epoxides such as *tert*-butyl glycidyl ether, 2,3-epoxypropyl isopropylether and 2,3-epoxypropyl phenylether (entries 4-7) to acetonides were not performed at standard conditions. Therefore, the following study will examine the suitable conditions for improving the yield in the conversion of these epoxides to acetonides.

4.4.3.1 The conversion of cyclohexene oxide to acetonide

Cyclohexene oxide was chosen as a representative of cyclic epoxide. The reaction of cyclohexene oxide with acetone was screened utilizing 10 wt% iron oxide-pillared bentonite at 60°C for 2 h. The reaction proceeded smoothly to give 2,2-dimethyl-hexahydro-benzo[1,3]dioxole **(20)** in excellent yield.

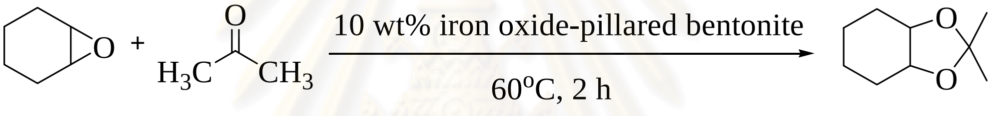

(20)

The isolated product was identified by ^{1}H NMR spectroscopy. The characterization of compound **20**; ^{1}H NMR ($CDCl_3$) δ (ppm): 1.24-1.00 (4H, m), 1.35 (6H, s), 2.58-2.07 (4H, m), 4.34-4.05 (2H, m).

4.4.3.2 The conversion of 1-dodecene oxide to acetonide

1-Dodecene oxide was chosen as a representative of terminal aliphatic epoxide. The reaction of 1-dodecene oxide with acetone could be carried out at 60°C for 2 h using 10 wt% iron oxide-pillared bentonite to furnish 4-decyl-2,2-dimethyl-1,3-dioxolane **(21)** with excellent yield.

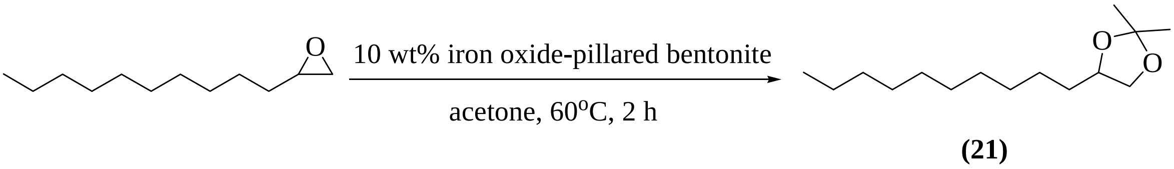

(21)

The isolated product was identified by ^{1}H NMR spectroscopy. The characterization of compound **21**; ^{1}H NMR ($CDCl_3$) δ (ppm): 0.81 (3H, t), 1.14 (16H, m), 1.29 (3H, s), 1.34 (3H, s), 1.56 (2H, m), 3.42 (1H, dd, *J* = 8.8, 7.2 Hz), 4.00 (2H, m).

4.4.3.3 The conversion of butyl glycidyl ether, *tert*-butyl glycidyl ether, 2,3-epoxypropyl isopropylether and 2,3-epoxypropyl phenylether to acetonides

Epoxides containing an ether functional group such as butyl glycidyl ether, *tert*-butyl glycidyl ether, 2,3-epoxypropyl isopropylether and 2,3-epoxypropyl phenylether to acetonides were examined. The effect of reaction time, reaction temperature and the amount of iron oxide-pillared bentonite for the conversion of butyl glycidyl ether to 4-(butoxymethyl)-2,2-dimethyl-1,3-dioxolane **(22)** were examined. The results are shown in Table 4.9.

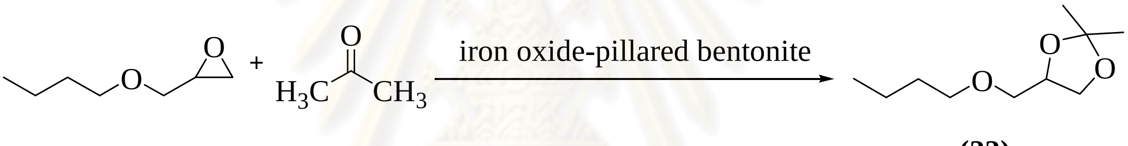

(22)

Table 4.9 The conversion of butyl glycidyl ether to acetonide catalyzed by iron oxide-pillared bentonite

Entry	**Time**	**Temp**	**Fe-pillared bentonite**	**% Yield**	**% Starting (recovered)**	**MB (%)**
1	15 min	RT	10 wt%	12.1	85.3	97.4
2	1 h	RT	10 wt%	25.6	71.1	96.7
3	2 h	RT	10 wt%	35.1	63.4	98.5
4	2 h	RT	30 wt%	75.5	20.9	96.4
5	2 h	reflux	10 wt%	88.0	7.3	95.3
6	2 h	reflux	30 wt%	95.8	0	95.8

Reaction conditions: butyl glycidyl ether 1 mmol, acetone in excess (3 mL), wt% iron oxide-pillared bentonite to butyl glycidyl ether.

According to the results from Table 4.9, the conversion of butyl glycidyl ether to **22** could be performed using iron oxide-pillared bentonite as a catalyst. At room temperature, more yield was obtained with increasing amount of iron oxide-pillared bentonite from 10 to 30 wt% (entries 3-4). In addition, the amount of the obtained product was slightly increased when reaction time increased (entries 1-3). At reflux temperature (60°C), the amount of the obtained product was slightly increased when the amount of iron oxide-pillared bentonite increased (entries 5-6). At the same amount of catalyst and reaction time, the yield at RT (30°C) was lower than that at reflux temperature (60°C) (entries 3 *vs* 5 and entries 4 *vs* 6). The reaction gave almost quantitative yield using 30 wt% iron oxide-pillared bentonites at 60°C for 2 h. It can be concluded that reaction temperature, reaction time and the amount of catalyst affected on the catalytic activity.

In summary, the suitable conditions for the conversion of butyl glycidyl ether to **22** were as follows: butyl glycidyl ether 1 mmol, acetone 3 mL, 30 wt% iron oxide-pillared bentonites to butyl glycidyl ether, reaction temperature at reflux (60°C) and reaction time for 2 h.

The isolated product was identified by ^{1}H NMR spectroscopy. The characterization of compound **22**; ^{1}H NMR ($CDCl_3$) δ (ppm): 0.84 (3H, t), 1.30 (3H, s), 1.34 (3H, s), 1.48 (4H, m), 3.49 (3H, m), 3.67 (2H, m), 3.99 (1H, dd, J = 8.0, 6.8 Hz), 4.20 (1H, quin).

The effect of reaction time, reaction temperature and the amount of iron oxide-pillared bentonite for the conversion of *tert*-butyl glycidyl ether to 4-(*tert*-butoxymethyl)-2,2-dimethyl-1,3-dioxolane **(23)** were examined. The results are shown in Table 4.10.

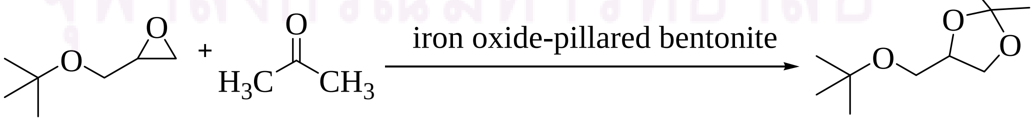

(23)

Table 4.10 The conversion of *tert*-butyl glycidyl ether to acetonide catalyzed by iron oxide-pillared bentonite

Entry	Time	Temp	Fe-pillared bentonite	% Yield	% Starting (recovered)	MB (%)
1	2 h	RT	10 wt%	24.0	69.4	93.4
2	2 h	RT	30 wt%	57.6	39.7	97.3
3	2 h	reflux	10 wt%	63.2	29.6	92.8
4	30 min	reflux	30 wt%	81.2	18.3	99.5
5	2 h	reflux	30 wt%	92.5	3.1	95.6
6	4 h	reflux	30 wt%	94.4	0	94.4

Reaction conditions: *tert*-butyl glycidyl ether 1 mmol, acetone in excess (3 mL), wt% catalyst to butyl glycidyl ether.

According to the results from Table 4.10, the conversion of *tert*-butyl glycidyl ether to **23** could be performed using iron oxide-pillared bentonite as a catalyst. At the same amount of catalyst and time, performing the reaction at 30°C gave lower yield than that at 60°C (entries 1 *vs* 3 and entries 2 *vs* 5). More yield could be obtained with increasing amount of iron oxide-pillared bentonite. The reaction gave almost quantitative yield using 30wt% iron oxide-pillared bentonite at 60°C for 4 h.

The isolated product was identified by ^{1}H NMR spectroscopy. The characterization of compound **23**; ^{1}H NMR ($CDCl_3$) δ (ppm): 1.13 (9H, s), 1.31 (3H, s), 1.38 (3H, s), 3.25 (1H, dd, J = 9.0, 6.4 Hz), 3.41 (1H, dd, J = 9.0, 5.6 Hz), 3.68 (1H, dd, J = 8.0, 5.6 Hz), 4.01 (1H, dd, J = 8.0, 6.4 Hz), 4.13 (1H, quin).

The conversion of 2,3-epoxypropyl isopropylether to 4-(isopropoxymethyl)-2,2-dimethyl-1,3-dioxolane **(24)** and 2,3-epoxypropyl phenylether to 2,2-dimethyl-4-(phenoxymethyl)-1,3-dioxolane **(25)** could be carried out at 60°C for 2 h using 10 wt% iron oxide-pillared bentonite as a catalyst in good yield.

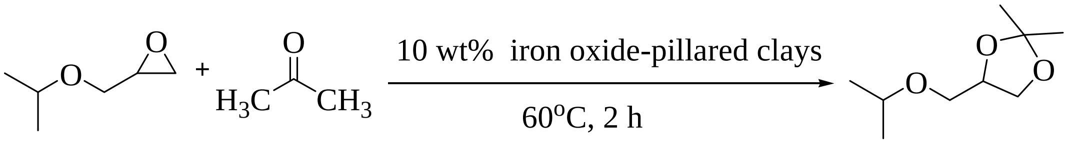

(24)

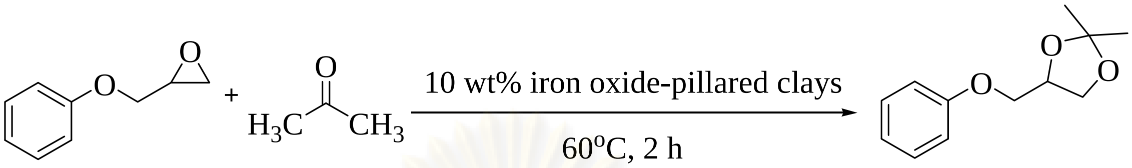

(25)

The isolated product was identified by ^{1}H NMR spectroscopy. The characterization of compound **24**; ^{1}H NMR ($CDCl_3$) δ (ppm): 1.09 (6H, d), 1.28 (3H, s), 1.34 (3H, s), 3.31 (1H, dd, *J* = 9.6, 6.0 Hz), 3.44 (1H, dd, *J* = 9.0, 6.4 Hz), 3.53 (1H, septet), 3.65 (1H, dd, *J* = 8.0, 6.2 Hz), 3.98 (1H, dd, *J* = 8.0, 6.4 Hz), 4.16 (1H, quin). The characterization of compound **25**; ^{1}H NMR ($CDCl_3$) δ (ppm): 1.38 (3H, s), 1.45 (3H, s), 3.89 (2H, ddd, *J* = 5.0, 9.2, 15.2 Hz), 4.01 (1H, dd, *J* = 9.0, 4.6 Hz), 4.12 (1H, dd, *J* = 14.4, 8.0 Hz), 4.45 (1H, quin), 6.91 (3H, m), 7.25 (2H, t).

4.4.4 Summary of the conversion of other epoxides to acetonides catalyzed by iron oxide-pillared bentonite

Various epoxides including cyclohexene oxide, 1-dodecene oxide, butyl glycidyl ether, *tert*-butyl glycidyl ether, 2,3-epoxypropyl isopropylether and 2,3-epoxypropyl phenylether were selected to perform the conversion of epoxides to acetonides catalyzed by 10 wt% iron oxide-pillared bentonite at 60°C for 2 h. The results are summarized in Table 4.11.

Table 4.11 The conversion of epoxides to acetonides catalyzed by iron oxide-pillared bentonite

Entry	Epoxides	Acetonides	% Yield
1	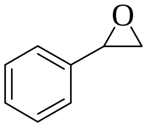	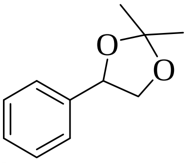	quant
2	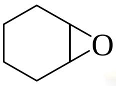	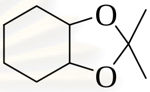	94.1
3	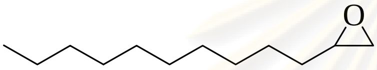	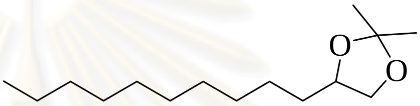	92.4
4	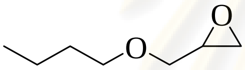	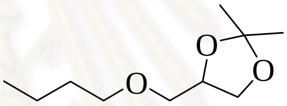	88.0
5	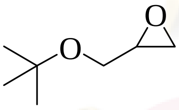	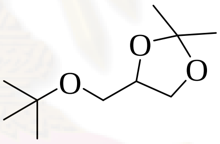	63.2
6	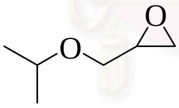	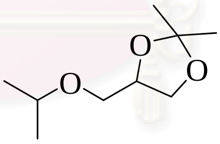	89.8
7	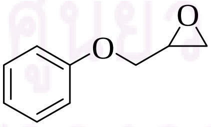	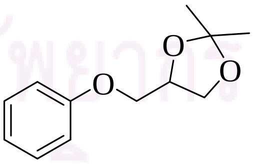	91.9

Reaction conditions: epoxide (1 mmol), acetone in excess (3 mL), 10 wt% iron oxide- pillared bentonite to epoxide at 60°C for 2 h.

As summarized in Table 4.11, high to excellent yields of acetonides were obtained in all cases. Various epoxides were reacted with acetone in the presence of catalytic amounts 10 wt% iron oxide-pillared bentonite to epoxide. The best result for this methodology was found for acetal formation with styrene oxide (entry 1). In a preliminary experiment, styrene oxide was stirred in the presence of 10 wt% iron oxide-pillared bentonite to styrene oxide and acetone at RT for 5 min to produce the **19** in quantitative yield.

In the case of cyclic epoxide such as cyclohexene oxide and terminal aliphatic epoxide such as 1-dodecene oxide, the reactions were performed with iron oxide-pillared bentonite catalyst (about 84 and 92% yield after 2 h, entries 2 and 3, respectively). The conversion of styrene oxide to the corresponding acetonide was much faster than cyclohexene oxide and 1-dodecene oxide. These results could be explained that the stability of the benzylic carbonium ion was formed during epoxide cleavage. In the case of the reaction of epoxides containing an ether functional group, the iron oxide-pillared bentonite could be catalyzed the efficient reaction of the epoxides with ethereal linkage on the epoxide ring such as butyl glycidyl ether, *tert*-butyl glycidyl ether, 2,3-epoxypropyl isopropylether and 2,3-epoxypropyl phenylether with acetone to gave their corresponding acetonides in high yields (entries 4-7, respectively), but lower conversions than that of styrene oxide under the same experimental conditions.

4.4.5 The conversion of styrene oxide with other carbonyl compounds to 1,3-dioxolanes catalyzed by iron oxide-pillared bentonite

Two carbonyl compounds: acetophenone and benzaldehyde were chosen to observe for the reaction with styrene oxide to form 1,3-dioxolanes at refluxing CH_2Cl_2 (40°C) for 2 h. The results are presented in Table 4.12.

Table 4.12 The conversion of styrene oxide to 1,3-dioxolane catalyzed by iron oxide-pillared bentonite

Entry	Carbonyl compounds	1,3-Dioxolanes	% Yield
1	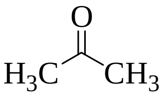	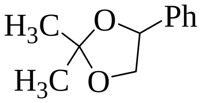	quant
2	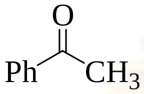	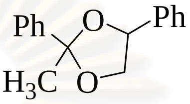	83
3	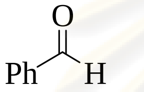	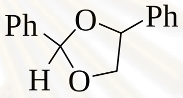	85

Reaction conditions: carbonyl compounds (2 mmol), styrene oxide (1 mmol), CH_2Cl_2 (3 mL), 10 wt% iron oxide-pillared bentonite to styrene oxide at refluxing CH_2Cl_2 (40°C) for 2 h.

Without iron oxide-pillared bentonite, no reaction occurred. The catalytic preparations were carried out in CH_2Cl_2; the carbonyl compounds were taken in small excess over the epoxide. Conditions for this reaction were 10 wt% iron oxide-pillared bentonites to styrene oxide at refluxing CH_2Cl_2 for 2 h. The best result was found in the case of styrene oxide with acetone to produce the acetonide in excellent yield (entry 1). The reactions also well proceeded when the following other carbonyl compounds: acetophenone and benzaldehyde were employed (entries 2-3). The products were attained in high yield. The yield of products was decreased when the steric hindrance of the substituents of carbonyl carbon increased. On the other hand, from the variation of carbonyl compounds such as acetophenone (83% yield) and benzaldehyde (85% yield), type of carbonyl compounds (ketone and aldehyde) did not affect on the catalytic activity of this reaction.

4.4.6 The mechanism for the formation of 1,3-dioxolane

The proposed mechanism describing the catalysis of the conversion of epoxide to 1,3-dioxolane is shown in scheme 4.1.

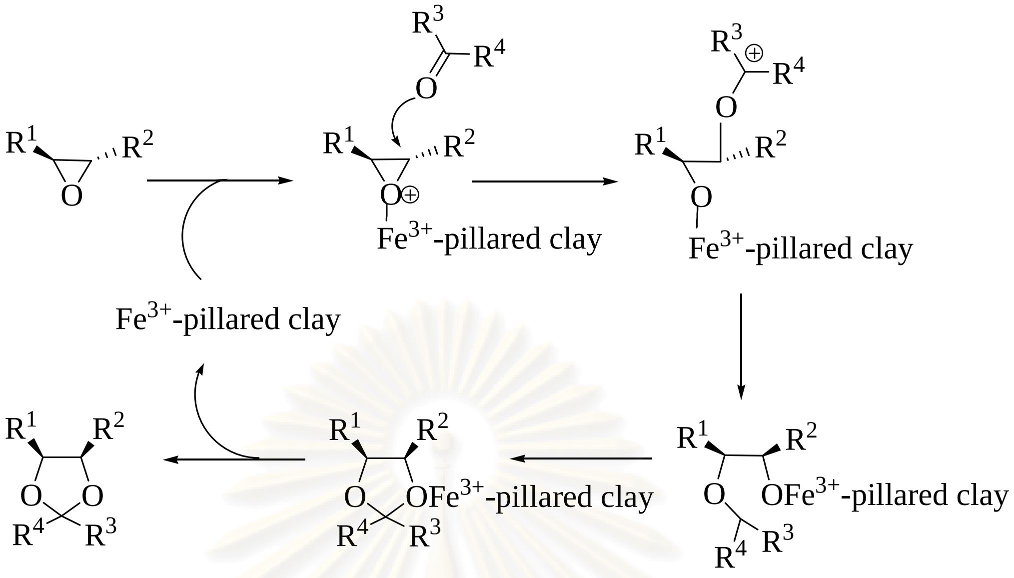

Scheme 4.1 Proposed mechanism for the formation of 1,3-dioxolane.

The proposed mechanism is shown in Scheme 4.1. Lewis acid-mediated reaction of an epoxide with a carbonyl compound was reported to proceed *via* the coordination of a metal cation of the catalyst with the epoxide oxygen, followed by nucleophilic ring-opening of the epoxide by the carbonyl oxygen and finally dioxolane ring formation. Because each step of the reaction is reversible, 1,3-dioxolanes could be converted to the corresponding ketone in the presence of catalytic iron oxide-pillared bentonite. Thus, acetal formation is sensitive to both structural factors such as steric hindrance which slow formation of the acetal and electronic factors which accelerate decomposition of the acetal.

4.4.7 Regenerated catalyst

4.4.6.1 The characterization of regenerated catalyst

The X-ray diffraction patterns of iron oxide-pillared bentonite and regenerated iron oxide-pillared bentonite for the conversion of styrene oxide to acetonide are shown in Figure 4.1.

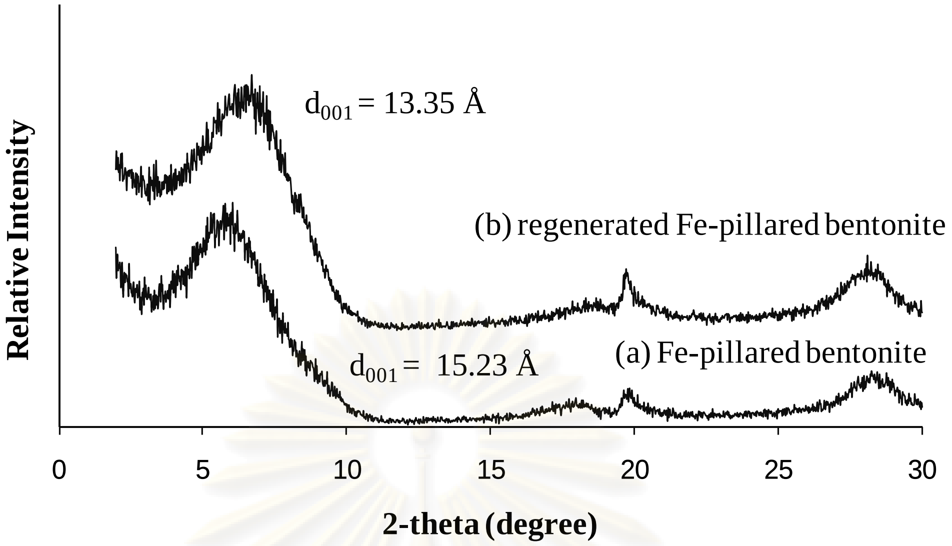

Figure 4.1 XRD patterns of (a) Fe-pillared bentonite and (b) regenerated Fe-pillared bentonite.

After the conversion of styrene oxide to acetonide was completed, the clay catalyst was filtered out of the reaction mixture, washed with EtOAc and calcined at 300°C for 5 h. The XRD pattern of regenerated iron oxide-pillared bentonite was similar to that of iron oxide-pillared bentonite. The broad (001) peak appeared at the same range (2θ of 4°-8°) as that of fresh iron oxide-pillared bentonite, indicating that the structure of catalyst was preserved upon regeneration process. Although the hightest point of d_{001} was around 13.35 Å which was smaller than the d_{001} of fresh iron oxide-pillared (15.23 Å). The collapse resulted from the re-calcination process and the local heat produced from decomposition of trapped organic species.

4.4.6.2 Nitrogen adsorption-desorption of regenerated catalyst

The nitrogen adsorption-desorption isotherms of iron oxide-pillared bentonite and regenerated iron oxide-pillared bentonite for the conversion of styrene oxide to acetonide are compared in Table 4.12.

Table 4.13 The BET specific surface area of iron oxide-pillared bentonite and regenerated iron oxide-pillared bentonite for the conversion of styrene oxide to acetonide

Entry	Samples	BET specific surface area (m^2/g)
1	Fe-pillared bentonite	155.52
2	Regenerated Fe-pillared bentonite#1	114.04

Table 4.13 shows the BET specific surface area of iron oxide-pillared bentonite and regenerated iron oxide-pillared bentonite. The BET specific surface area of regenerated catalyst decreased. The BET specific surface area of regenerated iron oxide-pillared bentonite was lower than iron oxide-pillared bentonite. There are two reasons: (i) the re-calcination process at 300°C was not enough to remove all organic residues that could block the pores of the catalyst, and (ii) the collapse of the d-spacing also caused the smaller pores; however, re-calcination process at higher 300°C caused the pillared structure change or collapse.

4.4.6.3 Temperature programmed desorption of regenerated catalyst

The total amount of acidity (mmol/g) of iron oxide-pillared bentonite and regenerated iron oxide-pillared bentonite for the conversion of styrene oxide to acetonide are compared in Table 4.14.

Table 4.14 The amount of acidity of iron oxide-pillared bentonite and regenerated iron oxide-pillared bentonite for the conversion of styrene oxide to acetonide

Entry	Samples	acidity (mmol/g)		Total amount of acidity (mmol/g)
		Weak acid sites	Strong acid sites	
1	Fe-pillared bentonite	0.618	3.108	3.726
2	Regenerated Fe-pillared bentonite#1	0.247	1.852	2.099

Table 4.14 shows the acidity of iron oxide-pillared bentonite and regenerated iron oxide-pillared bentonite. The acidity of regenerated iron oxide-pillared bentonite decreased. The acidity of regenerated iron oxide-pillared bentonite was lower than the iron oxide-pillared bentonite. It might due to the remaining organic residues in catalyst pores because the regenerated at 300°C may not completely destroy or decompose the organic compounds adsorbed on used catalyst.

4.4.6.4 Activity of regenerated iron oxide-pillared bentonite for the conversion of styrene oxide to acetonide

Iron oxide-pillared bentonite could be easily recovered by filtering the catalyst and washing with EtOAc, drying at 100°C in oven for 24 h and calcination. The recovered iron oxide-pillared bentonite was used in the next run. The results are summarized in Table 4.14.

Table 4.14 Activity of regenerated iron oxide-pillared bentonite for the conversion of styrene oxide to acetonide

Entry	**Run (times)**	**% Yield**
1	1	94.1
2	2	93.2
3	3	87.5

Reaction conditions: styrene oxide 1 mmol; acetone in excess (3 mL); 10 wt% iron oxide-pillared bentonite to styrene oxide at RT (30°C) for 5 min.

The regenerated iron oxide-pillared bentonite was used in the next run. The yield of the acetonide product remained 87% by the recovered catalyst for three times. The regenerated iron oxide-pillared bentonite exhibited lower activity than iron oxide-pillared bentonite, corresponding to the result of the collapse of d_{001} spacing and lower BET specific surface area.

4.4.7 Conclusion

The catalytic activities of iron oxide-pillared bentonite were performed for the conversion of styrene oxide to 1,3-dioxolanes. The optimized conditions were 10 wt% iron oxide-pillared bentonites to styrene oxide at RT for 5 min. The reaction could be performed to furnish **19** in almost quantitative yield. This method was carried out successfully furnishing the desired product in good to quantitative yields in short period of time under mild conditions. Under the same reaction condition, iron oxide-pillared bentonite showed better efficiency than iron oxide-pillared hectorite and iron oxide-pillared taeniolite because iron oxide-pillared bentonite had higher BET surface area and acidity than iron oxide-pillared hectorite and iron oxide-pillared taeniolite. These catalysts were commercially available, inexpensive, convenient, stable, reusable, recoverable and non-toxic heterogeneous catalysts, which made them a useful and a highly attractive process for the synthesis of acetonides.

The optimized conditions could be applied for other epoxides and carbonyl compounds. Various epoxides could be used to explore the scope of this reaction. From the variation of epoxides such as cyclohexene oxide (84% yield), 1-dodecene oxide (92% yield), butyl glycidyl ether (88% yield), *tert*-butyl glycidyl ether (63% yield), 2,3-epoxypropyl isopropyl ether (90% yield) and 2,3-epoxypropyl phenyl ether (92% yield), yields of acetonides greatly depended on the structure of the starting epoxides. All reactions were performed under mild conditions in good to excellent yields.

CHAPTER V

THE ISOMERIZATION OF α-PINENE BY CLAY CATALYSTS

5.1 Introduction

5.1.1 The isomerization of α-pinene

α-Pinenes (monoterpenes) are valuable and important natural raw materials for the production of cosmetics, pharmaceuticals, flavors, fragrances and food industries. α-Pinene is abundant in natural essential oils (monoterpene fraction) such as turpentine oil, pine oil and eucalyptus resins. The isomerization of α-pinene normally takes place in highly acidic conditions leading to the formation of a pinanyl cation. The transposition of pinanyl cation generates *p*-menthenyl and isobornyl cations which are rearranged through two pathways: one leading to bicyclic and tricyclic products (such as camphene, tricyclene, α-fenchene and bornylene) by transposition of the pinanyl cation to isobornyl cation. The other involves the rearrangement of pinanyl cation to *p*-menthenyl cation resulting in the formation of monocyclic products (such as limonene, *p*-cymene, α-terpinene, γ-terpinene, *m*-cymene, isoterpinolene and terpinolene) [93]. The proposed reaction pathway of α-pinene isomerization is shown in Scheme 5.1. Most of isomerized products are industrially valuable chemicals. Camphene is an important intermediate for the synthesis of camphor which is an important and valuable industrial product in fragrance and pharmaceutical industries. Limonene can be used as a precursor in carvone synthesis which is an important product in cosmetics and as a renewably-based solvent in cleaning products. The selectivity of α-pinene isomerization is highly depended on types of the heterogeneous catalysts.

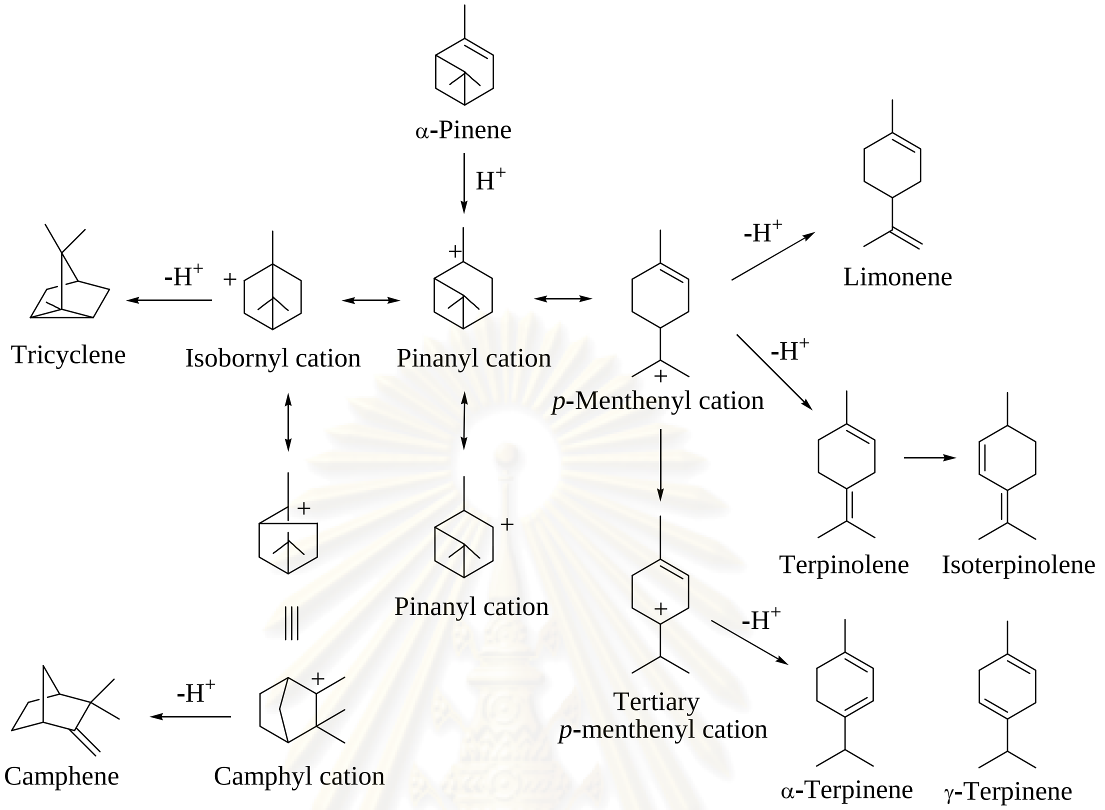

Scheme 5.1 The reaction pathway of α-pinene isomerization

5.1.2 Literature review on the isomerization of α-pinene

α-Pinene can be converted to bicyclic products (such as camphene, bornylene and α-fenchene), monocyclic products (such as limonene, *p*-cymene, α-terpinene, γ-terpinene, isoterpinolene terpinolene and *m*-cymene) and tricyclic products (such as tricyclene). The isomerization of α-pinene using acidic TiO_2 as a catalyst was the conventional process for the synthesis of camphene. The direct transformation of α-pinene into camphene has been previously reported using several Lewis acid catalysts [94].

In 1995, Stefanis and co-workers studied the catalytic effect of various acid catalysts such as a layered α-tin phosphate analogue (Al-PILP) and alumina-pillared clays (PILCs) compared with H^+-mordenite, NH_4^+-ZSM-5 (with SiO_2/Al_2O_3 ratios = 35 and 235) and the mid-pore zeolites USY for the isomerization of α-pinene. The results showed that the bicyclic product (camphene) gave the highest conversion for all catalysts. The order of catalytic activity of various catalysts is a follows: zeolites

USY > BP-PILC = ZSM-5 (35) > H+-mordenite. This result corresponded with the acidity of catalysts used [95].

In 1996, Severino and co-workers synthesized the hydrothermal treatment of zeolites Y and X for the transformation of α-pinene at 150°C. The reaction products were camphene, *p*-menthadienes and tricyclene [96].

In 1998, Lopez and co-workers tested the catalytic effect of various zeolites such as faujasite (FAU) zeolites and dealuminated mordenite (MOR) for isomerization of α-pinene at 120°C. Camphene and limonene as main products were obtained from this reaction. When using dealuminated mordenite as a catalyst, a selectivity of camphene/(limonene+camphene) greater than 0.54 and the maximum yields of camphene and limonene were obtained [97].

In 2001, Volzone and co-workers reported the use of acid dioctahedral and acid trioctahedral smectite clays as catalysts for the isomerization of α-pinene. The results showed that 50% conversion, 52.6-54.5% selectivity in camphene and 37.6-39.8% selectivity in limonene and their derivatives were obtained at 100°C after 1 h reaction. All acid smectite clays showed higher selectivity to camphene than limonene and its derivatives [98].

In 2002, Ferragina and co-workers addressed the use of γ-zirconium phosphate and rhodium γ-zirconium phosphate as efficient catalysts for the isomerization of α-pinene. γ-Zirconium phosphate displayed higher activity but lower reaction selectivity than rhodium γ-zirconium phosphate. γ-Zirconium phosphate gave higher yields of monocyclic compounds while the isomerization products on rhodium γ-zirconium phosphate were bicyclic terpenes [99].

In 2004, Valencia and co-workers described the isomerization of α-pinene using amberlyst 35 wet as an efficient catalyst. The effects of the amount of catalyst and reaction temperature were studied to search for the optimal conditions to maximize the yields of camphene. Amberlyst 35 wet could efficiently catalyze the reaction of α-pinene into camphene in good yields at 120°C. When the catalyst/α-pinene ratio was increased, the α-pinene conversion was increased and a fast transformation of camphene to other monocyclic products (limonene, *p*-cymene, α-terpinene, γ-terpinene and terpinolene) was observed [100].

In 2004, Yadav and co-workers addressed the isomerization of α-pinene using Ce^{3+}, Fe^{3+}, La^{3+}, Ag^{+}, Li^{+}, Ca^{2+} and Mg^{2+} exchanged clays and sulfuric acid treatment natural Indian montmorillonite as catalysts for the isomerization of α-pinene. Higher than 90% α-pinene conversion and 39-49% selectivity for camphene were obtained when using Ce^{3+}, Fe^{3+}, La^{3+} and Ag^{+} exchanged clays as catalysts. However, Li^{+}, Ca^{2+} and Mg^{2+} exchanged clays showed 4-12% conversion of α-pinene. In the case of acid treated clays, the isomerization of α-pinene was successfully performed at 150°C for 2 h affording the camphene selectivity from 39 to 49% and more than 96% conversion of α-pinene [93].

In 2005, Comelli and co-workers reported the use of sulfated zirconia having 15% H_2SO_4 as an efficient catalyst for the isomerization of α-pinene and the transformations of limonene, terpinolene and α-terpinene. 53% of camphene, 7.7% of limonene, 6.1% of tricyclene and 3.0% of terpinolene were attained from α-pinene isomerization at 120°C for 180 min. The products from the transformation of limonene were terpinolene, γ-terpinene and α-terpinene after 20 min reaction, whereas those from α-terpinene and terpinolene were *p*- and *m*-cymene, respectively [101].

The proposed reaction pathway for the isomerization of α-pinene using sulfated zirconia as a catalyst is shown in Scheme 5.2. The reaction pathway starts with the formation of pinanyl cation. The transposition of pinanyl cation generates *p*-menthenyl and isobornyl cations. The isobornyl cation generates bicyclic and tricyclic products such as camphene, tricyclene, α-fenchene and bornylene, while *p*-menthenyl cation leads to the formation of monocyclic products. The loss of H^+ from *p*-menthenyl cation generates limonene. The other monocyclic products (terpinolene, γ-terpinene and α-terpinene) are produced by the isomerization of limonene. The dehydrogenation of α-terpinene gives *p*-cymene and that of terpinolene yields *m*-cymene. The isomerization of terpinolene gives isoterpinolene [101].

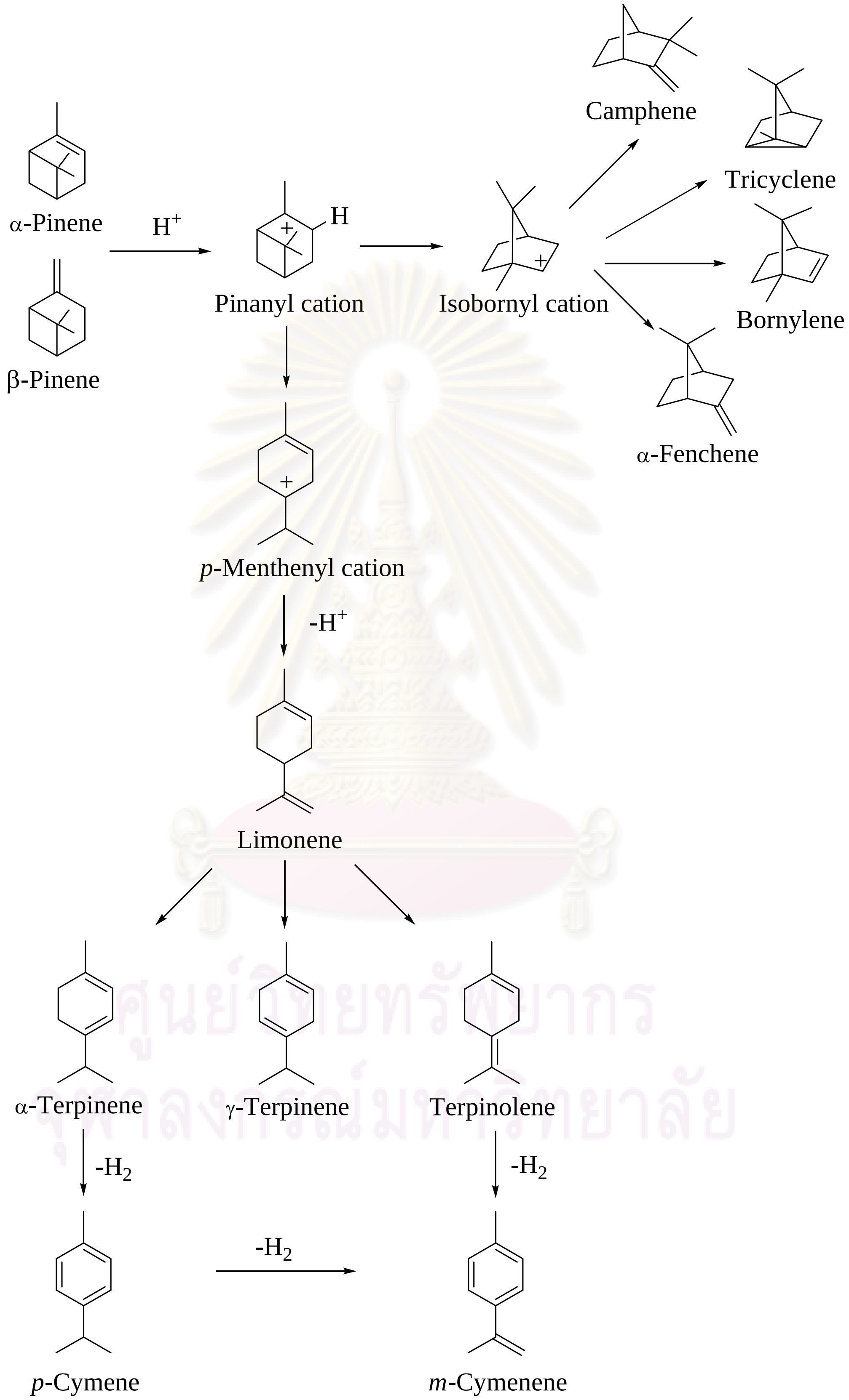

Scheme 5.2 Proposed reaction for the isomerization of α-pinene.

In 2009, Da Silva Rocha and co-workers studied the liquid-phase isomerization of longifolene and α-pinene using 0.15-5 wt% silica-supported $H_3PW_{12}O_{40}$ ($H_3PW_{12}O_{40}/SiO_2$) as an efficient and environmentally friendly heterogeneous catalyst under solvent-free conditions at 80-100°C. 50% Selectivity for camphene and 28% selectivity for limonene were obtained under optimized conditions (0.60 wt% $H_3PW_{12}O_{40}/SiO_2$) at 100°C for 60 min [102].

5.2 Scope of this work

According to the literature reviews, both homogeneous and heterogeneous catalysts could be employed as good catalysts for the isomerization of α-pinene. However, the disadvantage of some catalysts is the difficulty of separation and recovery of the catalyst, disposal of spent catalyst, high toxicity and expensive chemicals. The main features of this research focus on the isomerization of α-pinene catalyzed by iron oxide-pillared clays and metal chloride-impregnated aluminium oxide-pillared bentonite catalysts.

5.3 Experimental

5.3.1 General procedure

This section provides general information of general and/or specific reaction conditions and spectral data for compounds along with a representative ^1H NMR. The reactions were monitored by TLC on aluminium sheets precoated with silica gel (Merck’s, Kieselgel 60 PF_{254}). *Buchi* rotary evaporator connected to a vacuum pump was used for removal of solvents.

Chromatography: Gas chromatographic analysis was carried out on a Shimadzu Gas Chromatography instrument equipped with a flame ionization detector (FID) with N_2 as a carrier gas and a 30-m long HP-5 column (0.25-mm outer diameter, 0.25 μm film thickness). Column chromatography was performed on silica gel (Merck’s, kieselgel 60 G Art 7754 (70-230 mesh)).

^1H NMR spectra were recorded at 400 MHz on a Varian spectrometer. Chemical shifts are reported in ppm from tetramethylsilane with the solvent residue of $CDCl_3$ (7.26 ppm).

Chemicals: All solvents in this research were purified according to the procedures described in the standard methodology except for reagents and solvents that are reagent grade. The reagents are listed below:

1. α-pinene (Sigma-Aldrich, 98%)
2. camphene (Sigma-Aldrich, 95%)
3. tricyclene (Fluka Chemika, 98%)
4. limonene (Fluka Chemika, 98%)
5. terpinolene (Fluka Chemika, 85%)
6. α-terpinene (Sigma-Aldrich, 85%)
7. γ-terpinene (Fluka Chemika, 95%)
8. *p*-cymene (Fluka Chemika, 95%)

5.3.2 Syntheses

5.3.2.1 The general procedure for the isomerization of α-pinene

A typical reaction: α-pinene was added to a round bottom flask with 10 wt% of catalyst connected with a condenser for refluxing. The solution was continuous stirred for desired time and temperature. After the specific time or the reaction was finished, the catalyst was simply filtered out, washed the product with EtOAc. The solvent was evaporated to dryness under reduced pressure to afford the product. The product was analyzed by GC with the addition of an exact amount of an appropriate internal standard (cyclohexanone).

5.3.2.2 Optimum conditions for the isomerization of α-pinene

Effect of the amount of catalyst

The isomerization of α-pinene was performed according to the general procedure, but the amount of catalyst was changed to 10 and 30 wt% of catalyst to α-pinene.

Effect of the reaction time

The isomerization of α-pinene was performed according to the general procedure, but the reaction time was changed to 60, 120 and 180 min.

Effect of the reaction temperature

The isomerization of α-pinene was performed according to the general procedure, but the reaction temperature was changed to 100, 150 and 180°C.

5.3.3 Reuse of catalysts

The used $NdCl_3$-impregnated aluminium oxide-pillared bentonite was regenerated by calcinations at 450°C for 4 h. The structural characterization of the regenerated $NdCl_3$-impregnated aluminium oxide-pillared clays was carried out using XRD, N_2-adsorption/desorption and NH_3-TPD techniques. The regenerated catalyst was reused in the isomerization of α-pinene.

5.4 Results and discussion

5.4.1 Catalytic activities of iron oxide-pillared clay and metal chloride-impregnated aluminium oxide-pillared bentonite for the isomerization of α-pinene

Iron oxide-pillared clays (iron oxide-pillared bentonite and iron oxide-pillared hectorite) and the variation of metal chloride-impregnated aluminium oxide-pillared bentonite were employed to explore their catalytic activities for the conversion of α-pinene and selectivity to bicyclic or monocyclic products. Hectorite and bentonite clays were also employed for comparison. The effect of reaction time, reaction temperature and the amount of catalyst were varied to search for the optimized conditions. Moreover, the effect of type and acidity of catalyst on %conversion of α-pinene and selectivity towards the formation of bicyclic or monocyclic products was explored.

5.4.1.1 Effect of raw clays (bentonite and hectorite) and iron oxide-pillared clays on the reactivity of the isomerization of α-pinene

The catalytic activity of iron oxide-pillared clays (Fe-pillared clays) such as iron oxide-pillared bentonite and iron oxide-pillared hectorite was compared with montmorillonite, raw hectorite and iron oxide (Fe_2O_3, hematite) for the isomerization of α-pinene. Conditions studied were 10 wt% catalyst to α-pinene at 180°C for 2 h. The results are shown in Table 5.1.

Table 5.1 Effect of raw clays (montmorillonite, hectorite), Fe-pillared bentonite and Fe-pillared hectorite on the reactivity of the isomerization of α-pinene.

Entry	Catalyst	Conversion (%)	Selectivity (%)						
			Tri- and bicyclics		Monocyclics				
			Tricyclene	Camphene	Limonene	*p*-Cymene	α-Terpinene	γ-Terpinene	Terpinolene
1	Fe-pillared bentonite	100	-	18	69	2	3	3	5
2	Fe-pillared hectorite	100	-	16	70	3	5	2	-
3	montmorillonite	trace	-	-	-	-	-	-	-
4	Raw hectorite	trace	-	-	-	-	-	-	-
5	Fe_2O_3	trace	-	-	-	-	-	-	-
6	None	0	-	-	-	-	-	-	-

Reaction conditions: α-pinene 10 mmol, 10 wt% catalyst to α-pinene at 180°C for 2 h.

From Table 5.1, iron oxide-pillared bentonite and iron oxide-pillared hectorite were screened to observe their potentially catalytic ability. When the reaction was performed without catalyst, no product was observed. Using iron oxide-pillared bentonite and iron oxide-pillared hectorite at 180°C for 2 h, much higher %convension was observed (entries 1 and 2). With 100% α-pinene conversion, both iron oxide-pillared clays yielded limonene as a major product (69-70% selectivity) and camphene being a minor one. This study provided a clue that types of clays (bentonite or hectorite) are not essential for the isomerization of α-pinene.

5.4.1.2 Effect of metal chloride-impregnated aluminium oxide-pillared bentonite on the reactivity of the isomerization of α-pinene

The catalytic activity of metal chloride-impregnated Al-pillared bentonite (Al-PLC) was carried out. Six synthesized metal chloride-impregnated Al-PLC including $LaCl_3$/Al-PLC, $NdCl_3$/Al-PLC, $CeCl_3$/Al-PLC, $GdCl_3$/Al-PLC, $YbCl_3$/Al-PLC and $DyCl_3$/Al-PLC and Al-PLC were utilized to observe their potentially catalytic activity of the isomerization of α-pinene. Conditions for this reaction were 10 wt% catalyst to α-pinene at 180°C for 2 h. The results are shown in Table 5.2.

Table 5.2 Effect of Al-PLC and metal chloride-impregnated Al-PLC (MCl_3/Al-PLC) on the reactivity of the isomerization of α-pinene.

Entry	Catalyst	Conversion (%)	Selectivity (%)							
			Tri- and bicyclics		Monocyclics					Others
			Tricyclene	Camphene	Limonene	*p*-Cymene	α-Terpinene	γ-Terpinene	Terpinolene	
1	Al-PLC	85	5	27	37	6	7	5	8	5
2	$NdCl_3$/Al-PLC	100	3	37	23	6	9	9	10	3
3	$CeCl_3$/Al-PLC	39	-	35	39	4	3	6	8	5
4	$GdCl_3$/Al-PLC	16	-	37	39	3	5	3	9	4
5	$DyCl_3$/Al-PLC	9	-	33	43	-	7	4	10	3
6	$YbCl_3$/Al-PLC	6	-	52	48	-	-	-	-	-
7	$LaCl_3$/Al-PLC	trace	-	-	-	-	-	-	-	-

Reaction conditions: α-pinene 10 mmol, 10 wt% catalyst to α-pinene at 180°C for 2 h.

Table 5.2 demonstrates the comparative study on the effect of metal chloride-impregnated Al-PLC on the reactivity for the isomerization of α-pinene at 180°C for 2 h. The products attained were camphene, tricyclene, limonene, *p*-cymene, α-terpinene, γ-terpinene, terpinolene and others. Among metal chloride-impregnated Al-PLC studied, $NdCl_3$/Al-PLC displayed an excellent performance (entry 2). To illustrate this, the reaction catalyzed by $NdCl_3$/Al-PLC was performed at 180°C for 2 h affording 100% α-pinene conversion with the selectivity of 37% for camphene (major product) and 23% for limonene. In the case of Al-PLC (entry 1), 85% conversion for α-pinene with 27% selectivity for camphene and 37% for limonene (major product) were detected. It should however be noted that $CeCl_3$/Al-PLC, $GdCl_3$/Al-PLC, $YbCl_3$/Al-PLC and $DyCl_3$/Al-PLC showed poor %conversion for α-pinene. When the reaction was performed using $LaCl_3$/Al-PLC, no product was observed. According to the mentioned results, %α-pinene conversion and %selectivity ratio of bicyclic and tricyclic to monocyclic products were highly dependent on the acid strength of these catalysts and nature of metal chloride. This result was well corresponded with the acidity. $NdCl_3$/Al-PLC had the highest acidity, therefore this catalyst showed excellent performance in this reaction.

Comparing the results exhibited in Tables 5.1 and 5.2, under the same reaction conditions, two clay catalysts were employed: iron oxide-pillared bentonite and $NdCl_3$/Al-PLC. Iron oxide-pillared bentonite gave %conversion more or less the same as using $NdCl_3$/Al-PLC. For iron oxide-pillared bentonite, limonene was detected as a major product whereas using $NdCl_3$/Al-PLC, camphene was found as a main component. In addition, it was found that iron oxide-pillared bentonite exhibited higher activity, but lower selectivity to camphene than $NdCl_3$/Al-PLC. It has been suggested that the strong Lewis acid active sites can strongly affect on the selectivity. Iron oxide-pillared bentonite had the higher acidity than $NdCl_3$/Al-PLC, therefore this catalyst showed higher selectivity to limonene than $NdCl_3$/Al-PLC.

5.4.2 Comparative study on the effect of iron oxide-pillared bentonite and iron oxide-pillared hectorite for the isomerization of α-pinene

According to previous results (Table 5.1), iron oxide-pillared bentonite and iron oxide-pillared hectorite showed good activity for the isomerization of α-pinene.

Further investigation to search for optimized conditions in the isomerization of α-pinene was carried out. The amount of catalysts and reaction temperature were optimized.

5.4.2.1 Effect of the reaction temperature on the isomerization of α-pinene

Temperature is one of important parameters. The temperature examined was 150 and 180°C. The effect of the reaction temperature for the isomerization of α-pinene catalyzed by iron oxide-pillared bentonite and iron oxide-pillared hectorite was carried out and the results are presented in Table 5.3.

Table 5.3 Effect of the reaction temperature for the isomerization of α-pinene catalyzed by Fe-pillared bentonite and Fe-pillared hectorite

Entry	Catalyst	Temp (°C)	Conversion (%)	Selectivity (%)						
				Tri- and bicyclics		Monocyclics				
				Tricyclene	Camphene	Limonene	*p*-Cymene	α-Terpinene	γ-Terpinene	Terpinolene
1	Fe-pillared bentonite	150	84	-	27	43	8	4	6	12
2	Fe-pillared bentonite	180	100	-	18	69	2	3	3	5
3	Fe-pillared hectorite	150	79	-	30	45	12	3	4	6
4	Fe-pillared hectorite	180	100	-	16	70	3	5	2	4

Reaction conditions: α-pinene 10 mmol, 10 wt% catalyst to α-pinene for 2 h.

Table 5.3 demonstrates that the reaction temperature profoundly affected on %conversion and %selectivity of the reaction. %Conversion was slightly increased when reaction temperature increased. 100% conversion was achieved at 180°C for 2 h. Comparing between 150 and 180°C, both catalysts yielded limonene as a major product while camphene was a minor one. When the reaction temperature raised up, %selectivity in limonene was increased, but the selectivity in camphene was dropped. In addition, the selectivity towards the formation of monocyclic products including *p*-cymene, terpinolene, α-terpinene and γ-terpinene was decreased. It can be concluded that the reaction rate greatly increased with increasing the reaction temperature. The effect of reaction temperature has been documented to be effective on %conversion and %selectivity in the isomerization of α-pinene [95]. However, in previous reports when the reaction temperature was increased, the major (limonene) and minor products (camphene) were still the same. This could thus be summarized that the suitable reaction temperature for the isomerization of α-pinene is 180°C.

5.4.2.2 Effect of the amount of catalyst for the isomerization of α-pinene

The effect of the amount of iron oxide-pillared bentonite and iron oxide-pillared hectorite for the isomerization of α-pinene was examined. The results are presented in Table 5.4.

Table 5.4 Effect of the amount of catalyst for the isomerization of α-pinene catalyzed by Fe-pillared bentonite and Fe-pillared hectorite

Entry	Catalyst	Amount of catalyst	Conversion (%)	Selectivity (%)						
				Tri- and bicyclics		Monocyclics				
				Tricyclene	Camphene	Limonene	*p*-Cymene	α-Terpinene	γ-Terpinene	Terpinolene
1	Fe-pillared bentonite	10 wt%	84	-	27	43	8	4	6	12
2	Fe-pillared bentonite	30 wt%	100	-	15	73	12	-	-	-
3	Fe-pillared hectorite	10 wt%	79	-	30	45	12	3	4	6
4	Fe-pillared hectorite	30 wt%	100	-	8	77	15	-	-	-

Reaction conditions: α-pinene 10 mmol, wt% catalyst to α-pinene at 150°C for 2 h.

Table 5.4 displays that the amount of iron oxide-pillared bentonite and iron oxide-pillared hectorite profoundly affected on %conversion and %selectivity. When the amount of catalyst increased from 10 to 30 wt%, %conversion was increased. Using 30 wt% iron oxide-pillared bentonite as catalyst, %selectivity in limonene was increased from 43 to 73%. However, the selectivity to camphene was dropped from 27 to 15%. In the case of iron oxide-pillared hectorite, %selectivity in limonene was increased from 45 to 77%, but the selectivity to camphene was dropped from 30 to 8%. Therefore using large amounts of catalysts, limonene was an expected product. It has been suggested that the nature of acid active sites can strongly affect the balance between the two possible routes of isomerization of the pinanyl cation. Camphene and other bi- and tricyclic products are thought to preferentially form on Lewis acid sites, whereas monocyclic products on Bronsted acid sites [102-104]. It is surprising, therefore, that in spite of the strong Lewis acidity of iron oxide-pillared bentonite and iron oxide-pillared hectorite, the reactions occurred with up to 73 and 77% selectivity to limonene at a complete substrate conversion, respectively.

5.4.3 Comparative study on the effect of $NdCl_3$/Al-PLC and Al-PLC for the isomerization of α-pinene

Because of $NdCl_3$/Al-PLC and Al-PLC exhibiting good activity for the isomerization of α-pinene, further investigation was performed to find the optimized conditions. The amount of the catalyst, reaction temperature and reaction time were varied to search for the optimized conditions.

5.4.3.1 Effect of the reaction temperature for the isomerization of α-pinene

The temperature examined was 100, 150 and 180°C. The effect of the reaction temperature for the isomerization of α-pinene catalyzed $NdCl_3$/Al-PLC and Al-PLC were carried out and the results are presented in Table 5.5.

Table 5.5 Effect of the reaction temperature for the isomerization of α-pinene catalyzed by $NdCl_3$/Al-PLC and Al-PLC

Entry	Temp (°C)	Catalysts	Conversion (%)	Selectivity (%)							
				Tri- and bicyclics		Monocyclics					Others
				Tricyclene	Camphene	Limonene	*p*-Cymene	α-Terpinene	γ-Terpinene	Terpinolene	
1	100	$NdCl_3$/Al-PLC	44	-	30	50	-	4	-	16	-
2	150	$NdCl_3$/Al-PLC	98	2	33	28	4	6	5	22	-
3	180	$NdCl_3$/Al-PLC	100	3	37	23	6	9	9	10	3
4	100	Al-PLC	18	-	20	55	-	-	4	21	-
5	150	Al-PLC	74	1	25	40	3	6	4	18	3
6	180	Al-PLC	85	5	27	37	6	7	5	8	5

Reaction conditions: α-pinene 10 mmol, 10 wt% catalyst to α-pinene for 2 h.

From Table 5.5, the effect of the reaction temperature for catalytic isomerization of α-pinene with $NdCl_3$/Al-PLC and Al-PLC was studied. The reaction temperature profoundly affected on %conversion and %selectivity. %Conversion was slightly increased when the reaction temperature increased from 100 to 180°C. Using $NdCl_3$/Al-PLC as a catalyst at either 150 or 180°C, the main product was camphene**.** When the reaction was carried out at 100°C, the reaction was relatively slow, the main product was limonene. While using Al-PLC, the main product was limonene at every reaction temperature. When the reaction temperature raised up from 100 to 180°C, %selectivity in camphene was increased and the concentration of monocyclic products (*p*-cymene, α-terpinene, γ-terpinene and terpinolene) was also increased. It can thus be concluded, the reaction rate greatly increased with increasing the temperature.

5.4.3.2 Effect of the amount of catalyst for the isomerization of α-pinene

The effect of the amount of $NdCl_3$/Al-PLC and Al-PLC for the isomerization of α-pinene was examined. The results are shown in Table 5.6.

Table 5.6 Effect of the amount of catalyst for the isomerization of α-pinene catalyzed by $NdCl_3$/Al-PLC and Al-PLC

Entry	Amount of catalyst	Catalyst	Conversion (%)	Selectivity (%)							
				Tri- and bicyclics		Monocyclics					Others
				Tricyclene	Camphene	Limonene	*p*-Cymene	α-Terpinene	γ-Terpinene	Terpinolene	
1	10 wt%	$NdCl_3$/Al-PLC	87	4	32	27	5	9	9	12	2
2	30 wt%	$NdCl_3$/Al-PLC	100	6	35	57	-	-	-	-	12
3	10 wt%	Al-PLC	63	5	30	36	3	7	6	7	6
4	30 wt%	Al-PLC	100	4	31	56	4	2	-	3	-

Reaction conditions: α-pinene 10 mmol, wt% catalyst to α-pinene at 180°C for 1 h.

Table 5.6 displays that the amount of $NdCl_3$/Al-PLC and Al-PLC greatly affected on %conversion and %selectivity. When the amount of catalyst increased from 10 to 30 wt%, %conversion was slightly increased and the amount of limonene was increased, but that of camphene remained constant.

Using 30 wt% $NdCl_3$/Al-PLC, %selectivity in limonene was increased from 27 to 57%. In the case of Al-PLC, % selectivity in limonene was increased from 36 to 56%. All monocyclic products (*p*-cymene, α-terpinene, γ-terpinene and terpinolene) were decreased. Therefore using large amounts of catalysts, limonene is a major product. It has been suggested that the nature of acid active sites can strongly affect the balance between the two possible routes of isomerization of the pinanyl cation. Camphene and other bi- and tricyclic products are thought to preferentially form on strong acid sites, whereas monocyclic products on weak acid sites [102-104]. It is surprising, therefore, that in spite of the strong acidity of $NdCl_3$/Al-PLC and Al-PLC, the reactions occurred with up to 57 and 56% selectivity to limonene at a complete substrate conversion, respectively.

5.4.3.3 Effect of the reaction time for the isomerization of α-pinene

The effect of the reaction time for the isomerization of α-pinene catalyzed by $NdCl_3$/Al-PLC and Al-PLC were carried out and the results are presented in Table 5.7.

Table 5.7 demonstrates that the reaction time also affected on %conversion and %selectivity. When the reaction time increased from 60 to 180 min, the amount of limonene decreased. A fast transformation of limonene to other monocyclic products (*p*-cymene, α-terpinene, γ-terpinene and terpinolene) was observed when the reaction time increased.

Table 5.7 Effect of the reaction time for the isomerization of α-pinene catalyzed by $NdCl_3$/Al-PLC and Al-PLC

Entry	Time (min)	Catalyst	Conversion (%)	Selectivity (%)							
				Tri- and bicyclics		Monocyclics					Others
				Tricyclene	Camphene	Limonene	*p*-Cymene	α-Terpinene	γ-Terpinene	Terpinolene	
1	60	$NdCl_3$/Al-PLC	87	4	32	27	5	9	9	12	2
2	120	$NdCl_3$/Al-PLC	100	3	37	23	6	9	9	10	3
3	180	$NdCl_3$/Al-PLC	100	3	31	10	8	13	14	19	2
4	60	Al-PLC	63	5	30	36	3	7	6	7	6
5	120	Al-PLC	85	5	27	37	6	7	5	8	5
6	180	Al-PLC	100	6	26	20	10	14	8	12	4

Reaction conditions: α-pinene 10 mmol, 10wt% catalyst to α-pinene at 180°C.

5.5 Regenerated catalyst

5.5.1 The characterization of regenerated catalyst

The X-ray diffraction patterns of $NdCl_3$/Al-PLC and regenerated $NdCl_3$/Al-PLC for the isomerization of α-pinene are shown in Figure 5.1.

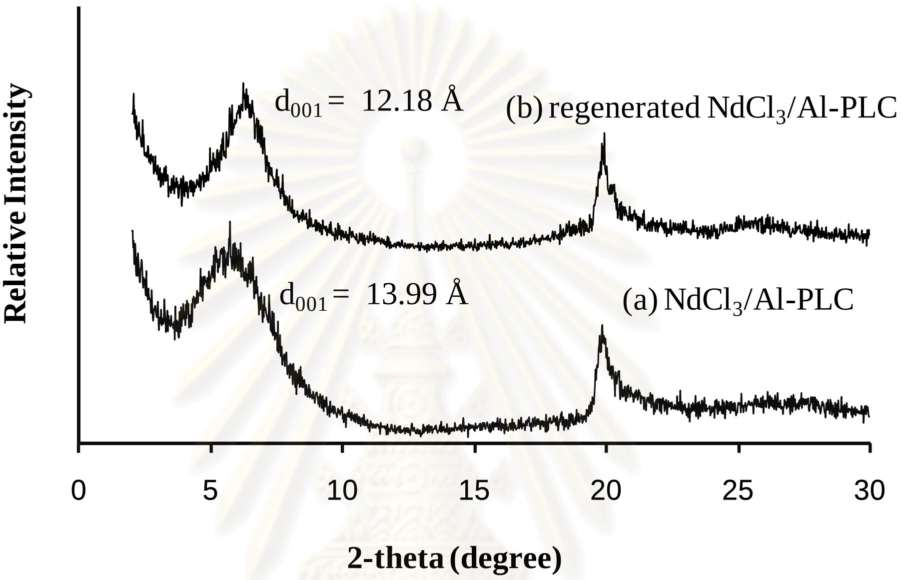

Figure 5.1 XRD patterns of (a) $NdCl_3$/Al-PLC and (b) regenerated $NdCl_3$/Al-PLC.

After the isomerization reaction had finished, the clay catalyst was filtered out, washed with EtOAc and calcined at 450°C for 4 h. The X-ray diffraction pattern of regenerated $NdCl_3$/Al-PLC was similar to that of $NdCl_3$/Al-PLC. The broad (001) peak appeared at the same range (2θ of 4°-8°) as that of fresh $NdCl_3$/Al-PLC, indicating that the structure of catalyst was preserved upon regeneration process. Although the hightest point of d_{001} was around 12 Å that was smaller than the d_{001} of fresh $NdCl_3$/Al-PLC. The collapse resulted from the re-calcination process and the local heat produced from decomposition of trapped organic species.

5.5.2 Nitrogen adsorption-desorption of regenerated catalyst

The nitrogen adsorption-desorption isotherms of $NdCl_3$/Al-PLC and regenerated $NdCl_3$/Al-PLC for the isomerization of α-pinene are shown in Table 5.8.

Table 5.8 The BET specific surface area of $NdCl_3$/Al-PLC and regenerated $NdCl_3$/Al-PLC for the isomerization of α-pinene

Entry	**Samples**	**BET specific surface area (m^2/g)**
1	$NdCl_3$/Al-PLC	127.25
2	regenerated $NdCl_3$/Al-PLC#1	86.57

Table 5.8 displays that the BET specific surface area of regenerated $NdCl_3$/Al-PLC was lower than that of $NdCl_3$/Al-PLC. The re-calcination process at 450°C seemed not enough to remove all organic residues that blocked the pores of the catalyst. Another possibility was the collapse of the d-spacing causing the smaller pores; however, re-calcination process at >300°C caused the impregnated pillared structure change or collapse.

5.5.3 Temperature programmed desorption of regenerated catalyst

The total acidity (mmol/g) of $NdCl_3$/Al-PLC and regenerated $NdCl_3$/Al-PLC for the isomerization of α-pinene are compared in Table 5.9.

Table 5.9 The acidity of $NdCl_3$/Al-PLC and regenerated $NdCl_3$/Al-PLC for the isomerization of α-pinene

Entry	**Samples**	**acidity (mmol/g)**		**Total acidity (mmol/g)**
		Weak acid sites	**Strong acid sites**	
1	$NdCl_3$/Al-PLC	0.600	2.899	3.499
2	regenerated $NdCl_3$/Al-PLC#1	0.225	1.416	1.641

From Table 5.9, the acidities of $NdCl_3$/Al-PLC and regenerated $NdCl_3$/Al-PLC were studied. The results demonstrated that the acidity of regenerated $NdCl_3$/Al-PLC was lower than that of $NdCl_3$/Al-PLC. The acidity of regenerated catalyst decreased. It was due to the remaining organic residues in catalyst pores because the regenerated process at 450°C may not completely destroy or decompose the organic compounds adsorbed on used catalyst.

5.5.4 Activity of regenerated $NdCl_3$/Al-PLC in the isomerization of α-pinene

The regenerated $NdCl_3$/Al-PLC was used as a catalyst in the isomerization of α-pinene. The results are presented in Table 5.10.

The regenerated $NdCl_3$/Al-PLC exhibited lower activity than $NdCl_3$/Al-PLC corresponding to the result of the collapse of d_{001} spacing, lower BET specific surface area and lower acidity.

Table 5.10 Activity of regenerated $NdCl_3$/Al-PLC for the isomerization of α-pinene

Entry	Run (times)	Conversion (%)	Selectivity (%)							
			Tri- and bicyclics		Monocyclics					Others
			Tricyclene	Camphene	Limonene	*p*-cymene	α-Terpinene	γ-Terpinene	Terpinolene	
1	1	100	3	37	23	6	9	9	10	3
2	2	96	5	34	19	9	7	10	14	2
3	3	89	5	36	17	8	9	5	16	4

Reaction conditions: α-pinene 10 mmol, 10 wt% $NdCl_3$/Al-PLC to α-pinene at 180°C for 2 h.

5.6 Conclusion

Clay catalysts have potential for the isomerization of α-pinene to a desired compound. The catalytic activities of iron oxide-pillared clays, Al-PLC and $NdCl_3$/Al-PLC and were evaluated. When using $NdCl_3$/Al-PLC, the main product was camphene, while using iron oxide-pillared clays and Al-PLC, the main product was limonene. The effects of reaction temperature, reaction time and the amount of catalysts were studied to search for the optimal conditions and selectivity of camphene and limonene production. These parameters greatly affected on %conversion and %selectivity. In the case of iron oxide-pillared clays, the reaction temperature and the amount of catalyst profoundly affected on %conversion and %selectivity. The major product was limonene. When reaction temperature or the amount of catalyst increased, %selectivity in limonene was increased, but the selectivity in camphene was decreased and the formation of monocyclic products was decreased. When using $NdCl_3$/Al-PLC and Al-PLC, the reaction time, reaction temperature and the amount of catalyst have an influence on the selectivity ratio of bicyclic and tricyclic to monocyclic products and %conversion increased. In the case of $NdCl_3$/Al-PLC, when reaction temperature was changed, the product was changed. At 100°C, the major product was limonene. When reaction temperature increased, %selectivity in limonene was decreased but the selectivity in camphene was increased, the major product was camphene. In the case of Al-PLC, the major product was limonene at every reaction temperature. The effect of the amount of catalyst was studied for both $NdCl_3$/Al-PLC and Al-PLC. When the amount of catalyst was increased, the amount of limonene was increased but the formation of camphene product remained constant around 30-35% whereas the amount of monocyclic products was decreased. The effect of the reaction time was examined for both $NdCl_3$/Al-PLC and Al-PLC. When the reaction time increased from 60 to 180 min, %α-pinene conversion was increased, but the amount of limonene was decreased. A fast transformation of limonene to other monocyclic products (*p*-cymene, α-terpinene, γ-terpinene and terpinolene) was obtained when the reaction time increased. Therefore using $NdCl_3$/Al-PLC, the optimized condition was 10 wt% $NdCl_3$/Al-PLC to α-pinene at 180°C for 2 h, the camphene is an expected product. While using iron oxide-pillared clays, the optimized condition was 10 wt% iron oxide-pillared clays to α-pinene at 180°C for 2 h, limonene was an expected product.

CHAPTER VI

CONCLUSION

The outcome from this research can be divided into four parts. The first part involves the synthesis and characterization of iron oxide-pillared clays, aluminium oxide-pillared bentonite and metal trichloride-impregnated aluminium oxide-pillared clay catalysts. The second, third and fourth parts involves the Friedel-Crafts acylation, the conversion of epoxides to acetonides and the isomerization of α-pinene catalyzed by iron oxide-pillared clays and metal chloride impragnated aluminium-pillared clays, respectively.

6.1 The synthesis and characterization of clay catalysts

Iron oxide-pillared clays including iron oxide-pillared bentonite, iron oxide-pillared hectorite and iron oxide-pillared taeniolite were synthesized by the intercalation of iron complexes into clay interlayers and calcination at 300°C for 5 h, whereas aluminium oxide-pillared bentonite was prepared by the intercalation method and calcination at 500°C for 1 h. The impregnation with metal chloride ($LaCl_3$, $NdCl_3$, $CeCl_3$, $GdCl_3$, $DyCl_3$ and $YbCl_3$) was carried out with calcination at 450°C for 4 h. The synthesized clays and raw clays were characterized using XRD, N_2 adsorption-desorption, NH_3-TPD and ICP-OES techniques. The XRD patterns of the iron oxide-pillared clays and metal chloride-impregnated aluminium oxide-pillared bentonite indicate that the layered structure of clay is sustained. The d_{001} basal spacings of iron oxide-pillared bentonite, iron oxide-pillared hectorite, iron oxide-pillared taeniolite and aluminium oxide-pillared bentonite are reported for 15.23, 14.88, 13.94 and 16.36 Å, respectively. The d_{001} basal spacings of all synthesized of metal chloride-impregnated aluminium oxide-pillared clays are about 14-15 Å. The N_2 adsorption-desorption isotherms of all synthesized catalysts suggested the distorted reversible type IV isotherm, indicating their mesoporous structure. The BET specific surface areas of all synthesized catalysts were higher than those of pure clays. In the case of iron oxide-pillared clays group, iron oxide-pillared bentonite exhibited the highest surface area (155.52 m^2/g of clay). From the results of NH_3-TPD, the amounts of acidity of all synthesized clay catalysts were higher than those of pure clays. Iron oxide-pillared bentonite exhibited the highest acidity (3.726 mmol/g of clay). The iron chloride content in iron oxide-pillared bentonite was 10.14 wt%, measuring by ICP-OES.

These synthesized catalysts were used for acid-catalyzed reactions (1) the Friedel-Crafts acylation, (2) the conversion of epoxides to acetonides and (3) isomerization reaction. The catalytic activity of synthesized clays was compared with raw clays. The synthesized clays provided significantly higher yield than raw clays of all types. These acid-catalyzed reactions could smoothly be proceeded in the presence of synthesized clays as efficient catalysts to furnish the corresponding products in good to excellent yield. The excellent and quantitative yield of products in all reactions was obtained.

6.2 The Friedel-Crafts acylation catalyzed by iron oxide-pillared bentonite

The main aim of this part is to search for the optimized conditions for the Friedel-Crafts acylation catalyzed by iron oxide-pillared bentonite. This new catalytic system was applied to the Friedel-Crafts acylation of various aromatic compounds and acid chlorides. The Friedel-Crafts acylation of anisole with benzoyl chloride catalyzed by iron oxide-pillared bentonite could be carried out to furnish 4-methoxy-benzophenone in excellent yield with good selectivity. The optimized conditions were anisole 1 mmol, benzoyl chloride 3 mmol, 30 wt% iron oxide-pillared bentonite to anisole, reaction temperature at refluxing 1,4-dioxane for 2 h. The optimized conditions were also applied for the variation of both aromatic compounds and acid chlorides.

6.3 The conversion of epoxides to acetonides catalyzed by iron oxide-pillared clays

The goal of this session is to search for the optimized conditions for the conversion of epoxides to acetonides catalyzed by iron oxide-pillared bentonite compared with iron oxide-pillared hectorite and iron oxide-pillared taeniolite. Under the same reaction conditions, iron oxide-pillared bentonite showed better efficiency than iron oxide-pillared hectorite and iron oxide-pillared taeniolite. The former iron oxide-pillared clay had the highest BET surface area and acidity. This new catalytic system was applied to the conversion of various epoxides and carbonyl compounds to acetonides. The reaction of styrene oxide with acetone catalyzed by iron oxide-pillared bentonite could be performed to furnish 2,2-dimethyl-4-phenyl-1,3-dioxolane in quantitative yield in short period of time under mild conditions. The optimized conditions were 10 wt% iron oxide-pillared bentonites to styrene oxide at RT for 5 min. The optimized conditions were also applied for the variation of both epoxides and carbonyl compounds.

6.4 The isomerization of α-pinene

The main aim of this part is to search for the optimized conditions for the isomerization of α-pinene catalyzed by iron oxide-pillared bentonite, iron oxide-pillared hectorite, $NdCl_3$/Al-PLC and Al-PLC. Using $NdCl_3$/Al-PLC, the main product was camphene, whereas using iron oxide-pillared bentonite, iron oxide-pillared hectorite and Al-PLC, the main product was limonene. The optimized conditions for the isomerization of α-pinene reaction were 30 wt% catalysts to α-pinene at 180°C for 2 h.

6.5 Propose for the future work

This research concerns with the methodology development for the reactions catalyzed by clay. Other types of pillared oxides such as indium oxide-pillared clay or nickel oxide-pillared clay and types of metal trichloride-impregnated aluminium oxide-pillared clays such as indium or gallium should be used in order to improve yield and selectivity of those acid catalyzed reactions. In Friedel-Crafts acylation, more aromatic compounds and acid chlorides should be tested to expand the scope of the reaction. Various epoxides and carbonyl compounds should be further tested. In the isomerization reaction, the obtained methodology and optimized conditions for the isomerization of α-pinene should be applied for the isomerization of other substrates.

REFERENCES

[1] Nagendrappa, G. Organic synthesis using clay and clay-supported catalysts. *Appl. Clay Sci.*, 2010, Articles in press.

[2] Clark, J. H. Solid acids for green chemistry. *Acc. Chem. Res.*, 2002, *35*: 791-797.

[3] Okuhara, T. Water-tolerant solid acid catalysts. *Chem. Rev.*, 2002, *102*: 3641-3666.

[4] Azzouz, A., et al. Assessment of acid-base strength distribution of ion-exchanged montmorillonites through NH_3 and CO_2-TPD measurements. *Thermochim. Acta*, 2006, *449*: 27-34.

[5] Venaruzzo, J. L., Volzone, C., Rueda, M. L., and Ortiga, J. Modified bentonitic clay minerals as adsorbents of CO, CO_2 and SO_2 gases. *Micropor. Mesopor. Mater.*, 2002, *56*: 73-80.

[6] Gil, A., Gandia, L. M., and Vicente, M. A. Recent Advances in the synthesis and catalytic applications of pillared clays. *Catal. Rev.-Sci. Eng.*, 2000, *42*: 145-212.

[7] Centi, G., and Perathoner, S. Catalysis by layered materials: A review. *Micropor. Mesopor. Mater.*, 2008, *107*: 3-15.

[8] Bruce, W. D., and Hare, D. Inorganic materials. 2nd ed., New York, John Wiley& Sons, Inc., 1997.

[9] Shichi, T., and Takagi, K. Clay minerals as photochemical reaction fields. *J. Photochem. Photobiol. C: Photochem. Rev.*, 2000, *1*: 113-130.

[10] Moore, D. M., and Reynolds, Jr. R. C. X-Ray Diffraction and the Identification and Analysis of Clay Minerals. New York, USA, Oxford University Press, 1989.

[11] Rajamathi, M., Thomas, G. S., and Kamath, P. V. The many ways of making anionic clays. *Proc. Indian Acad. Sci (Chem. Sci.)*, 2001, *113*: 671-680.

[12] Lambert, J. F., and Poncelet, G. Acidity in pillared clay: origin and catalytic manifestations. *Topic in Catal.*, 1997, *4*: 43-56.

[13] Novozhilov, A. I., Samoilovich, M. I., Anikin, I. N., and Sergeev-Bobr, A. A. Investigation of structural defects in the crystals of synthetic mica

(fluorophlogopite and taeniolite) by the EPR method. All-Union Scientific-Research Institute of Mineral Raw Materials, Aleksandrov. Translated from Zhurnal Strukturnoi Khimii, 1971, *12*: 562-566.

[14] Varma, R. S. Clay and clay-supported reagents in organic synthesis. *Tetrahedron*, 2002, *58*: 1235-1255.

[15] Schoonheydt, R. A., Pinnavaia, T., Lagaly, G., and Gangas, N. Pillared clays and pillared layered solids. *Pure Appl. Chem.*, 1999, *71*: 2367-2371.

[16] Vicente, M. A., et al. Preparation and characterization of vanadium catalysts supported over alumina-pillared clays. *Catal. Today*, 2003, *78*: 181-190.

[17] Gonzalez, F., Pesquera, C., Blanco, C., Benito, I., and Mendioroz, S. Synthesis and characterization of Al-Ga pillared clays with high thermal and hydrothermal stability. *Inorg. Chem.*, 1992, *31*: 727.

[18] Sawangkam, P. Synthesis of tangsten containing MCM-41 catalyst and their activity for olefin metathesis. Master’s Thesis, Department of Chemistry, Faculty of Science, Chulalongkorn University, 2005.

[19] Basic operating principles of the sorptomatic. [online] Available from: http://saf.chem.ox.ac.uk./Instruments/BET/sorpoptprin. [2010.11.15].

[20] Analysis software user’s manual, BELSORP, BEL JAPAN, INC. 57.

[21] Tago, T., Okubo, Y., Mukia, S. R., Tanaka, T., and Masuda, T. Simultaneous characterization of acidic and basic properties of solid catalysts by a new TPD method and their correlation to reaction rates. *App. Catal. A: General*, 2005, *290*: 54-64.

[22] Inductive coupled plasma atomic emission spectroscopy. [online] Available from: http://en.wikipedia.org/wiki/Inductive coupled plasma atomic emission spectroscopy. [2009.10.26].

[23] Manning, T. J., and Grow, R. W. Inductively coupled plasma-atomic emission spectrometry. *The Chem. Educator*, 1997, *2*: 1-19.

[24] Nagendrappa, G. Organic synthesis under solvent free-conditions: An environmentally benign procedure-I. *Resonance*, 2002, *7*: 59-68.

[25] Paolis, O. D., Teixeira, L., and Torok, B. Synthesis of quinolines by a solid acid-catalyzed microwave-assisted domino cyclization-aromatization approach. *Tetrahedron Lett.*, 2009, *50*: 2939-2942.

[26] Fabra, M. J., Fraile, J. M., Herrerias, C. I., Lahoz, F. J., Mayoral, J. A., and Perez, I. Surface-enhanced stereoselectivity in Mukaiyama aldol reactions catalyzed by clay-supported bis(oxazoline)-copper complexes. *Chem. Commun.*, 2008, *42*: 5402-5404.

[27] Kulkarni, A., Abid, M., Torok, B., and Huang, X. A direct synthesis of β-carbolines via a three-step one-pot domino approach with a bifunctional Pd/C/K10 catalyst. *Tetrahedron Lett.*, 2009, *50*: 1791-1794.

[28] Kamath, C. R., Shinde, A. B., and Samant, S. D. Diels-Alder reaction ofpyran-2(H)-ones. Part 5 Diels-Alder reaction of 4, 6-disubstituted pyran-2(H)-ones with 1, 4-naphthoquinone and N-phenylmaleimide under dry state adsorbed condition (DSAC) on montmorillonite K10, filtrol-24, bentonite, pyrophillite; and Al^{3+}, Zn^{2+}, Fe^{3+} exchanged montmorillonite K10 and bentonite. *Indian J. Chem.*, 2000, *39*: 270-276.

[29] Yadav, G. D., and Bhagat, R. D. Clean esterification of mandelic acid over $Cs_{2.5}H_{0.5}PW_{12}O_{40}$ supported on acid treated clay. *Clean Technol. Environ. Policy*, 2005, *7*: 245-251.

[30] Yadav, G. D., and George, G. Single step synthesis of 4-hydroxybenzophenone via esterification and Fries rearrangement: novelty of cesium substituted heteropoly acid supported on clay. *J. Mol. Catal. A: Chem.*, 2008, *292*: 54-61.

[31] Ilina, I. V., Volcho, K. P., Korchagina, D. V., Barkhash, V. A., and Salakhutdinov, N. F. Reactions of allyl alcohols of the pinene series and of their epoxides in the presence of montmorillonite clay. *Helv. Chim. Acta*, 2007, *90*: 353-368.

[32] Castanheiro, R. A. P., Pinto, M. M. M., Cravo, S. M. M., Pinto, D. C. G. A., Silva, A. M. S., and Kijjoa, A. Improved methodologies for synthesis of prenylated xanthones by microwave irradiation and combination of

heterogeneous catalysis (K10 clay) with microwave irradiation. *Tetrahedron*, 2009, *65*: 3848-3857.

[33] Singh, V., Khurana, A., Kaur, I., Sapehiyia, V., Kad, G. L., and Singh, J. Microwave assisted facile synthesis of elvirol, curcuphenol and sesquichamaenol using montmorillonite K10 clay in dry media. *J. Chem. Soc. Perkin Trans.*, 2002, *1*: 1766-1768.

[34] Kanjanaboonmalert, T. Synthesis and catalytic activity in alkylation reaction of iron and gallium-dopes iron oxides pillared clays. Master’s Thesis, Department of Chemistry, Faculty of Science, Chulalongkorn University, 2004.

[35] Masaleh, M. Catalytic cracking of polypropylene and polyethylene using zirconium/aluminium oxide-pillared clay. Master’s Thesis, Department of Chemistry, Faculty of Science, Chulalongkorn University, 2008.

[36] Kameshima, Y., Yoshizawa, A., Nakajima, A., and Okada, K. Solid acidities of SiO_2-TiO_2/montmorillonite composites synthesized under different pH conditions. *Appl. Clay Sci.* 2009, *46*: 181-184.

[37] Olejnik, S., Posner, A. M., and Quirk, J. P. Swelling of montmorillonite in polar organic liquids. *Clays & Clay Min.*, 1974, *22*: 361-365.

[38] Wang, M., and Muhammed, M. Novel synthesis of Al_{13}-cluster based alumina. *Nanostructured Mat.*, 1999, *11*: 1219-1229.

[39] Thomas, B., and Sugunan, S. Effect of rare earth metal ions on the structural properties of NaFAU-Y zeolite and vapour phase alkylation of benene with 1-octene. *Indian J. Chem. Tech.*, 2005, *12*: 676-688.

[40] Rai, K. M. L., Musad, E. A., Jagadish, R. L., and Shivakumar, K. N. Convenient method for the Friedel-Crafts acylation of benzene derivatives using silver nitrate as catalyst. *Synth. Commun.*, 2011, *41*: 953-955.

[41] Bai, G. Y., Dou, H. Y., Qiu, M. D., He, F., Fan, X. X., and Ma, Z. Friedel-Crafts acylation of anisole over Cr-doped Hβ zeolite. *Res. Chem. Intermed.*, 2010, *36*: 483-490.

[42] Kaur, J., Kozhevnikova, E. F., Griffin, K., Harrison, B., and Kozhevnikov, I. V. Friedel-Crafts acylation and related reactions catalyzed by heteropoly acids. *Kinet. Catal.*, 2003, *44*: 175-182.

[43] El-Sharkawy, E. A., and Al-Shihry, S. S. Friedel-Crafts acylation of toluene using superacid catalysts in a solvent-free medium. *Monatsh. Chem.*, 2010, *141*: 259-267.

[44] Hu, R. J., and Li, B. G. Novel solid acid catalyst, bentonite-supported polytrifluoro-methanesulfosiloxane for Friedel-Crafts acylation of ferrocene. *Catal. Lett.*, 2004, *98*: 43-47.

[45] Katritzky, A. R., Jiang, R., and Suzuki, K. *N*-Tfa- and *N*-Fmoc-(α-aminoacyl) benzotriazoles as chiral *C*-acylating reagents under Friedel-Crafts reaction conditions. *J. Org. Chem.*, 2005, *70*: 4993-5000.

[46] Calloway, N. O. The Friedel-Crafts Syntheses. *Chem. Rev.*, 1935, *17*: 327-392.

[47] Baudry, D. B., Bouazza, A., Desmurs, J. R., Dormond, A., and Richard, S. Uranium^{IV} and uranyle salts, efficient and reusable catalysts for acylation of aromatic compounds. *J. Mol. Catal. A: Chem.*, 2000, *164*: 195-204.

[48] Hwang, J. P., Prakash, G. K. S., and Olah, G. A. Trifluoromethanesulfonic acid catalyzed novel Friedel-Crafts acylation of aromatics with methyl benzoate. *Tetrahedron*, 2000, *56*: 7199-7203.

[49] Laidlawa, P., Bethell, D., Brownb, S. M., and Hutchings, G. J. Benzoylation of substituted arenes using Zn-and Fe-exchanged zeolites as catalysts. *J. Mol. Catal. A: Chem.*, 2001, *174*: 187-191.

[50] Patil, P. T., Malshe, K. M., Kumar, P., Dongare, M. K., and Kemnitz E. Benzoylation of anisole over borate zirconia solid acid catalyst. *Catal. Commun.*, 2002, *3*: 411-416.

[51] Choudhary, V. R., and Jana S. K. Benzoylation of benzene and substituted benzenes by benzoyl chloride over In_2O_3/Si-MCM-41 catalyst. *J. Mol. Catal. A: Chem.*, 2002, *184*: 247-255.

[52] Duris, F., Baudry, D. B., Dormond, A., Desmurs, J. R., and Bernard, J. M. Lanthanide bis(trifluoromethylsulfonyl)amides vs. trifluoromethyl sulfonates as catalysts for Friedel-Crafts acylations. *J. Mol. Catal. A: Chem.*, 2002, *188*: 97-104.

[53] Kawamura, M., Cui, D. M., Hayashi, T., and Shimada, S. Lewis acid-catalyzed Friedel-Crafts acylation reaction using carboxylic acids as acylating agents. *Tetrahedron Lett.*, 2003, *44*; 7715-7717.

[54] Sheemol, V. N, Tyagi, B., and Jasra, R.V. Acylation of toluene using rare earth cation exchanged zeolite β as solid acid catalyst. *J. Mol. Catal. A: Chem.*, 2004, *215*: 201-208.

[55] Sawant, D. P., Devassy, B. M., and Halligudi, S.B. Friedel-Crafts benzoylation of diphenyl oxide over zirconia supported 12-tungstophosphoric acid. *J. Mol. Catal. A: Chem.*, 2004, *217*: 211-217.

[56] Deutsch, J., Trunschke, A., Müller, D., Quaschning, V., Kemnitz, E., and Lieske, H. Acetylation and benzoylation of various aromatics on sulfated zirconia. *J. Mol. Catal. A: Chem.*, 2004, *207*: 51-57.

[57] Melero, J. A., Grieken, R. V., Morales, G., and Nuno, V. Friedel-Crafts acylation of aromatic compounds over arenesulfonic containing mesostructured SBA-15 materials. *Catal. Commun.*, 2004, *5*: 131-136.

[58] Gopalakrishnan, M., Sureshkumar, P., Kanagarajan, V., and Thanusu, J. Aluminium metal powder (atomized) catalyzed Friedel-Crafts acylation in solvent-free conditions: A facile and rapid synthesis of aryl ketones under microwave irradiation. *Catal. Commun.*, 2005, *6*: 753-756.

[59] Jana, S. K. Advances in liquid-phase Friedel-Crafts acylation of aromatics catalyzed by heterogeneous solids. *Catal. Sur. Asia*, 2006, *10*: 98-109.

[60] Yadav, G. D., and Badure, O. V. Selective acylation of 1,3-dibenzyloxybenzene to 3,5-dibenzyloxyacetophenone over cesium modified dodecatungsto phosphoric acid (DTP) on clay. *App. Catal. A: Gen.*, 2008, *348*: 16-25.

[61] Tamilselvan, P., Basavaraju, Y. B., Murugesan, R., and Sampathkumar, E. Cobalt(II) acetylacetonate catalyzed Friedel-Crafts acylation of anisole, thioanisole, and toluene. *Catal. Commun.*, 2008, *10*: 300-303.

[62] Farkas, J., Bekassy, S., Agai, B., Hegedus, M., and Figueras, F. Acylation of resorcinol on clay catalysts. *Synth. Commun.*, 2000, *30*: 2479-2485.

[63] Choudhary, V. R., Jana, S. K., and Mandale, A. B. Highly active, reusable and moisture insensitive catalyst obtained from basic Ga-Mg-hydrotalcite anionic clay for Friedel-Crafts type benzylation and acylation reactions. *Catal. Lett.*, 2001, *74*: 95-98.

[64] Yadav, G. D., Asthana, N. S., and Kamble, V. S. Cesium-substituted dodecatungsto-phosphoric acid on K-10 clay for benzoylation of anisole with benzoyl chloride. *J. Catal.*, 2003, *217*: 88-99.

[65] Choudhary, V. R., Patil, K. Y., and Jana, S. K. Acylation of aromatic alcohols and phenols over $InCl_3$/montmorillonite K-10 catalysts. *J. Chem. Sci.*, 2004, *116*: 175-177.

[66] Singh, D. U., and Samant, S. D. Comparative study of benzylation of benzene using benzyl chloride in the presence of pillared bentonite; ion-exchanged and pillaring solution impregnated montmorillonite K10. *J. Mol. Catal. A: Chem.*, 2004, *223*: 111-116.

[67] Choudhary, V. R., and Jha, R. $GaAlCl_x$-grafted Mont.K-10 clay: Highly active and stable solid catalyst for the Friedel-Crafts type benzylation and acylation reactions. *Catal. Commun.*, 2008, *9*: 1101-1105.

[68] Goodrich, P., Hardacre, C., Mehdi, H., Nancarrow, P., Rooney, D. W., and Thompson, J. M. Kinetic study of the metal triflate catalyzed benzoylation of anisole in an ionic liquid. *Ind. Eng. Chem. Res.*, 2006, *45*: 6640-6647.

[69] Quaschning, V., Auroux, A., Deutsch, J., Lieske, H., and Kemnitz, E. Microcalorimetric and catalytic studies on sulfated zirconia catalysts of different preparations. *J. Catal.*, 2001, *203*: 426-433.

[70] Carey, F. A. <u>Organic chemistry</u>, New York, McGraw-Hill, 1992.

[71] Kasemsuknimit, A. One-pot synthesis of aryl ketone from carboxylic acid via Friedel-Craft acylation. Master’s Thesis, Department of Chemistry, Faculty of Science, Chulalongkorn University, 2008.

[72] Wang, B., Gu, Y., Song, G., Yang, T., Yang, L., and Suo, J. An efficient procedure for protection of carbonyls catalyzed by sulfamic acid. *J. Mol. Catal. A: Chem.*, 2005, *233*: 121-126.

[73] Mori, A., and Yamamoto, H. Resolution of ketones *via* chiral acetals. Kinetic approach. *J. Org. Chem.*, 1985**,** *50*: 5444-5446.

[74] Hirano, K., Iwahama, T., Sakaguchi, S., and Ishii, Y. *N*-Hydroxyphthalimide-catalyzed radical addition of 1,3-dioxolanes and molecular oxygen to alkenes under ambient conditions: a new route to β-oxycarbonyl compounds. *Chem. Commun.*, 2000, *24*: 2457-2458.

[75] Clode, D. M. Carbohydrate cyclic acetal formation and migration. *Chem. Rev.*, 1979, *79*: 491-513.

[76] Torok, D. S., Figueroa, J. J., and Scott, W. J. 1,3-Dioxolane formation via lewis acid-catalyzed reaction of ketones with oxiranes. *J. Org. Chem.*, 1993, *58*: 7274-7276.

[77] Iranpoor, N., and Zeynizadeh, B. Efficient and catalytic conversion of epoxides to 1,3-dioxolanes with $TiO(TFA)_2$ or $TiCl_3(OTf)$. *J. Chem. Res.*, 1998, *8*: 466-467.

[78] Iranpoor, N., and Kazemi F. Ru(III) catalyses the conversion of epoxides to 1,3-dioxolanes. *Synth. Commun.*, 1998, *28*: 3189-3193.

[79] Mohammadpoor, B. I., Khosropour, A. R., and Aliyan, H. Efficient conversion of epoxide to 1,3-dioxolanes catalyzed by bismuth (III) salts. *Synth. Commun.*, 2001, *31*: 3411–3416.

[80] Vyvyan, J. R., Meyer, J. A., and Meyer, K. D. Conversion of epoxides to 1,3-dioxolanes catalyzed by tin(II) chloride. *J. Org. Chem.*, 2003, *68*: 9144-9147.

[81] Procopio, A., Dalpozzo, R., De Nino, A., Maiuolo, L., Nardi, M., and Russo, B. Synthesis of acetonides from epoxides catalyzed by Erbium(III) Triflate. *Adv. Synth. Catal.*, 2005, *347*: 1447-1450.

[82] Saha, S., Mandal, S. K., and Roy, S. C. Fe(III) chloride catalyzed conversion of epoxides to acetonides. *Tetrahedron Lett.*, 2008, *49*: 5928-5930.

[83] Zeynizadeh, B., and Sadighnia, L. Catalytic conversion of epoxides to 1,3-dioxolanes with phosphomolybdic acid (PMA) in solution and under solvent-free conditions. *Phosphorus, Sulfur Silicon Relat. Elem.*, 2008, *183*: 2274-2279.

[84] Ponde, D., Borate, H. B., Sudalai, A., Ravlndranathan, T., and Deshpande, V. H. Natural kaolinitic clay: A remarkable reusable solid catalyst for the selective functional protection of aldehydes and ketones. *Tetrahedron Lett.*, 1996, *37*: 4605-4608.

[85] Ballini, R., Bosica, G., Frullanti, B., Maggi, R., Sartori, G., and Schroer, F. 1,3-Dioxolanes from carbonyl compounds over zeolite HSZ-360 as a reusable, heterogeneous catalyst. *Tetrahedron Lett.*, 1998, *39*: 1615-1618.

[86] Ledneczki, I., Daranyi, M., Ferenc F., and Molnar, A. SAC-13 silica nanocomposite solid acid catalyst in organic synthesis. *Catal. Today*, 2005, *100*: 437-440.

[87] Bucsi, I., Meleg, A., Molnar, A., and Bartok, M. Brønsted acid catalyzed formation of 1,3-dioxolanes from oxiranes and ketones. *J. Mol. Catal. A: Chem.*, 2001, *168*: 47-52.

[88] Wu, H. H., Yang, F., Cui, P., Tang, J., and He, M.Y. An efficient procedure for protection of carbonyls in Brønsted acidic ionic liquid [Hmim]BF_4. *Tetrahedron Lett.*, 2004, *45*: 4963-4965.

[89] Duan, Z., Gu, Y., and Deng, Y. Green and moisture-stable Lewis acidic ionic liquids (choline chloride. $xZnCl_2$) catalyzed protection of carbonyls at room temperature under solvent-free conditions. *Catal. Commun.*, 2006, *7*: 651-656.

[90] Srivastava, P., and Srivastava, R. A novel method for the protection of amino alcohols and carbonyl compounds over a heterogeneous, reusable catalyst. *Catal. Commun.*, 2008, *9*: 645-649.

[91] Shirini, F., Sadeghzadeh, P., and Abedini, M. Silica sulfuric acid: A versatile reagent for oxathioacetalyzation of carbonyl compounds and deprotection of 1,3-oxathiolanes. *Chinese Chem Lett.*, 2009, *20*: 1457-1460.

[92] Amrute, A. P., Sahoo, S., Bordoloi, A., Hwang, Y. K., Hwang, J. S., and Halligudi, S. B. MoO_3/SiO_2: An efficient and selective catalyst for the synthesis 1,3-dioxolane and 1,3-dioxane. *Catal. Commun.*, 2009, *10*: 1404-1409.

[93] Yadav, M. K., Chudasama, C. D., and Jasra, R. V. Isomerisation of α-pinene using modified montmorillonite clays. *J. Mol. Catal. A: Chem.,* 2004, *216*: 51-59.

[94] Grzonaa, L., Masinia, O., Comellia, N., Ponzib, E., and Ponzia, M. Deactivation of $H_3PW_{12}O_{40}/TiO_2$ catalyst used in the production of camphene. *React. Kinet. Catal. Lett.*, 2005, *84*: 199-204.

[95] Stefanis, A. D., Perez, G., Ursini, O., and Tomlinson, A. A. G. PLS versus zeolites as sorbents and catalysts II. Terpene conversions in alumina-pillared clays and phosphates and medium pore zeolites. *App. Catal. A: Gen.*, 1995, *132*: 353-365.

[96] Severino, A., Esculcas, A., Rocha, J., Vital, J., and Lobo, L. S. Effect of extra-lattice aluminium species on the activity, selectivity and stability of acid zeolites in the liquid phase isomerisation of α-pinene. *App. Catal. A: Gen.*, 1996, *142*: 255-278.

[97] Lopez, C. M., Machado1, F. J., Rodrigueza, K., Mendez, B., Hasegawa, M., and Pekerar, S. Selective liquid-phase transformation of α-pinene over dealuminated mordenites and Y zeolites. *App. Catal. A: Gen.*, 1998, *173*: 75-85.

[98] Volzone, C., Masini, O., Comelli, N. A., Grzona, L. M., Ponzi, E. N., and Ponzi, M. I. Production of camphene and limonene from pinene over acid di- and trioctahedral smectite clays. *App. Catal. A: Gen.*, 2001, *214*: 213-218.

[99] Ferragina, C., Cafarelli, P., and Perez, G. Selective isomerization of α-pinene. *React. Kinet. Catal. Lett.*, 2002, *77*: 173-179

[100] Valencia, O. C., Sanchez, A. R., Martinez, V. C., and Elguezabal, A. A. Ion exchange resins as catalyst for the isomerization of α-pinene to camphene. *Bioresource Tech.*, 2004, *93*: 119-123.

[101] Comelli, N. A., Ponzi, E. N., and Ponzi, M. I. Isomerization of α-pinene, α-terpinene, and terpinolene on sulfated zirconia. *JAOCS,* 2005, *82*: 531-535.

[102] Da Silva Rocha, K. A., Robles, D. P. A., Kozhevnikov, I. V., and Gusevskaya, E. V. Phosphotungstic heteropoly acid as efficient heterogeneous

catalyst for solvent-free isomerization of α-pinene and longifolene. *App. Catal. A: Gen.*, 2009, *352*: 188-192.

[103] Gunduz, G., Dimitrova, R., Yilmaz, S., and Dimotrov, L. Liquid phase transformation of α-pinene over Beta zeolites containing aluminium or boron, titanium and vanadium as lattice ions. *App. Catal. A: Gen.*, 2005, *282*: 61-65.

[104] Rachwalik, R., Olejniczak, Z., Jiao, J., Huang, J., Hunger, M., and Sulikwoski, B. Isomerization of *α*-pinene over dealuminated ferrierite-type zeolites. *J. Catal.*, 2007, *252*: 161-170.

VITA

Miss Piyarat Trikittiwong was born on January 17, 1982 in Bangkok, Thailand. She graduated with Bachelor's Degree of Science in Chemistry from Faculty of Science, Mahidol University in 2004 and Master's Degree of Science in Petrochemistry and Polymer Science Program from Faculty of Science, Chulalongkorn University in 2005. She continued her study in Petrochemistry Program in 2005 and completed in 2010. During her studies towards the Doctor of Philosophy's Degree, she was supported by research grant for this Doctor of Philosophy's Degree from Office of the Higher Education Commission, Thailand during 2005-2010, and was awarded conference scholarship by National Center of Excellence for Petroleum, Petrochemicals, and Advance Meterials.

Her present address is 61 Lardya Road, Somdejjaophraya, Klongsan, Bangkok, 10600, Thailand.